

# MICROBIAL COMMUNITIES IN OLIGOTROPHIC MARINE ECOSYSTEMS

---

**Kajan, Katarina**

**Doctoral thesis / Doktorski rad**

**2023**

*Degree Grantor / Ustanova koja je dodijelila akademski / stručni stupanj:* **University of Zagreb, Faculty of Science / Sveučilište u Zagrebu, Prirodoslovno-matematički fakultet**

*Permanent link / Trajna poveznica:* <https://um.nsk.hr/um:nbn:hr:217:767270>

*Rights / Prava:* [In copyright](#)/[Zaštićeno autorskim pravom.](#)

*Download date / Datum preuzimanja:* **2025-03-14**



*Repository / Repozitorij:*

[Repository of the Faculty of Science - University of Zagreb](#)





University of Zagreb

Faculty of Science  
Department of Geology

Katarina Kajan

**MICROBIAL COMMUNITIES  
IN OLIGOTROPHIC MARINE  
ECOSYSTEMS**

DOCTORAL DISSERTATION

Zagreb, 2023



University of Zagreb

Faculty of Science  
Department of Geology

Katarina Kajan

# **MICROBIAL COMMUNITIES IN OLIGOTROPHIC MARINE ECOSYSTEMS**

DOCTORAL DISSERTATION

Supervisor:  
Sandi Orlić, PhD

Zagreb, 2023



University of Zagreb

Prirodoslovno-matematički fakultet  
Geološki odsjek

Katarina Kajan

**MIKROBNE ZAJEDNICE U  
OLIGOTROFNIM MORSKIM  
EKOSUSTAVIMA**

DOKTORSKI RAD

Mentor:  
Dr.sc. Sandi Orlić

Zagreb, 2023

This doctoral dissertation was carried out within the Postgraduate program of Interdisciplinary Doctoral Study in Oceanology at the Department of Geology, Faculty of Science, University of Zagreb, under the supervision of Dr. sc. Sandi Orlić at Laboratory for Precipitation Processes, Division of Materials Chemistry, Ruđer Bošković Institute, Zagreb and Center of Excellence for Science and Technology-Integration of Mediterranean Region (STIM), University of Split, Split, Croatia. The research was performed in the frame of the project STIM–REI, Contract Number: KK.01.1.1.01.0003, a project funded by the European Union through the European Regional Development Fund – the Operational Programme Competitiveness and Cohesion 2014-2020 (KK.01.1.1.01); principal investigator Prof. Dr. Dr. h.c. Vlasta Bonačić-Koutecký. Part of the experimental research was carried out at the University of Vienna (Austria), while part of the bioinformatics analyses was carried out at the University of Kaiserslautern (Germany), University of Vienna (Austria), and Swedish University of Agricultural Sciences, Uppsala (Sweden).

## ACKNOWLEDGEMENTS

*I thank to my PhD supervisor and mentor dr.sc. Sandi Orlić, who supported and guided me in every way, gave me space and time, and lead me in the right direction to become independent. Moreover, his relentless efforts in securing crucial collaborations significantly contributed to the scientific work essential for my PhD.*

*My appreciation goes to all the members of the dissertation committee for their useful comments, corrections, and assistance.*

*I thank to all present and former members of the Laboratory for Precipitation Processes who were always ready to lend a hand whenever needed.*

*I extend my thanks to all my collaborators and colleagues who contributed to the creation of this dissertation and guided me on the scientific path with their diligent and selfless work. This dissertation and many publications could not have been carried out without them.*

*I express my gratitude to Branko Jalžić, a brave speleo scuba diver, and other members of the Croatian Biospeleological Society for their assistance in conducting underwater sampling in anchialine environments.*

*A special mention must go to Anita Rogošić for her help and support throughout the STIM-REI project, especially with all the administrative procedures.*

*Thanks to my friends for always being there with their limitless support and understanding.*

*Finally, I must express my very profound gratitude to my family, for providing me with unfailing support and continuous encouragement throughout my years of study, and through the process of researching and writing this thesis. This accomplishment would not have been possible without them. Thank you!*

## **MICROBIAL COMMUNITIES IN OLIGOTROPHIC MARINE ECOSYSTEMS**

KATARINA KAJAN

Faculty of Science, Department of Geology

Oligotrophic ecosystems are characterized by low nutrient concentration and low primary production. Climate change and anthropogenic nutrient loading affect the microbial communities of oligotrophic marine ecosystems, and therefore, understanding the essential functions of microbial communities is extremely important for understanding environmental changes. However, studying uncultured microorganisms and complex microbial communities in oligotrophic ecosystems remains a scientific challenge. This dissertation investigated the diversity and composition of microbial communities and their response to individual environmental conditions using modern molecular methods in an oligotrophic open ecosystem such as an ocean gyre and in semi-closed ecosystems such as coastal anchialine speleological objects. The results show that the physicochemical gradients, including light penetration, oxygen concentration, and salinity, along with nutrient limitation, play a crucial role in defining the microbial community composition and dynamics within the studied oligotrophic marine environments. Specifically, the protistan communities in the ultra-oligotrophic South Pacific Gyre are influenced by the depth of light penetration, while site-specific parameters influence the fungal communities. Additionally, the composition of protistan and prokaryotic communities in anchialine pits and caves undergoes changes along the salinity gradient within the water column, demonstrating a high degree of site-specificity in their diversity. Moreover, the diversity, activity, and function of the prokaryotic community in anchialine speleological object depends on the availability of oxygen and the stratification of the salinity gradient. The research provides insight into the microbial community's biodiversity and ecological role, expanding the knowledge of oligotrophic marine ecosystems.

(106 pages, 39 figures, 1 table, 291 references, original in English)

Keywords: microbial community, ocean gyre, anchialine speleological object, metagenomics

Supervisor: Sandi Orlić, PhD, Senior Scientist

Reviewers: Sunčica Bosak, PhD, Associate Professor

Neven Cukrov, PhD, Senior Scientist

Jelena Godrijan, PhD, Research Associate

## **MIKROBNE ZAJEDNICE U OLIGOTROFNIM MORSKIM EKOSUSTAVIMA**

KATARINA KAJAN

Prirodoslovno-matematički fakultet, Geološki odsjek

Oligotrofne ekosustave karakterizira niska koncentracija nutrijenata i niska razina primarne produkcije. Klimatske promjene te antropogeno opterećenje hranjivim tvarima utječu na mikrobne zajednice morskih oligotrofnih ekosustava te je stoga poznavanje osnova njihovog funkcioniranja od iznimne važnosti za razumijevanje okolišnih promjena. Međutim, istraživanje raznolikosti nekultiviranih mikroorganizama i metaboličkog potencijala kompleksnih mikrobni zajednica u oligotrofnim ekosustavima još uvijek predstavlja značajan znanstveni izazov. U ovom doktorskom radu istraživana je raznolikost i sastav mikrobni zajednica i njihov odgovor na pojedinačne uvjete okoliša korištenjem suvremenih molekularnih metoda u oligotrofnom otvorenom ekosustavu kao što je oceanski vrtlog i u poluzatvorenim ekosustavima kao što su obalni anhidralni speleološki objekti. Rezultati pokazuju da fizikalno-kemijski gradijenti, uključujući dubinu prodora svjetlosti, koncentraciju kisika i salinitet, zajedno s ograničenjem hranjivih tvari, igraju ključnu ulogu u definiranju sastava i dinamike mikrobne zajednice u istraživanim oligotrofnim morskim ekosustavima. Na prisutnost zajednica protista u ultra-oligotrofnom vrtlogu južnog Tihog oceana utječe dubina prodora svjetlosti, dok obrasci specifični za mjesto također utječu na prisutnost zajednica gljiva. Sastav zajednica protista i prokariota u anhidralnim jamama i špiljama mijenja se duž gradijenta saliniteta unutar vodenog stupca, dodatno pokazujući visok stupanj specifičnosti lokacije u njihovoj raznolikosti. Štoviše, raznolikost, aktivnost i funkcija prokariotske zajednice u anhidralnom speleološkom objektu duž gradijent saliniteta, ovisi o dostupnosti kisika. Istraživanje pruža uvid u bioraznolikost i ekološku ulogu mikrobne zajednice, proširujući znanje o oligotrofnim morskim ekosustavima.

(106 stranica, 39 slika, 1 tablica, 291 literaturna navoda, jezik izvornika: engleski)

Ključne riječi: mikrobna zajednica, oceanski vrtlog, anhidralni speleološki objekt, metagenomika

Mentor: dr.sc. Sandi Orlić, znanstveni savjetnik

Ocjenjivači: izv. prof. dr. sc. Sunčica Bosak

dr. sc. Neven Cukrov, znanstveni savjetnik

dr. sc. Jelena Godrijan, znanstvena suradnica

## **EXTENDED SUMMARY**

The carbon cycle results from numerous biotic interactions, where the function and productivity of microbial communities are directly related to their diversity and composition. Understanding the fundamental processes that regulate microbial communities in oligotrophic ecosystems is essential for predicting ecosystem functioning and maintenance, allowing better management and conservation plans. Modern molecular methods allow detailed exploration of taxonomic and genetic diversity, and the role of microbial communities in nutrient cycling in diverse marine ecosystems. The study of uncultured microorganisms and the metabolic potential of complex microbial communities in oligotrophic ecosystems is still a major scientific challenge. In today's marine ecosystems, the abundance, distribution, diversity, interaction, and functions of marine microorganisms are directly or indirectly affected by climate change and anthropogenic impacts, leading to changes in nutrient cycling, loss of microbial diversity and biomass, local extinctions, and community changes.

Oligotrophic ecosystems are defined as areas with extremely low levels of nutrients, and organisms classified as oligotrophic are those that have adapted to thrive in such nutrient-poor conditions (Browning and Moore, 2023; Moore et al., 2013). Although the South Pacific Gyre has been referred to as a "biological desert", it plays a significant role in the global carbon and nitrogen cycle according to estimates obtained from satellite remote sensing data (Claustre et al., 2008; Guidi et al., 2016). The main reason for the lack of microbial data on the South Pacific Gyre is its great depth and distance from the coast, which limits scientific expeditions due to difficult sampling conditions and high costs. Previous research has mainly focused on studying the prokaryotic and photosynthetic protistan community (Walsh et al., 2015; Reintjes et al., 2019), so little is known about the diversity of the other functional groups of protists and fungi and their potential ecological role.

In contrast, to open ocean ecosystems, the ecological niches of coastal and semi-closed anchialine ecosystems are additionally limited by light and oxygen resources (Duque et al., 2020; Pakes, 2013). Anchialine ecosystems are defined as "tidally-influenced subterranean estuary located within crevicular and cavernous karst and volcanic terrains that extend inland to the limit of seawater penetration" (Bishop et al., 2015). Geographic isolation and abiotic influences such as halocline, chemocline, and oxycline are recognized promoters of the evolution of organisms in these habitats (Pachiadaki et al., 2014). Despite unfavorable growth conditions and numerous limiting factors, microorganisms evolved in the ecological niches of anchialine ecosystems (Calderón-Gutiérrez et al., 2018). Anchialine caves along the Adriatic

coast are spatially complex habitats that are generally accessible only to speleologists and divers because technical difficulties in sampling limit access to the systems.

Studying microbial communities becomes especially challenging within specific oligotrophic environments like stratified water bodies, including anchialine speleological objects or ultra-oligotrophic ecosystems such as ocean gyres. In these ecosystems, a substantial portion of the microbial community often consists of organisms that remain uncharacterized or have not been isolated yet. Recognizing the metabolic traits exhibited by anchialine microbial communities is crucial for gaining insights into the survival mechanisms of complex ecosystems in extreme environments and for evaluating their susceptibility to environmental shifts. Despite the diversity found in anchialine ecosystems, our comprehension of their metabolic functions remains limited.

The main focus of this dissertation was to gain insight into the diversity and composition of microbial communities and the influence of individual environmental conditions in nutrient-depleted environments using modern molecular methods in an oligotrophic open ecosystem such as an ocean gyre and a semi-closed ecosystem such as coastal anchialine speleological objects. This doctoral dissertation includes results presented in the form of three research areas of nutrient-depleted environments, which adequately address the aims and hypotheses of the dissertation. The aims of this dissertation were to: I) analyze the diversity and vertical distribution of protistan and fungal communities in the water column of the ultra-oligotrophic South Pacific Gyre; II) analyze the diversity of protistan and prokaryotic communities in the water column of anchialine pits and caves, and III) analyze the diversity, function and activity of the prokaryotic community in the anoxic water column of an anchialine speleological object.

This doctoral dissertation is structured in six chapters. The introduction gives an overview of the knowledge of the microbial communities and studied oligotrophic ecosystems, highlighting the results of the previous studies. The following three chapters (Materials and methods, Results, and Discussion) are divided into three subchapters according to the oligotrophic research area and accompanying aims and hypotheses. The three subchapters are divided as follows: I) diversity patterns of protists and fungi in the water column of the ultra-oligotrophic South Pacific Gyre area, II) diversity patterns of prokaryotes and protists in the water column of anchialine pits and caves in the area of Kornati National Park, and III) diversity and activity patterns of prokaryotes together with their functional diversity in the water column of the anchialine speleological object in the Martinska area. The second chapter covers materials and methods used in the dissertation. The third chapter presents the results of the previously listed

research areas in three subchapters. The fourth chapter constitutes a detailed discussion that brings together the results of this doctoral dissertation in the given research area. The main conclusions are given in the fifth chapter. At the very end, there is an overview of the literature sources used.

The results presented in this dissertation under the second subchapter: II) *diversity patterns of prokaryotes and protists in the water column of anchialine pits and caves in the area of Kornati National Park* are published as: **Kajan K**, Cukrov N, Cukrov N, Bishop-Pierce R, Orlic S. Microeukaryotic and Prokaryotic Diversity of Anchialine Caves from Eastern Adriatic Sea Islands. *Microbial ecology* (Kajan et al., 2022).

The scientific contribution of this dissertation is that it provides detailed insight into the biodiversity of the microbial community and their ecological role, expanding the current knowledge of marine oligotrophic ecosystems. The dissertation underscores the critical role of physicochemical gradients, including light penetration, oxygen concentration, salinity, and nutrient limitation, in shaping the composition and dynamics of the microbial community. Understanding these drivers can aid in predicting how microbial communities may respond to environmental changes. The dissertation also provides new insights into the current understanding of sulfur cycling in anchialine speleological object and biogeochemical cycling potential of the stratified microbial communities, together with their functional distribution. Moreover, this is the first attempt of applying metagenomics, BONCAT and CARDFISH approaches on the water samples of anchialine ecosystems in Croatia. The overall research and results presented in this dissertation represent a step forward in understanding the basis for further research on the diversity and functional characteristics of microbial communities in marine oligotrophic ecosystems, particularly in coastal anchialine ecosystems and ocean gyres. Overall, this research provides a foundation for future studies in this field and emphasizes the importance of considering site-specific conditions and environmental drivers when studying microbial diversity and function. This work will ultimately contribute to better management and protection of oligotrophic marine ecosystems, especially anchialine speleological objects in Croatia.

## PROŠIRENI SAŽETAK

Ciklus ugljika rezultat je brojnih biotičkih interakcija, gdje su funkcija i produktivnost mikrobnih zajednica izravno povezani s njihovom raznolikošću i sastavom. Razumijevanje temeljnih procesa koji reguliraju mikrobnje zajednice u oligotrofnim ekosustavima bitno je za predviđanje funkcioniranja i održavanja ekosustava, što omogućuje bolje upravljanje i donošenje planova očuvanja. Suvremene molekularne metode omogućuju detaljno istraživanje taksonomske i genetske raznolikosti te uloge mikrobnih zajednica u kruženju nutrijenata u različitim morskim ekosustavima. Proučavanje nekultiviranih mikroorganizama i metaboličkog potencijala složenih mikrobnih zajednica u oligotrofnim ekosustavima još uvijek je veliki znanstveni izazov. U današnjim morskim ekosustavima, brojnost, distribucija, raznolikost, interakcija i funkcije morskih mikroorganizama izravno su ili neizravno pod utjecajem klimatskih promjena i antropogenih utjecaja, što dovodi do promjena u kruženju hranjivih tvari, gubitka mikrobnje raznolikosti i biomase, lokalnog izumiranja i promjene zajednica.

Oligotrofni ekosustavi definiraju se kao područja s iznimno niskim razinama hranjivih tvari, a organizmi klasificirani kao oligotrofni su oni koji su se prilagodili za razvoj u takvim uvjetima siromašnim hranjivim tvarima (Browning i Moore, 2023; Moore i sur., 2013). Iako se vrtloga južnog Tihog oceana naziva "biološkom pustinjom", igra značajnu ulogu u globalnom ciklusu ugljika i dušika prema procjenama dobivenim iz satelitskih podataka daljinskog istraživanja (Claustre i sur., 2008; Guidi i sur., 2016). Glavni razlog nedostatka mikrobnih podataka vrtloga južnog Tihog oceana je njegova velika dubina i udaljenost od obale, što ograničava znanstvene ekspedicije zbog teških uvjeta uzorkovanja i visokih troškova. Prethodna istraživanja uglavnom su bila usmjerena na proučavanje zajednice prokariota i fotosintetski aktivnih protista (Walsh i sur., 2015; Reintjes i sur., 2019). Kao rezultat toga, se malo zna o raznolikosti raznolikosti protista i gljiva te o njihovoj potencijalnoj ekološkoj ulozi.

Za razliku od otvorenog oceanskog ekosustava, ekološke niše anhidralnih ekosustava su priobalnog i poluzatvorenog tipa te su dodatno ograničeni resursima svjetlosti i kisika (Duque i sur., 2020; Pakes, 2013). Anhidralni ekosustavi definirani su kao „podzemni estuariji unutar pukotinskih i kavernoznih krških i vulkanskih terena, koji se protežu u unutrašnjost do granica prodora morske vode” (Bishop i sur., 2015). Geografska izolacija, zajedno s abiotičkim pritiscima, kao što su haloklina, kemoklina i oksiklina, priznati su promotori evolucije organizama u tim staništima (Pachiadaki i sur., 2014). Unatoč nepovoljnim uvjetima rasta i mnogim ograničavajućim čimbenicima, mikroorganizmi se mogu razvijati u ekološkim nišama anhidralnih ekosustava (Calderón-Gutiérrez i sur., 2018). Anhidralne špilje i jame uz jadransku

obalu prostorno su složena staništa, te zbog tehničkih poteškoća u uzorkovanju koji ograničavaju pristup sustavima dostupna su većim dijelom samo speleolozima i ronionicima.

Proučavanje mikrobnih zajednica postaje posebno izazovno unutar specifičnih oligotrofnih ekosustava poput stratificiranih vodenih tijela, uključujući anhijalne speleološke objekte ili ultra-oligotrofne ekosustave poput oceanskih vrtloga. U tim ekosustavima, znatan dio mikrobne zajednice često se sastoji od organizama koji ostaju nedetektirani ili još nisu izolirani. Uvid u metabolički potencijal mikrobnih zajednica anhijalnih ekosustava ključan je za stjecanje uvida u mehanizme preživljavanja složenih ekosustava u ekstremnim okruženjima i za procjenu njihove osjetljivosti na promjene u okolišu. Unatoč raznolikosti koja se nalazi u anhijalnim ekosustavima, naše razumijevanje njihovih metaboličkih funkcija ostaje ograničeno.

Glavni fokus ovog doktorskog rada bio je steći uvid u raznolikost i sastav mikrobnih zajednica i utjecaj pojedinih okolišnih uvjeta u okolišima osiromašenim hranjivim tvarima primjenom molekularnih metoda na području oligotrofnog otvorenog ekosustava kao što je oceanski vrtlog i poluzatvorenog ekosustava kao što su priobalni anhijalni speleološki objekti. Ovaj doktorski rad uključuje rezultate prikazane u obliku tri područja istraživanja okoliša osiromašenih hranjivim tvarima, koji na odgovarajući način odgovaraju ciljevima i hipotezama rada. Ciljevi ovog doktorskog rada bili su: I) analizirati raznolikost i vertikalnu rasprostranjenost u stupcu vode zajednice protista i gljiva na području ultra-oligotrofnog vrtloga južnog Tihog oceana, II) analizirati raznolikost zajednice protista i prokariota u stupcu vode anhijalnih jama i špilja, i III) analizirati raznolikost, funkciju i aktivnost prokariotske zajednice u anoksičnom vodenom stupcu anhijalnog speleološkog objekta.

Ovaj doktorski rad prikazan je u šest poglavlja. U uvodu je dan literaturni pregled o mikrobnim zajednicama i proučavanim oligotrofnim ekosustavima, s naglaskom na rezultate dosadašnjih istraživanja. Sljedeća tri poglavlja (Materijali i metode, Rezultati i Rasprava) podijeljena su u tri potpoglavlja prema području istraživanja oligotrofnog ekosustava te pratećim ciljevima i hipotezama. Tri su potpoglavlja podijeljena na sljedeći način: I) obrasci raznolikosti protista i gljiva u vodenom stupcu ultra-oligotrofnog vrtloga južnog Tihog oceana, II) obrasci raznolikosti prokariota i protista u vodenom stupcu anhijalnih jama i špilja na području Nacionalnog parka Kornati, i III) raznolikost i obrasci aktivnosti prokariota zajedno s njihovom funkcionalnom raznolikošću u vodenom stupcu anhijalnog speleološkog objekta na području Martinske. Drugo poglavlje pokriva materijale i metode korištene u doktorskom radu. U trećem poglavlju prikazani su rezultati prethodno navedenih područja istraživanja u tri potpoglavlja. Četvrto poglavlje predstavlja detaljnu raspravu koja objedinjuje rezultate ovog doktorskog rada

u zadanom području istraživanja. Glavni zaključci dani su u petom poglavlju. Na samom kraju je pregled korištenih izvora literature.

Rezultati prikazani u ovom radu pod drugim potpoglavljem: II) obrasci raznolikosti prokariota i protista u vodenom stupcu anhijalinih jama i špilja na području Nacionalnog parka Kornati objavljeni su pod: **Kajan K**, Cukrov N, Cukrov N, Bishop-Pierce R, Orlić S. Microeukaryotic and Prokaryotic Diversity of Anchialine Caves from Eastern Adriatic Sea Islands. *Microbial ecology* (Kajan et al., 2022).

Znanstveni doprinos ovog doktorskog rada je u tome što prikazuje detaljan uvid u bioraznolikost mikrobne zajednice i njihovu ekološku ulogu, proširujući dosadašnje spoznaje o morskim oligotrofnim ekosustavima. Također naglašava kritičnu ulogu fizikalno-kemijskih gradijenata, uključujući prodiranje svjetla, koncentraciju kisika, salinitet i ograničenje hranjivih tvari, u oblikovanju sastava i dinamike mikrobne zajednice. Razumijevanje ovih pokretača može pomoći u predviđanju kako mikrobne zajednice mogu odgovoriti na promjene u okolišu. Doktorski rad također daje nove uvide u trenutno razumijevanje kruženja sumpora u anhijalinskom speleološkom objektu i potencijal biogeokemijskog kruženja stratificiranih mikrobnih zajednica, zajedno s njihovom funkcionalnom distribucijom. Štoviše, ovo je prvi pokušaj primjene metagenomike, BONCAT i CARDFISH pristupa na uzorcima vode anhijalnih ekosustava u Hrvatskoj. Ukupna istraživanja i rezultati prikazani u ovom radu predstavljaju korak naprijed u razumijevanju temelja za daljnja istraživanja raznolikosti i funkcionalnih karakteristika mikrobnih zajednica u morskim oligotrofnim ekosustavima, posebice u obalnim anhijalinskim ekosustavima i oceanskim vrtlozima. Štoviše, ovo istraživanje pruža temelj za buduće studije u ovom području i naglašava važnost razmatranja uvjeta specifičnih za lokaciju i ekoloških pokretača pri proučavanju mikrobne raznolikosti i funkcije. Ovaj će rad u konačnici doprinijeti boljem upravljanju i zaštiti oligotrofnih morskih ekosustava, posebice anhijalinih speleoloških objekata u Hrvatskoj.

# TABLE OF CONTENTS

<b>EXTENDED SUMMARY</b>	i
<b>PROŠIRENI SAŽETAK</b>	iv
<b>1. INTRODUCTION</b>	1
<b>1.1. Marine microbial communities</b> .....	1
<b>1.2. Oligotrophic marine ecosystems</b> .....	4
1.2.1. Open ocean systems – Subtropical Gyres .....	5
1.2.2. Semi-closed ecosystems – Coastal anchialine speleological objects .....	7
<b>1.3. Dissertation outline</b> .....	10
<b>2. MATERIALS AND METHODS</b>	12
<b>2.1. Study area: ultra-oligotrophic South Pacific Gyre</b> .....	12
2.1.1. Site description, sample collection and DNA extraction .....	12
2.1.2. Environmental measurements .....	13
2.1.3. Amplicon sequencing and analysis .....	13
2.1.4. Statistical analysis and data visualization .....	13
<b>2.2. Study area: anchialine pits and caves in the area of National Park Kornati</b> ....	15
2.2.1. Site description, sample collection and DNA extraction .....	15
2.2.2. Environmental measurements .....	16
2.2.3. Amplicon sequencing and analysis .....	17
2.2.4. Statistical analysis and data visualization .....	18
<b>2.3. Study area: anchialine speleological object in the Martinska area</b> .....	19
2.3.1. Site description, sample collection and DNA extraction .....	19
2.3.3. Amplicon sequencing and analysis .....	21
2.3.4. Incubation experiment – BONCAT and CARD-FISH .....	22
2.3.5. Image processing and analysis .....	23
2.3.6. Metagenome sequencing, assembly and binning .....	24
2.3.7. Functional annotation .....	24
2.3.8. Statistical analysis and data visualization .....	25
<b>3. RESULTS</b>	26
<b>3.1. Diversity patterns of protists and fungi in the water column of the ultra-oligotrophic South Pacific Gyre area</b> .....	26

3.1.1. Environmental characteristics of South Pacific Gyre .....	26
3.1.2. Community composition, diversity and assembly of protists along the SPG ....	27
3.1.3. Community composition and diversity of fungi along the SPG .....	33
<b>3.2. Diversity patterns of prokaryotes and protists in the water column of anchialine pits and caves in the area of National Park Kornati.....</b>	<b>37</b>
3.2.1. Environmental characteristics of anchialine water columns .....	37
3.2.2. Taxonomic composition and diversity of the prokaryotic community .....	38
3.2.3. Taxonomic composition and diversity of the protistan and fungal community.	41
3.2.4. Co-occurrence patterns of microbial communities .....	43
<b>3.3. Diversity patterns of prokaryotes in the water column of the anchialine speleological object in the Martinska area .....</b>	<b>50</b>
3.3.1. Environmental characteristics of anchialine speleological object.....	50
3.3.2. Prokaryotic diversity, activity and community structure .....	51
3.3.3. Functional gene diversity and metabolic potential of the prokaryotic community	58
<b>4. DISCUSSION</b>	<b>67</b>
<b>4.1. Diversity patterns of protists and fungi in the water column of the ultra-oligotrophic south Pacific Gyre area.....</b>	<b>67</b>
<b>4.2. Diversity patterns of prokaryotes and protists in the water column of anchialine pits and caves in the area of Kornati National Park.....</b>	<b>71</b>
<b>4.3. Diversity patterns of prokaryotes in the water column of the anchialine speleological object in the Martinska area .....</b>	<b>76</b>
<b>5. CONCLUSIONS</b>	<b>79</b>
<b>6. LITERATURE</b>	<b>82</b>
<b>SUPPLEMENTARY MATERIALS</b>	<b>i</b>
Supplementary material 1 .....	i
Supplementary material 2 .....	ii
Supplementary material 3 .....	vi
Supplementary material 4 .....	viii
<b>CURRICULUM VITAE</b>	<b>xiv</b>

# 1. INTRODUCTION

## 1.1. Marine microbial communities

Aquatic microbial communities are affected by many environmental factors that determine their diversity and abundance (Lima-Mendez et al., 2015; Lozupone and Knight, 2007). Life in marine ecosystems is governed by broad ecological gradients of physical, chemical, and hydrological parameters such as temperature, light intensity, salinity, pressure, nutrient availability, etc. (Field et al., 1998; Follows and Oguz, 2005). The marine habitat is the largest on Earth, covering 70% of its surface and its second-largest carbon reservoir ( $38 \times 10^3$  Gt C; Ciais et al., 2013; Ducklow et al., 2001). Marine microorganisms play fundamental roles in global biogeochemical nutrient cycling in these habitats by metabolizing approximately half of the yearly organic carbon production in the ocean (Azam and Malfatti, 2007; Fuhrman, 2009; Legendre et al., 2015). The carbon cycle results from numerous biotic interactions, where the function and productivity of microbial communities are directly related to their diversity and composition (Devries, 2022; Hutchins and Fu, 2017; Siegel et al., 2023; Worden et al., 2015). A diverse consortium of marine microorganisms is forming the foundation of the marine food web, including prokaryotes (Archaea and Bacteria), protists, fungi, and viruses, which have adapted to diverse environments with different forms, functions, and strategies (Ibarbalz et al., 2019; Nayfach et al., 2021; Seymour et al., 2017; Stocker, 2012). They account for nearly 90% of the biomass, are responsible for about 98% of primary production, and play a fundamental role in maintaining the structure and function of marine ecosystems (Field et al., 1998; Longhurst et al., 1995). The high abundance and activity of microorganisms drive the biological carbon pump and directly impacts the global carbon cycle (Azam and Malfatti, 2007; Siegel et al., 2023). The biological pumps are important in regulating air-sea carbon exchange and the global carbon cycle (Ducklow et al., 2001; Iversen, 2023).

Marine phytoplankton accounts for ~1% of the world's photosynthetic biomass, while it contributes to nearly half of the world's primary production (Calbet and Landry, 2004; Field et al., 1998). Phytoplankton is a collective term used to describe marine primary producers, including phototrophic prokaryotes and phototrophic protists. Primary producers fix CO<sub>2</sub> using solar energy (photolithotrophically) or reduced inorganic compounds (chemolithotrophically) (Azam and Malfatti, 2007; Garritano et al., 2022). This energy is used to synthesize simple organic molecules from dissolved inorganic carbon (Moran et al., 2022). These simple inorganic compounds can then be utilized to synthesize more complex cellular materials such as lipids, amino acids, proteins, and carbohydrates, which often contain other nutrients like

nitrogen, phosphorus, sulfur, and iron. Phytoplankton makes this fixed material available to the marine food web through several processes. Initially, within the marine food web, primary consumers (zooplankton) feed on phytoplankton biomass, which can subsequently serve as sustenance for secondary consumers (fish), facilitating the transfer of matter throughout the food chain. Alternatively, phytoplankton also actively release between 10-50% of the produced organic matter from their cells in the form of dissolved organic matter (DOM; Thornton, 2014). DOM is predominantly accessible to marine heterotrophic microorganisms. Consequently, roughly half of the organic material derived from phytoplankton, or approximately one-quarter of global primary production, is controlled by marine microorganisms (Kujawinski, 2011; Kujawinski et al., 2016). Global marine primary production distribution exhibits marked heterogeneity, characterized by extensive regions with low production and smaller patches of high productivity. This variability arises from shifts in physicochemical conditions that govern and limit phytoplankton growth, encompassing factors such as sunlight availability (irradiance), temperature, and the presence and concentration of crucial inorganic nutrients like iron, phosphorus, and nitrogen (Howarth, 1988; Liang et al., 2023; Richardson and Bendtsen, 2019). Limitations in any of these elements impose constraints on primary production, thereby influencing the carbon influx through the biological carbon pump. The primary contributor to this high degree of heterogeneity is the prevalence of vast, nutrient-poor (oligotrophic) regions in the surface oceans, where essential nutrients like iron, phosphorus, and nitrogen are present in extremely low concentrations (Bristow et al., 2017; Howarth, 1988). In contrast, localized areas of elevated primary production are predominantly located in coastal regions, where the mixing of water masses or the upwelling of nutrient-rich deep waters occurs, significantly enhancing nutrient availability (Wallace et al., 2014). These conditions promote phytoplankton blooms, which play a pivotal role in capturing CO<sub>2</sub> and converting it into organic matter, driving the biological carbon pump (Ducklow et al., 2001; Inomura et al., 2022). Although phytoplankton fixes a significant amount of CO<sub>2</sub>, their biomass represents only a minor portion of the overall organic carbon present in the oceans (3 Gt C out of approximately 700 Gt C; Piontek et al., 2010). The large discrepancy between the amount of fixed carbon and phytoplankton biomass is due to extremely high rates of organic matter turnover in the oceans. Marine protists form a diverse and heterogeneous community, encompassing the majority of eukaryotic diversity in the oceans (Ohtsuka et al., 2015). They consist of primary producers (autotrophs), heterotrophs (phagotrophs and parasites), and a wide range of lineages exhibiting various mixotrophic strategies (Adl et al., 2019; Caron et al., 2012). These different groups occupy specific niches within the marine food web and play crucial roles in biogeochemical

cycles. Studies have shown that marine protists are responsible for approximately 50% of annual planktonic photosynthetic primary productivity, and they consume around 66% of this productivity, as well as an additional 10% of bacterial primary productivity (Caron et al., 2012; Steele et al., 2011).

Marine bacteria and archaea degrade between 75-95% of the organic matter derived from phytoplankton within a few days to weeks after its formation (Moran et al., 2016; Sanz-Sáez et al., 2020). This significantly impacts the marine carbon cycle, as a large portion of the fixed carbon is directly converted back into CO<sub>2</sub>. However, the remineralization of DOM affects the carbon cycle and also the other biogeochemical cycles since DOM contains many essential nutrients (N, P, Fe; Moran et al., 2016). The release of nutrients through DOM remineralization makes them available to higher levels of marine organisms (Moran et al., 2022). In these areas, the biological supply of nutrients from DOM remineralization by heterotrophic microorganisms dictates primary production. The active role of heterotrophic microorganisms in the cycling of DOM is referred to as the microbial loop (Benner, 2011).

Particulate organic matter often leads to the formation of aggregates. Due to their adhesive properties, aggregates often bind additional materials such as living and dead marine phytoplankton or zooplankton cells, transparent exopolymer particles, fecal pellets, and inorganic minerals (Simon et al., 2002). Aggregates serve as a source of organic matter in a highly nutrient-limiting environment, and therefore, they are quickly colonized by selective marine prokaryotes from the surrounding water column (Simon et al., 2002). The attachment of selective prokaryotic groups to aggregates has resulted in the general categorization of marine bacteria into two different lifestyles: free-living and particle-associated. The particle-associated fraction is often further categorized into size fractions based on the method used for their separation, such as sequential filtration through filters of different pore sizes. The difference between the two prokaryotic fractions is based on the exposure of prokaryotes to different selective forces (e.g., nutrient availability), which is assumed to drive organisms to gradually become phylogenetically and functionally distinct (Ngugi et al., 2023). Free-living bacteria are defined as pelagic bacteria adapted to grow at low levels of nutrients and substrates, such as *Prochlorococcus*, SAR11, or SAR86 (Bryant, 2003; Flombaum et al., 2013; Giovannoni, 2017; Partensky et al., 1999; West et al., 2016). Free-living prokaryotes typically have smaller genomes with fewer gene copies, reduced metabolic capabilities, and a decreased number of genes encoding transcription and signal transduction (Ngugi et al., 2023). In contrast, particle-associated bacteria typically exhibit high metabolic diversity, high hydrolytic activity, and large genomes with a range of genes encoding substrate utilization and uptake. These

organisms are predominantly heterotrophic, with specializations for the degradation of complex organic molecules found in aggregates. Some bacteria are known to transition between free-living and particle-associated lifestyles, depending on chemical triggers and substrate availability. Additionally, many marine bacteria are motile and show chemotaxis towards substrate hotspots so that they can exist as both free-living and particle-associated bacteria (Keestra et al., 2022; Raina et al., 2023; York, 2022).

The majority of marine primary production is consumed and respired in the euphotic zone, while the remainder (5-25%) is exported to the mesopelagic zone and below (Siegel et al., 2014). Once in the deep sea, exported particulate organic carbon is degraded and respired, resulting in attenuation of particulate organic carbon flux and accumulation of suspended and dissolved forms of carbon at depth (Herndl and Reinthaler, 2013). Despite extensive study, there remains a need to better quantify mechanisms of supply and demand for carbon in the mesopelagic zone (Boyd and Kennedy, 2021; Siegel et al., 2023), including the roles of zooplankton therein (Shea et al., 2023; Steinberg and Landry, 2017).

The significance of aquatic ecosystems as fungal habitats has often been neglected despite the potential importance of fungi in organic matter cycling and food web dynamics (Amend et al., 2019; Richards et al., 2012). Recent advancements in methodologies have shed light on the role of fungi in various aquatic systems (Grossart et al., 2019), but a comprehensive conceptual framework is still lacking (Cunliffe, 2023; Tedersoo et al., 2022). Understanding fungal diversity, abundance, ecological function, and interactions with other microorganisms is largely speculative and unexplored (Coleine et al., 2022; Sen et al., 2022). However, it has been proposed that fungi have the capacity to significantly influence the structure, stability, and functionality of aquatic food webs through symbiotic and parasitic interactions with other organisms and degradation of organic matter (Amend et al., 2019; Baltar et al., 2021; Gareth Jones et al., 2022; Kumar et al., 2021).

### **1.2. Oligotrophic marine ecosystems**

Oligotrophic ecosystems are defined as areas with extremely low levels of nutrients, and organisms classified as oligotrophic are those that have adapted to thrive in such nutrient-poor conditions (Browning and Moore, 2023; Moore et al., 2013). Specifically, oligotrophic microorganisms are adapted to thrive in environments with very low nutrient fluxes, typically around 0.1 mg of C L<sup>-1</sup> per day (Noell et al., 2023; Poindexter, 1981). They achieve maximal growth rates under these conditions and are inhibited in their growth by high nutrient

concentrations, generally be thought of as K strategists. In contrast, copiotrophs, also termed opportunists or r strategists, are adapted to make the most of high nutrient concentrations by maximizing time spent in nutrient patches or attached to sinking particles, which results in them occupying a very different spatial niche than oligotrophs (Lever et al., 2015; Poindexter, 1981). Most knowledge about microbial growth and metabolism comes from highly productive ecosystems, where microorganisms exhibit rapid growth rates and higher abundance, in contrast to oligotrophic ecosystems (Hoehler and Jørgensen, 2013; Howarth, 1988).

Despite the low nutrient content, marine microorganisms in oligotrophic ecosystems contribute significantly to biogeochemical nutrient cycling, oxygen production, and organic matter degradation (de Vargas et al., 2015; Roshan and DeVries, 2017). Vast expanses of the world's oceans are predominantly nutrient-limited (Smith, 1984), but the seasonal input of high amounts of organic matter, mainly from phytoplankton blooms, prompt significant changes in substrate availability (Bristow et al., 2017).

### **1.2.1. Open ocean systems – Subtropical Gyres**

Oligotrophic ocean gyres are large marine ecosystems that account for 60% of the ocean and 40% of the Earth's surface (Raimbault and Garcia, 2008) and have been described as ocean deserts due to their characteristically low nutrient concentrations and productivity (Dai et al., 2023; Irwin and Oliver, 2009; Kletou and M., 2012). Despite their low productivity, these subtropical gyres contribute significantly, accounting for 30-50% of the global oceanic primary productivity (Carr et al., 2006; Xiang et al., 2023). The subtropical gyres in the North Pacific, North Atlantic, South Pacific, South Atlantic, and South Indian Ocean maintain their ultraoligotrophic status year-round, with the South Pacific gyre near Easter Island exhibiting the lowest productivity (Morel et al., 2007).

Oligotrophic subtropical gyres cover ~40% of the Earth's surface by area and are expanding globally (McClain et al., 2004; Polovina et al., 2008). Nonetheless, these regions account for ~20% of total marine primary production due to their vast size (Shiozaki et al., 2018). Oligotrophic subtropical gyres are microbially dominated systems; cyanobacteria are the major primary producers (Flombaum et al., 2013; Grob et al., 2007), while heterotrophic bacteria and archaea modulate carbon and nutrient cycling (Azam and Malfatti, 2007). Carbon export in these regions is closely related to the composition of the microbial community (Guidi et al., 2016; Letscher et al., 2015).

The South Pacific Gyre (SPG) is the largest oligotrophic subtropical gyre, with a total area of 37 million km<sup>2</sup>, accounting for 10% of the entire ocean surface area (Polovina et al., 2008). The surface waters of the SPG are a unique ultra-oligotrophic habitat with the lowest chlorophyll *a* concentration and low surface nitrate concentrations (Morel et al., 2007; Raimbault et al., 2008; Signorini et al., 2015). Although the SPG has been referred to as a "biological desert", it plays a significant role in the global carbon and nitrogen cycle according to estimates obtained from satellite remote sensing data (Claustre et al., 2008; Guidi et al., 2016). Due to its distance from continental sources, it receives the lowest atmospheric iron flux worldwide (Wagner et al., 2008). Within the central gyre, both phytoplankton and heterotrophic bacteria face nitrogen limitations but not iron constraints, which only limit primary production along the gyre's periphery (Bonnet et al., 2008). Surface waters (shallower than 180 meters) contain undetectable nitrate ions and only trace amounts of regenerated nitrogen. Despite the nitrogen shortage, there is no evidence of nitrogen fixation (N<sub>2</sub> fixation), and *nifH* gene abundances are remarkably low compared to the North Pacific gyre (Bonnet et al., 2008). This suggests that autotrophic communities have adapted to thrive under low iron conditions, and common photoautotrophic nitrogen-fixing organisms are not favored due to their higher iron requirements. Despite significant nitrogen depletion leading to low chlorophyll biomass, the South Pacific gyre, with its characteristic reduced vertical mixing, can accumulate organic matter (Ko et al., 2018; Raimbault et al., 2008), which can support active regeneration processes during stratification (Raimbault and Garcia, 2007).

In the clear waters of the gyre's center, autotrophic eukaryotes transition to smaller cells (less than 2 micrometers) compared to more eutrophic conditions (Masquelier and Vaultot, 2008). Flow cytometry sorting conducted in the most oligotrophic areas of the gyre has led to the discovery of several novel lineages of photosynthetic picoeukaryotes, including a prasinophyte clade unique to the central region of the gyre (Shi et al., 2011). Dominant picophytoplankton in the region include pelagophytes, chrysophytes, and haptophytes (Shi et al., 2011). Coccolithophores, important unicellular calcifying haptophytes, are present at low abundances, with maximum cell concentrations recorded at depths between 150 and 200 meters (Beaufort et al., 2008). Additionally, high taxonomic diversity is observed in microzooplankton tintinnids, inversely correlated with chlorophyll concentration and positively related to the depth of the maximum chlorophyll layer (Dolan et al., 2007). Furthermore, larger microplankton, such as diatoms, can adapt to the ultraoligotrophic conditions of this region through symbiotic relationships with other species (Gómez, 2007).

There is a growing body of evidence suggesting that this expansive oceanic area, once considered net heterotrophic, may, in fact, be net autotrophic (Bender and Jönsson, 2016). The deep layers below the euphotic zones may significantly contribute to carbon fixation, fueling heterotrophic processes in the upper layer (Claustre et al., 2008). However, this remains a subject of debate, as some studies indicate that net community production is closely balanced or slightly net heterotrophic, while data from oxygen sensors deployed on profiling floats suggest that the system is net autotrophic year-round (Riser and Johnson, 2008). The main reason for the lack of microbial data on the SPG is its great depth and distance from the coast, which limits scientific expeditions due to difficult sampling conditions and high costs. Previous research has mainly focused on studying the prokaryotic and photosynthetic protistan community (Reintjes et al., 2019; Walsh et al., 2015; West et al., 2016), so little is known about the diversity of the other functional groups of protists and fungi and their potential ecological role. Understanding the interactions between physical and biological processes in subtropical gyres is critical for determining the magnitude and variability of carbon transported from the surface to the deep ocean (Roshan and DeVries, 2017).

### **1.2.2. Semi-closed ecosystems – Coastal anchialine speleological objects**

In contrast to open ocean ecosystems, the ecological niches of coastal and semi-closed anchialine ecosystems are additionally limited by light and oxygen resources (Duque et al., 2020; Pakes, 2013). Anchialine ecosystems are defined as “tidally-influenced subterranean estuaries within crevicular and cavernous karst and volcanic terrains that extend inland to the limit of seawater penetration” (Bishop et al., 2015). Due to the sea and groundwater connections, they possess both seawater and freshwater influences (Iliffe, 2000; Sket, 1996). These ecosystems exhibit a wide variety of morphological, physicochemical, and biological characteristics, which has a direct association with rainfall seasonality, influencing the vertical stratification within the water columns. Although they have a worldwide distribution, habitats fitting this ecosystem definition are considered relatively rare, and located in tropical and moderately warm climatic zones (Bailey et al., 2017; van Hengstum et al., 2019). Many anchialine speleological objects were formed during the Quaternary period (approximately 2.5 million years ago to the present) because of cyclical sea-level changes (Mylroie and Mylroie, 2011; Pérez-Moreno et al., 2016). Therefore, these anchialine speleological objects can be hundreds to thousands of years old and contain detailed records of environmental change and landscape evolution. To date, many anchialine ecosystems, such as subterranean estuaries, blue holes, sinks, caves, pits, cenotes, aquifers, etc., have been partially explored, including the

Saipan Blue Hole (the Pacific Ocean), the Dahab Blue Hole (Egypt), the Faanu Madugau's Blue Hole (the Indian Ocean), the Gozo Blue Hole (the Mediterranean Sea), the Dean's Blue Hole (the Bahama Islands), etc. (B. C. Gonzalez et al., 2011, 2012; H. He et al., 2019; P. He et al., 2020; Liu et al., 2019; Patin et al., 2021).

Anchialine ecosystem habitats represent an important long-term reservoir of species diversity and endemism maintained by limiting light, nutrients, and oxygen resources (Bishop et al., 2015; Iliffe, 2000). Geographic isolation and biotic pressures, such as halocline, chemocline and oxycline, are acknowledged promoters of evolution in organisms in these habitats (Pachiadaki et al., 2014). Defined clines in anchialine ecosystems act as a selecting barrier affecting species distribution, making them exquisite models for species diversity research (Culver and Pipan, 2019; B. C. Gonzalez et al., 2011, 2017; T. M. Iliffe, 2018; Pérez-Moreno et al., 2016). Although parameters such as temperature, light resources, nutrient limitation, etc., remain relatively stable, these factors may differ considerably between and within the anchialine ecosystem (Barton et al., 2010).

The availability of various physicochemical microhabitats in anchialine speleological objects make them ideal systems to study microbial community structure and discover novel chemosynthetic metabolisms (Ruiz-González et al., 2021). These extreme environments are formed in porous rocks, such as limestone, and often lack light. Here, water exchange with the landlocked marine habitat is severely restricted (T. M. Iliffe and Alvarez, 2018), resulting in stable gradients, often including anoxic and sulfidic marine layers underlying brackish water layers (Pohlman et al., 1997). The distinct halocline at which these marine and brackish waters meet is often called the zone of mixing. Methane may also be present where anoxic marine water sulfates are biogenically reduced in anoxic sediments (Brankovits et al., 2017; Seymour et al., 2007), making these interfaces potentially viable habitats for chemosynthetic microbes. Anchialine habitats thus contain both the highly structured environment and redox gradients necessary for the persistence of highly structured chemosynthetic communities. These metabolisms are especially important in cave ecosystems that have historically been characterized by a low nutrient supply (Gray and Engel, 2013).

Thus far, we have begun to understand better the importance and function of microorganisms and how microbial diversity is distributed across environments, yet the microbial community of anchialine ecosystems is still poorly investigated compared to other aquatic environments. Most studies conducted in anchialine speleological objects documented endemism among eukaryotes (Becking et al., 2011; Chlebicki and Jakus, 2019; B. Gonzalez et al., 2020; Havird and Santos, 2016; Pérez-García et al., 2018; Pohlman, 2011). Relatively few studies have

attempted to record the full diversity of microbial communities in anchialine ecosystems (B. C. Gonzalez, 2010; H. He et al., 2019; Hoffman et al., 2018; Krstulović et al., 2013; Liu et al., 2019), even though these studies resulted in descriptions of new species using novel molecular tools.

Anchialine speleological objects represent a unique and understudied environment common in the area of the eastern Adriatic coast (Cuculić et al., 2011; Rossi and Cukrov, 2017; Žic et al., 2008). The coast of Croatia is largely karstified and extends for more than 6,000 km, where hundreds of anchialine ecosystems have been recorded (Surić et al., 2010). In the region of the eastern Adriatic Sea, the majority of anchialine ecological studies have been based on the taxonomic research of stygobiotic metazoans (Kršinić, 2005), the distribution of trace metals (Kwokal et al., 2014), and iodine species and nutrients (Žic et al., 2011). Technical difficulties in sampling anchialine ecosystems limit the ability to study microbial communities. These environments along the Adriatic coast are spatially complex habitats accessible only by speleologists and scuba divers.

### 1.3. Dissertation outline

The main focus of this dissertation was to gain insight into the diversity and composition of microbial communities and the influence of individual environmental conditions in nutrient-depleted environments using modern molecular methods in an oligotrophic open ecosystem such as an ocean gyre and a semi-closed ecosystems such as coastal anchialine speleological objects. This doctoral dissertation includes results presented in the form of three research areas of nutrient-depleted environments, which adequately address the aims and hypotheses of the dissertation (**Figure 1**).

**Aims** of the dissertation are:

1. Analyze the diversity and vertical distribution of protistan and fungal communities in the water column of the ultra-oligotrophic South Pacific Gyre.
2. Analyze the diversity of protistan and prokaryotic communities in the water column of anchialine pits and caves.
3. Analyze the diversity, function and activity of the prokaryotic community in the anoxic water column of an anchialine speleological object.

**Hypothesis** of the dissertation are:

1. The presence of protist and fungal communities in the ultra-oligotrophic South Pacific Gyre depends on the depth of light penetration (photic zone).
2. The composition of protistan and prokaryotic communities in anchialine pits and caves changes with the salinity gradient.
3. The diversity, activity and function of the prokaryotic community in anchialine speleological object depends on the availability of oxygen and the salinity gradient.

The dissertation is structured in six chapters, as described below. The introduction gives an overview of the knowledge of the microbial communities and studied oligotrophic ecosystems, highlighting the results of the previous studies. The following three chapters (*Materials and methods*, *Results*, and *Discussion*) are divided into three subchapters according to the research area and accompanying aims and hypotheses (**Figure 1**). The three subchapters are divided as follows: I) diversity patterns of protists and fungi in the water column of the ultra-oligotrophic South Pacific Gyre area, II) diversity patterns of prokaryotes and protists in the water column

of anchialine pits and caves in the area of Kornati National Park, and III) diversity and activity patterns of prokaryotes together with their functional diversity in the water column of the anchialine speleological object in the Martinska area. The second chapter covers materials and methods used in the dissertation. The third chapter presents the results of the previously listed research areas in three subchapters. The fourth chapter constitutes a detailed discussion that brings together the results of this doctoral dissertation in the given research area. The main conclusions are given in the fifth chapter. At the very end, there is an overview of the literature sources used.

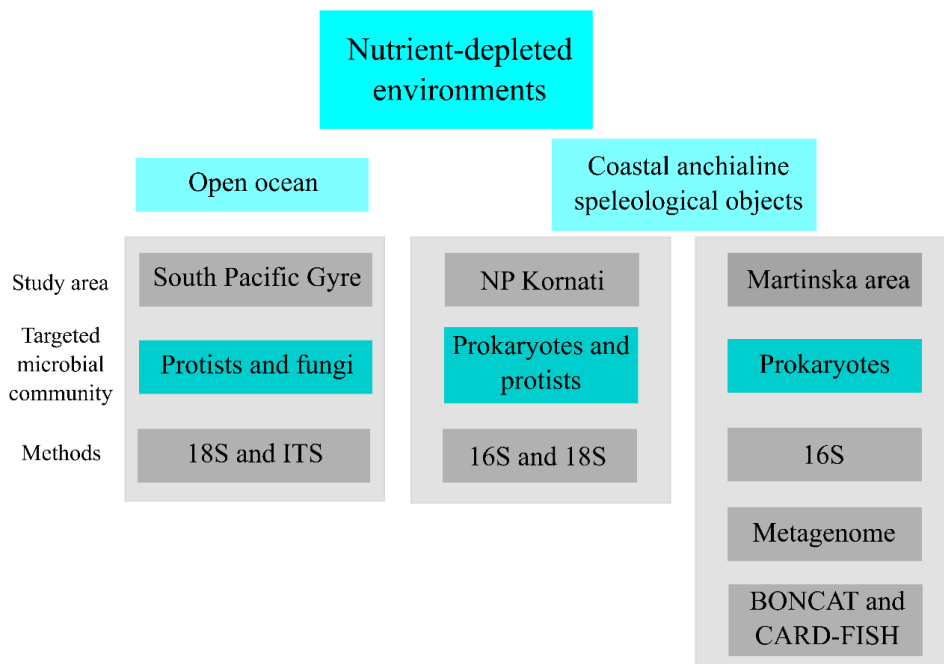


**Figure 1.** Schematic overview of dissertation structure.

The results presented in this dissertation under the second subchapter: II) *diversity patterns of prokaryotes and protists in the water column of anchialine pits and caves in the area of Kornati National Park* are published as: **Kajan K**, Cukrov N, Cukrov N, Bishop-Pierce R, Orlić S. Microeukaryotic and Prokaryotic Diversity of Anchialine Caves from Eastern Adriatic Sea Islands. *Microbial ecology* (Kajan et al., 2022)

## 2. MATERIALS AND METHODS

### 2.1. Study area: ultra-oligotrophic South Pacific Gyre

#### 2.1.1. Site description, sample collection and DNA extraction

Sampling was carried out at 15 stations along a transect from Antofagasta (Chile) to Wellington (New Zealand) during the R/V Sonne “UltraPac” cruise (SO245) in the austral summer from December 17, 2015 to January 28, 2016 (**Figure 2**). A transect along the South Pacific Ocean covered a length of 7,000 km and a depth of up to 5,000 km. A total of 152 samples were taken from multiple depths at 11 stations (five intermediate stations: 1, 3, 5, 7, 9; six main stations: 2, 4, 6, 8, 10, 12). Six sampling stations covered the central gyre region (stations 4 to 9), three sampling stations on the northern east side of the gyre (Southeast Pacific), and two stations in the Southwest Pacific. In total, eight water samples were taken throughout the water column on the intermediate stations in the range of 20 to 500 m, while 12 to 15 samples were on the main stations with a maximal depth of 50 to 100 m above the seafloor (Reintjes et al., 2016). In the gyre region at station 8 within the vertical profile of 300 m, the diurnal variation of the microbial community was evaluated. Water samples at nine depths were taken over 24 hours at four time points: 2 AM, 8 AM, 2 PM, and 9 PM. A total of 1-2 L of the water sample was filtered onto 47-mm polycarbonate filters (pore size 0.2  $\mu\text{m}$ ), which were stored at  $-80^{\circ}$  until DNA extraction.

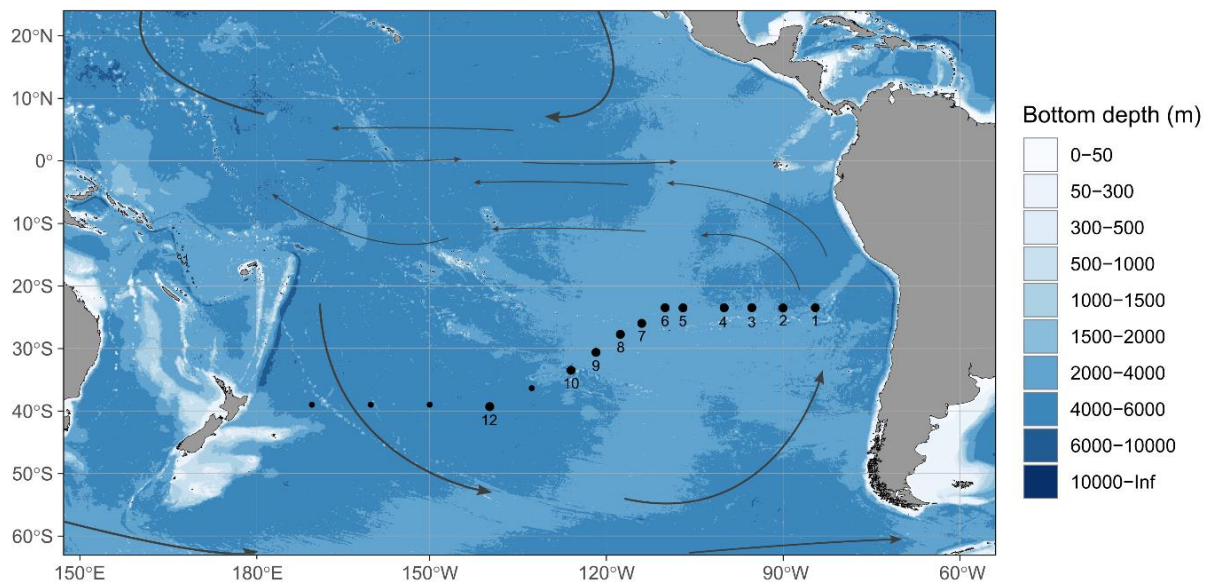


**Figure 2.** Map of sampling stations along the SO245 UltraPac transect. Black dots denote sampling stations; samples used in the following study were taken at the enumerated dots. Gray arrows show the main ocean currents.

### **2.1.2. Environmental measurements**

A Niskin rosette with a Seabird SBE 911+ CTD (Seabird Scientific, WA, USA) was used to collect samples and measure physicochemical parameters at 11 stations. Physical oceanography, oxygen, and nutrient data are available via the Pangea database (Ferdelman, 2019; Zielinski et al., 2018).

### **2.1.3. Amplicon sequencing and analysis**

The V4 region of the 18S rRNA gene was amplified with primers TAREuk454FWD1 and TAREukREV3 (Stoeck et al., 2010), and the ITS2 region of the fungal rRNA with primer pair ITS3-Mix1-Mix2, ITS3-mkmix2 and a reverse primer ITS4 (Tedersoo et al., 2015; Wurzbacher et al., 2017), using a unique dual barcoding two-step PCR approach (UDB-H12) as described by Pjevac et al. (2021). Amplicons were sequenced in paired-end mode (v3 chemistry, 2x 300 bp; Illumina, San Diego, CA, United States) on a MiSeq platform (Illumina, San Diego, CA, United States) at the Joint Microbiome Facility of the Medical University of Vienna and the University of Vienna. Sequence data were processed in R using DADA2 following the workflow by Callahan et al. (2016). Amplicon sequence variants (ASVs) were inferred across all samples in pooled mode. Further details on sequence trimming and settings for quality filtering are described in Pjevac et al. (2021). Taxonomic assignment was done by mapping 18S V4 ASV sequences against the PR2 reference database (v. 4.12.0; Guillou et al., 2013) and ITS ASV sequences against the UNITE reference database (v. 04.02.2020; Nilsson et al., 2019). The sequences assigned to protistan taxa with 18S V4 and fungal taxa with ITS2 were retained for further analysis. Furthermore, functional groups were identified according to the taxonomical classification of protistan ASVs as autotrophs, mixotrophs, parasites, osmotrophs, and phagotrophs. The functional assignment was determined based on Adl et al. (2019) and literature reviews (Reczuga et al., 2020; Suter et al., 2022). The identified fungal taxa were assigned to functional groups with the FUNGuild tool (Nguyen et al., 2016) into pathotrophs, saprotrophs, symbiotrophs, etc. ASVs that did not match any functional group in the database were categorized as ‘Unknown’.

### **2.1.4. Statistical analysis and data visualization**

All analyses and visualizations were performed using R v. 4.2.2 (R Core Team, 2020) in R studio using packages ‘phyloseq’ (McMurdie and Holmes, 2013), ‘tidyverse’ (Wickham et al., 2019), ‘vegan’ (Oksanen et al., 2020), ‘ggplot2’ (Wickham, 2016), ‘pheatmap’ (Kolde, 2012)

and 'ggVennDiagram' (Gao et al., 2021). Prior to analyses, the standardization method of the ASV tables was applied according to Gutiérrez-Rodríguez et al. (2022). Samples from diel sampling at station 8 with four time points (2 AM, 8 AM, 2 PM and 9 PM) were analyzed separately, including only samples taken at 2 PM to compare them with other stations.

Principal coordinate analysis (PCoA) was performed on the Bray-Curtis distance matrix at the ASV level. To evaluate compositional differences in microbial communities among the sampling station, depth, and radiation zone among the samples, a permutational multivariate analysis of variance (PERMANOVA) was performed using the function *adonis2* in package 'vegan', with 999 permutations. The distance-decay relationship was evaluated using linear regression by comparing the Bray-Curtis community distance matrix of protistan and fungal communities with geographic and environmental distance. The Mantel test was used to determine the driving environmental factors (Euclidean distance) on protistan and fungal community diversity based on the Bray-Curtis distance ('linkET' package).

The biodiversity ecological null model was used to evaluate processes driving protistan assembly (Stegen et al., 2013, 2015). Based on the standardized abundance ASV table and amplicon phylogenetic tree, the  $\beta$ -nearest taxon index ( $\beta$ NTI) of microbial communities was calculated. In order to test if there was a significant difference between molecular and phylogenetic turnover between the observed microbial assemblages, the  $\beta$ -mean nearest taxon index ( $\beta$ MNTD) was calculated. Further, the  $\beta$ NTI was calculated as the difference between the observed  $\beta$ MNTD and the null distribution. Deterministic processes (variable or homogeneous selection) dominated when  $\beta$ NTI is greater than 2 or less than -2. Values within the  $-2 < \beta$ NTI < 2 range indicate the dominance of stochastic processes (homogenizing dispersal or dispersal limitation) or random drift. Based on the abundance of microbial communities, the Raup-Crick (RC) beta diversity was calculated to distinguish stochastic processes. Assemblies were structured by dispersal limitation if RC >+0.95, homogenizing dispersal if RC <-0.95, or random processes acting alone to undominated if RC falls between -0.95 and +0.95.

## 2.2. Study area: anchialine pits and caves in the area of National Park Kornati

### 2.2.1. Site description, sample collection and DNA extraction

Sampling was conducted in National Park Kornati, situated in the eastern part of the Adriatic Sea, Croatia. Four anchialine speleological objects located on different islands: Vjetruša (VG), Blitvica (BP), Živa Voda (ZVP), and Gravnjača (GKV), were sampled in June 2016 during the expedition of the Croatian Biospeleological Society members (**Figure 3, Table 1**). The sampling depths were determined following the vertical salinity gradient. Within each anchialine speleological object, three water samples were collected, spanning the following areas: the region encompassing fresh to brackish surface water (above the halocline), the region within the halocline, and the seawater region (below the halocline). Water samples for molecular and chemical analysis were collected in bottles with a total of 2 L from progressively increasing depths to ensure the collection of undisturbed water (Humphreys et al., 1999). Water samples (1 L) were filtered on 0.2  $\mu\text{m}$  pore size polycarbonate filters. The extraction of total genomic DNA from filters was carried out using the DNeasy PowerWater kit (Qiagen GmbH Hilden, Germany), following the manufacturer's guidelines.



**Figure 3.** Location of anchialine speleological objects on the islands of National Park Kornati. Vjetruša (VG), Blitvica (BP), Gravnjača (GKV) and Živa Voda (ZVP).

**Table 1.** Location and characteristics of the sampled anchialine speleological objects.

	Vjetruša (island Guštac; VG)	Blitvica (island Piškera; BP)	Gravrnjača (island Kurba Vela; GKV)	Živa Voda (island Panitula Vela; ZVP)
Location	43°46'27.2"N 15°20'59.3"E	43°45'54.8"N 15°21'09.5"E	43°42'16.4"N 15°28'23.0"E	43°45'40.54"N 15°20'29.65"E
Distance from the coast (m)	120	100	30	50
Cave depth (m)	60	70	40	10
Water depth (m)	24	50	31	6

### 2.2.2. Environmental measurements

Salinity stratification in the anchialine water column was determined by an instant CTD probe (EXO2, YSI, USA), taken at each station before all other samples. Physical parameters (salinity, pH, dissolved oxygen (DO) and water temperature) were measured with depth *in situ* using diver-carried multiparameter data loggers Hach HQ40D Portable Multi-Parameter Meter (Hach Company, Loveland, CO, USA). Concentrations of total nitrogen (TN), ammonium with organic nitrogen ( $\text{N-NH}_4^+ + \text{Norg}$ ), nitrogen-nitrite ( $\text{N-NO}_2^-$ ), nitrogen-nitrate ( $\text{N-NO}_3^-$ ), orthophosphate ( $\text{PO}_4^{3-}$ ) and total dissolved carbon (TOC) were determined in collected water samples (300 mL). The concentrations of nutrients were measured on a Perkin Elmer Lambda 25 UV/Vis spectrometer. Nitrate, nitrite and ammonium were measured according to J. Z. Zhang and Fischer (2006) with method detection limits of  $0.5 \mu\text{mol L}^{-1}$ ,  $0.03 \mu\text{mol L}^{-1}$  and  $0.4 \mu\text{mol L}^{-1}$ , respectively, with overall precision  $\pm 10\%$ . Orthophosphate concentrations were analyzed according to ISO 6878:1998(E). The method is based on the formation of the phosphomolybdate complex, which is subsequently reduced with ascorbic acid to form a strongly colored blue molybdenum complex, and the absorbance is measured spectrometrically at 880 nm. Detection limits in orthophosphate analyses were  $0.04 \mu\text{mol L}^{-1}$  and  $0.15 \mu\text{mol L}^{-1}$ , respectively, while precision was typically better than  $\pm 10\%$ .

A sample aliquot was filtered on 25 mm glass filters (GFF, Whatman) using an all-glass filtering system (Wheaton) under vacuum to determine the total organic carbon content. All glass equipment (filter, tubes, filtering system) was calcined at  $450 \text{ }^\circ\text{C}$  for 4 h before use. The resulting dissolved fraction was stored in a 24 mL glass tube equipped with a teflon/silicone septum (Wheaton), poisoned with  $50 \mu\text{L}$  of  $1 \text{ mol L}^{-1} \text{ NaN}_3$  (Aldrich), and stored in the dark at  $4 \text{ }^\circ\text{C}$  until analysis. Filters were dried to constant weight at  $60 \text{ }^\circ\text{C}$  and then exposed to HCl fumes for 4 h to remove all inorganic carbon (Lorrain et al., 2003). The dissolved organic

carbon concentrations were determined using a Shimadzu TOC-VCSH analyzer and the high-temperature (680 °C) catalytic oxidation method with IR detection of CO<sub>2</sub> (Benner and Strom, 1993), and calibrated using potassium hydrogen phthalate (Fisher Scientific, Analytical Reagent grade; Louis et al., 2009). The particulate organic carbon concentration on the filters was determined using the same equipment via the Shimadzu SSM-5000 module, which uses catalytic oxidation at 950 °C and is calibrated using glucose (Fisher Scientific, Analytical Reagent grade). The sum of the DOC and the POC yielded the TOC content up to 10% accuracy. Precision was typically better than ±5%.

### 2.2.3. Amplicon sequencing and analysis

The hypervariable V9 region of the eukaryotic SSU rRNA gene was amplified using the primer pair 1391F (5'-GTACACACCGCCCGTC-3') and EukB (5'-TGATCCTTCTGCAGGTTACCTAC-3') following the protocol of Stoeck et al. (2010). For the prokaryotic dataset, the hypervariable V4 region of the 16S rRNA gene was amplified using primer pair 515F (5'-GTGCCAGCMGCCGCGGTAA-3') and 806R (5'-GGACTACHVHHHTWTCTAAT-3') (Caporaso et al., 2011). To minimize PCR-bias, three individual reactions per sample were prepared and pooled prior to sequencing. Paired-end sequencing of purified 18S V9 amplicons was conducted on an Illumina NextSeq platform generating 150-bp reads (SeqIT GmbH and Co. KG, Kaiserslautern, Germany). The prokaryotic reads were sequenced on an Illumina MiSeq platform generating 250-bp paired-end reads (MR DNA, Molecular Research LP, Shallowater, TX, USA).

Paired-end reads were quality-trimmed using the *bbduk* function and merged using the *bbmerge* function of the BBDMap package (v. 38.71; <https://sourceforge.net/projects/bbmap/>) and quality-filtered using the *split\_libraries.py* script implemented in QIIME v. 1.8.0 to remove low quality reads (Caporaso et al., 2010). Only reads with exact barcodes and primers, unambiguous nucleotides, and a minimum length of 90 (18S V9 region) and 250 (16S V4 region) base pairs were retained. Chimeric sequences, representing sequencing artifacts, were identified and removed using UCHIME (Edgar et al., 2011). Non-chimeric reads were clustered into Operational Taxonomic Units (OTUs) with SWARM (v. 3.0.0; Mahé et al., 2015) using  $d = 1$ , clustering amplicons using a local clustering threshold. Taxonomic assignment of 18S OTUs was done using *blastn* in BLAST (v. 2.9.0; Altschul et al., 1990) against the NCBI nucleotide database. Prokaryotic OTUs were blasted against the SILVA database (SILVA release 132; December 13, 2017). Nontarget OTUs (metazoans and embryophytes in the 18S dataset; chloroplasts in the 16S dataset), singletons, and doubletons were excluded. The resulting OTUs

were further filtered by the quality of the blast results ( $\geq 98\%$  identity). The taxonomic classification of the 18S dataset at the phylum level was further verified against the nomenclature available through Adl et al. (2019).

In order to minimize sequencing-related biases and facilitate sample comparisons, a standardization among samples was performed by randomly subsampling the table of OTUs to the minimum read level using the *rrarefy* function of the R package ‘vegan’ (Oksanen et al., 2020). The resulting tables were used as a basis for further statistical analyses.

#### **2.2.4. Statistical analysis and data visualization**

All statistical analyses were performed in the R environment (v. 4.0.4; R Core Team, 2020) and visualized using the ‘ggplot2’ package (Wickham, 2016). The alpha diversity was estimated as the OTU richness, Shannon-Wiener, and Simpson index for each microbial community (‘vegan’ package). Shared and unique OTUs of prokaryotic and protistan communities were distinguished through a Venn diagram (package ‘VennDiagram’; Chenn, 2018). Prior to beta diversity analysis, Hellinger transformation was applied to datasets of microbial communities. The similarity of the protistan and prokaryotic community between the anchialine speleological objects and the sampling depths were tested by principal coordinate analysis (PCoA) based on Bray-Curtis distance (package ‘ape’; Paradis and Schliep, 2019). Permutational multivariate analysis of variance (PERMANOVA) was used to test whether the partitioning of microbial communities was affected significantly by the anchialine speleological object or the sampling depth (package ‘vegan’). The function *envfit* of the package ‘vegan’ was applied to the results of PCoA to evaluate the correlations with environmental factors and the significance of regression by permutations test. A Co-Inertia Analysis (CIA) based on the PCoA results was used to assess the correlation of microbial communities using the ‘ade4’ package (Dray and Dufour, 2007). The significance of CIA results was evaluated using the Monte-Carlo test.

## 2.3. Study area: anchialine speleological object in the Martinska area

### 2.3.1. Site description, sample collection and DNA extraction

Preliminary research by members of the Croatian Biospeleological Society has determined the gradient of salinity and anoxia in the anchialine speleological object in the Martinska area (Sarcophagus cave (SC); cave in Čapljina). The anchialine speleological object is located in the karstic Upper Cretaceous (Senon) limestone with rare fragments of dolomite in the eastern coastal area of the Adriatic Sea near the Krka River estuary, Croatia (**Figure 4**). The carbonate rocks of the karst area contain channels and fissures porosity that store and transfer a significant amount of groundwater of different salinities (Bishop et al., 2015). The climate in this area is Mediterranean, with dry and hot summers and mild, rainy winters (Filipčić, 1998). The mean annual precipitation in 2021 at the Šibenik meteorological station was 748 mm (Croatian Meteorological and Hydrological Service, [www.meteo.hr](http://www.meteo.hr)).

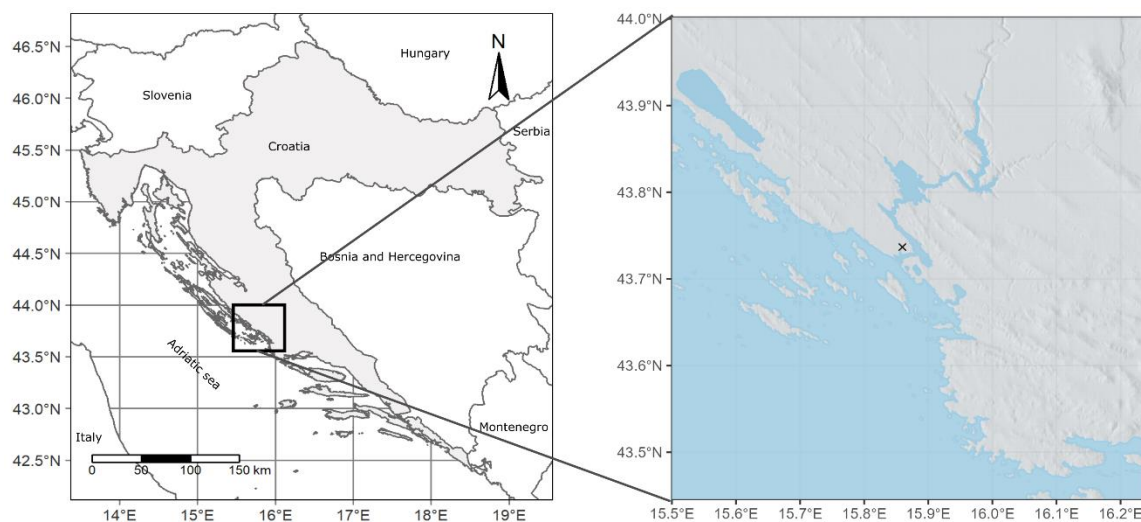


**Figure 4.** Sampling site area. The map displays the position of the explored speleological object passage. The study site (designated by x) is situated 580 m inland from the nearest coastline.

The investigated anchialine speleological object had no visible signs of direct or indirect anthropogenic influence; therefore, it is presumed to be a pristine habitat. However, a stone sarcophagus brought to the southeast of the entrance indicates that throughout history, the anchialine speleological object was used to feed livestock, most likely goats and sheep. The small vertical entrance shaft of the speleological object is located approximately 580 m from the estuary shore at an elevation of 5 m from the sea level (**Figure 4**). The total depth of the speleological object is approximately 18 m, with the vertical shaft channel measuring

approximately 8 m. This includes a dry part of 6 m and a submerged part of 2 m, variable due to tide variations. The known depth of the water body is around 12 m (**Figure 5**).

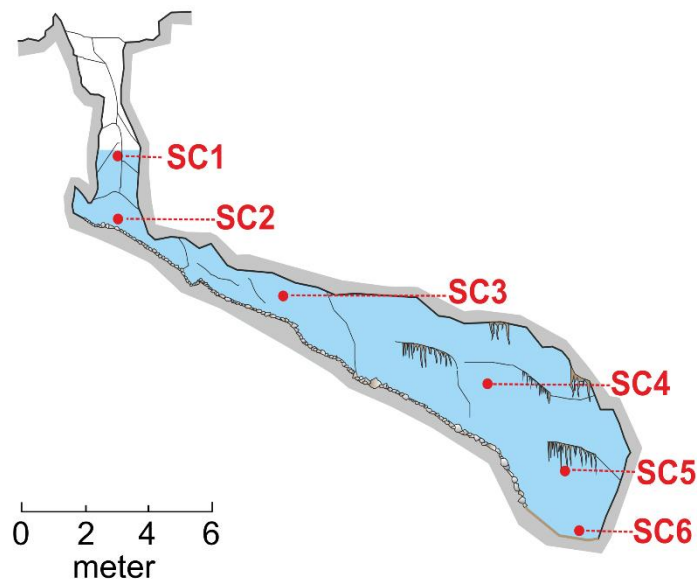


**Figure 5.** Topology of the anchialine speleological object in the Martinska area with a marked depth of samples taken in 2021. Adapted from the plan of Vedran Jalžić.

Water samples were collected at six depths along the salinity gradient at 0, 2, 4, 7, 10, and 12 m in March (17.03.), April (14.04.) and August (30.08.) in 2021 (**Figure 5**). Samples from the first two depths were collected using a Niskin bottle. A professional cave scuba diver collected samples from depths below 3 m into sterile polycarbonate bottles. For the March and April samplings, 2 L of water was collected from each depth, whereas for the August sampling, 5 L of water was collected from each depth in a Niskin bottle carried by the diver.

From each bottle, 50 mL of water sample was kept for CARD-FISH analysis. To perform BONCAT method in anoxic conditions, water samples were collected separately in glass vials of 65 mL (in April and August). Samples for chemical analysis were collected in acid-cleaned LDPE (Nalgene) bottles and stored at -20 °C until analysis, which was performed within one month.

To collect the biomass, water samples were filtered on 0.22 µm pore-size polycarbonate filters (Whatman Nuclepore Track-Etch Membrane, diam. 47 mm). Filtrates were used for chemical characterization, and filters were stored at -20 °C until further processing. Total genomic DNA from filters was extracted using the DNeasy PowerWater Kit (Qiagen, Inc., Valencia, CA, USA) following the manufacturer's instruction.

### 2.3.2. Environmental measurements

Physical parameters (temperature, salinity, conductivity, dissolved oxygen, pH, TDS and chlorophyll) were measured in situ along the depth using a diver-carried Multisensor CTD probe (EXO2, YSI, USA).

Concentrations of the cations ( $\text{Ca}^{2+}$ ,  $\text{Mg}^{2+}$ ,  $\text{Na}^{+}$ ), anions ( $\text{Cl}^{-}$ ,  $\text{SO}_4^{2-}$ ), and dissolved organic carbon (DOC) were determined in filtered water samples in the Hydrochemical Laboratory of the Croatian Geological Survey. The concentrations of cations and anions were measured on Dionex ICS-6000 DC (Thermo Fisher Scientific, Waltham, MA, USA). DOC was analyzed using the HACH QBD1200 analyzer (Lenntech, Delfgauw, Netherlands).

Nutrients were analyzed using a UV/Vis spectrophotometer (Specord 200 Plus, Analytikjena, Germany) in unfiltered samples according to Strickland and Parsons (1972) for the determination of ammonium ( $\text{NH}_4^{+}$ ), phosphate ( $\text{PO}_4^{3-}$ ), nitrite ( $\text{NO}_2^{-}$ ), and silicate ( $\text{SiO}_4^{4-}$ ). Nitrates ( $\text{NO}_3^{-}$ ) were analyzed according to the vanadium reduction protocol (Pai et al., 2021). Samples for reduced sulfur species (RSS) analysis were collected without exposure to oxygen and analyzed within 24 hours. The total reduced sulfur species (RSS<sub>tot</sub>) were analyzed by electrochemical methods at the hanging mercury electrode (663 VA Stand) connected to the potentiostat (PG STAT 128N, Methrom, Netherlands) as previously described (Bura-Nakić et al., 2009; Marguš et al., 2015). Briefly, RSS<sub>tot</sub> accumulation occurs at -0.2 V (vs. Aa/AgCl) on the Hg electrode surface and forms HgS. The reduction of the formed HgS occurs at -0.68 V (vs. Ag/AgCl) under the given experimental conditions when the potential of the Hg electrode is shifted to more negative values. The current of the detected peak is proportional to the concentration of RSS<sub>tot</sub>. To distinguish between volatile and non-volatile RSS, samples are acidified and purged with nitrogen. After restoring the pH, the samples are analyzed as described and the concentration of the non-volatile fraction (RSS<sub>nv</sub>) is determined.

### 2.3.3. Amplicon sequencing and analysis

A portion of the extracted DNA was used to amplify the hypervariable V4 region of the prokaryotic 16S rRNA gene using primer pair 515F (5'-GTGYCAGCMGCCGCGGTAA-3'; Parada et al., 2016) and 806R (5'-GGACTACNVGGGTWTCTAAT-3'; Apprill et al., 2015), modified with two 16 bp sequences which allow for sample barcoding in a second PCR step (Pjevac et al., 2021). As described in detail in Pjevac et al. (2021), samples were amplified, barcoded, purified, normalized, and prepared for sequencing on an Illumina MiSeq System in paired-end mode (v3 chemistry, 2x 300 bp; Illumina, San Diego, CA, United States) at the Joint

Microbiome Facility of the Medical University of Vienna and the University of Vienna. Sequence data were processed in R using DADA2 following the workflow by Callahan et al. (2016). Amplicon sequence variants (ASVs) were inferred across all samples in pooled mode. Further details on sequence trimming and settings for quality filtering are described in Pjevac et al. (2021). Taxonomic assignment was done by mapping 16S V4 ASV sequences against the SILVA SSU Ref NR 99 database (v. 138.1). The sequences assigned to prokaryotic taxa with 16S V4 region were kept for further analysis. Prior to analysis, chloroplast and mitochondrial sequences were removed and the ASV table was rarefied to the same total number of sequences (*rrarefy*; package ‘vegan’; Oksanen et al., 2020).

### **2.3.4. Incubation experiment – BONCAT and CARD-FISH**

Water samples collected for CARD-FISH (catalyzed reporter deposition - fluorescent *in situ* hybridization) were fixed with formaldehyde (2%; v/v) and filtered on 0.2  $\mu\text{m}$  Nuclepore TrackEtch polycarbonate membranes (Whatman, Maidstone, UK). Filters were air-dried and stored at  $-20\text{ }^{\circ}\text{C}$  until further analysis. The bioorthogonal noncanonical amino acid tagging (BONCAT) is increasingly used to monitor cellular activity in complex microbial communities (Hatzenpichler et al., 2014; Sebastián et al., 2019) and additional practical approach to the available molecular tools for analyzing microbial community function (Steward et al., 2020). By combining sequencing methods with quantitative CARD-FISH analysis, it is possible to obtain a detailed description of the community structure and determine the spatial and temporal changes in the community. BONCAT method was applied to water samples collected in glass vials with a total of 65 mL. To monitor microbial cell activity, L-Homopropargylglycine (HPG) was added to the samples with injection at a final concentration of  $50\text{ }\mu\text{mol L}^{-1}$ . All incubations were performed in the dark at  $15\text{ }^{\circ}\text{C}$ . The samples were removed from the incubator after 24 hours of incubation and fixed with paraformaldehyde at a final concentration of 3% (v/v) for 1 h, at room temperature, in the dark. Samples were then filtered onto a 0.2  $\mu\text{m}$  pore size filter Nuclepore TrackEtch polycarbonate membranes (Whatman, Maidstone, UK), examined under a microscope using 4',6-diamidino-2-phenylindole (DAPI) staining ( $10\text{ }\mu\text{g }\mu\text{L}^{-1}$ ), and filters were stored at  $-20\text{ }^{\circ}\text{C}$  until the click reaction was performed.

BONCAT was performed according to Hatzenpichler and Orphan (2015) and adjusted according to Kostešić et al. (2023). Briefly, filter pieces were placed sequentially in 50, 80, and 96% EtOH for 3 min to dehydrate and permeabilize the cells. For the Cu(I)-catalyzed click reaction, a dye premix was prepared to contain  $1.25\text{ }\mu\text{L}$  of a  $20\text{ mmol L}^{-1}$   $\text{CuSO}_4$  solution,  $1\text{ }\mu\text{L}$  of a  $2.5\text{ mmol L}^{-1}$  Cy5,5-alkyne dye, and  $2.5\text{ }\mu\text{L}$  of a  $50\text{ mmol L}^{-1}$  tris-

hydroxypropyltriazolylmethylamine (THPTA) chelating agent. While allowing the dye-premix to react, 12.5  $\mu\text{L}$  of each 100  $\text{mmol L}^{-1}$  sodium ascorbate and 100  $\text{mmol L}^{-1}$  aminoguanidine hydrochloride were added to 221  $\mu\text{L}$  phosphate buffered saline (PBS). After the dye-premix was mixed with the rest of the buffer, the filters were added directly to the click mix and incubated at room temperature in the dark for 1 hour. Filters were then washed 3 times in PBS for 3 minutes each, dehydrated in 50% EtOH for 3 minutes, and stored at  $-20\text{ }^{\circ}\text{C}$  until the CARD-FISH procedure.

CARD-FISH was performed according to Schmidt et al., (2012). Briefly, after the filters thawed, they were dehydrated in a series of EtOH and embedded in 0.1% low melting point agarose. Permeabilization was performed with a 10  $\text{mg mL}^{-1}$  lysozyme solution for 1 hour and 60  $\text{U mL}^{-1}$  achromopeptidase solution for 30 minutes, both at  $37\text{ }^{\circ}\text{C}$ , followed by incubation in 0.1  $\text{mol L}^{-1}$  HCl for 1 minute at room temperature. Inactivation of endogenous peroxidases was achieved by 3%  $\text{H}_2\text{O}_2$  treatment. Subsequently, 1.5  $\mu\text{L}$  of a 50  $\text{ng }\mu\text{L}^{-1}$  HRP-probe solution was added to 400  $\mu\text{L}$  of hybridization buffer of corresponding stringency. Filters were added directly to the solution and hybridized overnight at  $46\text{ }^{\circ}\text{C}$ . The tyramide signal was amplified by catalyzed reporter deposition (CARD; Kubota, 2013) to improve the detection of microorganisms. Prior to tyramide signal amplification, washing was performed in a washing buffer at  $48\text{ }^{\circ}\text{C}$  for 10 min in a water bath and in Triton-X-PBS for 5 min. Filters were placed in a mixture of 1 mL of amplification buffer and 2  $\mu\text{L}$  of tyramide solution (Alexa Fluor 488), incubated at  $46\text{ }^{\circ}\text{C}$  for 20 minutes, washed in Triton-X-PBS, MQ water, and absolute EtOH. After drying, filters were placed on the slide and embedded in Citifluor Vectashield DAPI solution (10  $\mu\text{g }\mu\text{L}^{-1}$ ). The oligonucleotide probe used for CARD-FISH was probe mixture EUBI-III targeting the majority of bacteria (**Table S1**; Amann et al., 1995; Daims et al., 1999). The NONEUB probe was used as a negative control for hybridizations.

### 2.3.5. Image processing and analysis

Images of the samples were acquired using a Zeiss Axio Imager.Z2 (Zeiss, Jena, Germany) fluorescence motorized microscope including the software package AxioVision (Zeiss, Jena, Germany) at a resolution of 1232 x 1028 pixels. For each sample, 4-10 fields of view and their overlay were acquired in each channel individually. After inspection of the samples on the microscope, cell density was performed using the *dai*me software (v. 2.2.3; Daims et al., 2006) and further calculated manually. Images were processed with 2D filter histogram stretching and noise reduction to remove any background noise before automatic segmentation in custom

mode within the range of 20 – 255 pixels. After carefully examining the segmentation, the CARD-FISH positive cells were determined against BONCAT positive ones and vice versa.

### 2.3.6. Metagenome sequencing, assembly and binning

Extracted DNA from the depth profile collected on August (30.08.2021) was used for metagenome sequencing (PE150) using Illumina - NovaSeq 6000 (Eurofins Genomics Europe Sequencing GmbH, Germany). Metagenomic reads were trimmed using *cutadapt* (v. 2.10; Martin, 2011). Trimmed reads were then assembled using *megahit* (v. 1.1.2; D. Li et al., 2015). Assembled contigs shorter than 1 kbp were removed using *seqtk* ([github.com/lh3/seqtk](https://github.com/lh3/seqtk)). To bin the assembled contigs, metagenomic reads were mapped to the assemblies using *minimap2* (v. 2.17; H. Li, 2018). The calculated read mappings were then converted using *samtools* (v. 1.11; H. Li et al., 2009) and binned using *MetaBAT2* (v. 2.15; Kang et al., 2019). All generated metagenomes were co-assembled and binned into combined Metagenome Assembled Genomes (MAGs) following the same method to improve the binning outcome.

Reconstructed MAGs were then quality-checked using *QUAST* (v. 5.0.2; Gurevich et al., 2013) and *CheckM* (v. 1.1.1; Parks et al., 2015). MAGs with completeness  $\geq 50\%$  and contamination  $\leq 10\%$  were used for further analysis. Taxonomic affiliation of these MAGs was then assigned using *GTDBtk* (v. 1.5.0; Chaumeil et al., 2020).

Genome abundance was calculated as the fraction of the total reads mapping to the contigs in a given bin. These counts were then normalized for the depth of the sequenced metagenomes. The threshold for cumulative abundance of MAGs was set at a minimum of 2 per depth.

### 2.3.7. Functional annotation

Gene prediction on good-quality MAGs was done using *Prodigal* (Hyatt et al., 2010) and initially annotated using *Prokka* (Seemann, 2014). Further functional annotation of the predicted proteins was done using *eggno-mapper* (v. 2.2.1) with the eggno-mapper\_5.0 database (Cantalapiedra et al., 2021; Huerta-Cepas et al., 2019). The eggno-mapper output was used to assign enzyme EC numbers, KEGG orthologs (Kyoto Encyclopedia of Genes and Genomes; KOs), Cazy annotations, pathways, and modules to the predicted genes. All annotations of key genes were further inspected and manually checked for their conserved domains using NLM's Conserved Domain Database (CDD) search (Lu et al., 2020). The KEGG database was used to assign pathways, brite, and modules of KOs (Kanehisa et al., 2023). MAGs were additionally functionally annotated using *Metabolic* (v. 4.0; Zhou et al., 2022) with default parameters. The

resulting figures including summary scheme of biogeochemical cycling processes at the total community scale in the anchialine speleological object were presented.

For each annotated KO within the MAGs, its cumulative abundance was assigned as MAGs abundance for each depth. The annotated KOs were further classified into two categories: prevalent and rare, based on the summation of their cumulative abundances across all depths. The KOs' cutoff point was determined based on the frequency histogram, resulting in a threshold of a cumulative abundance sum of 2000.

#### **2.3.8. Statistical analysis and data visualization**

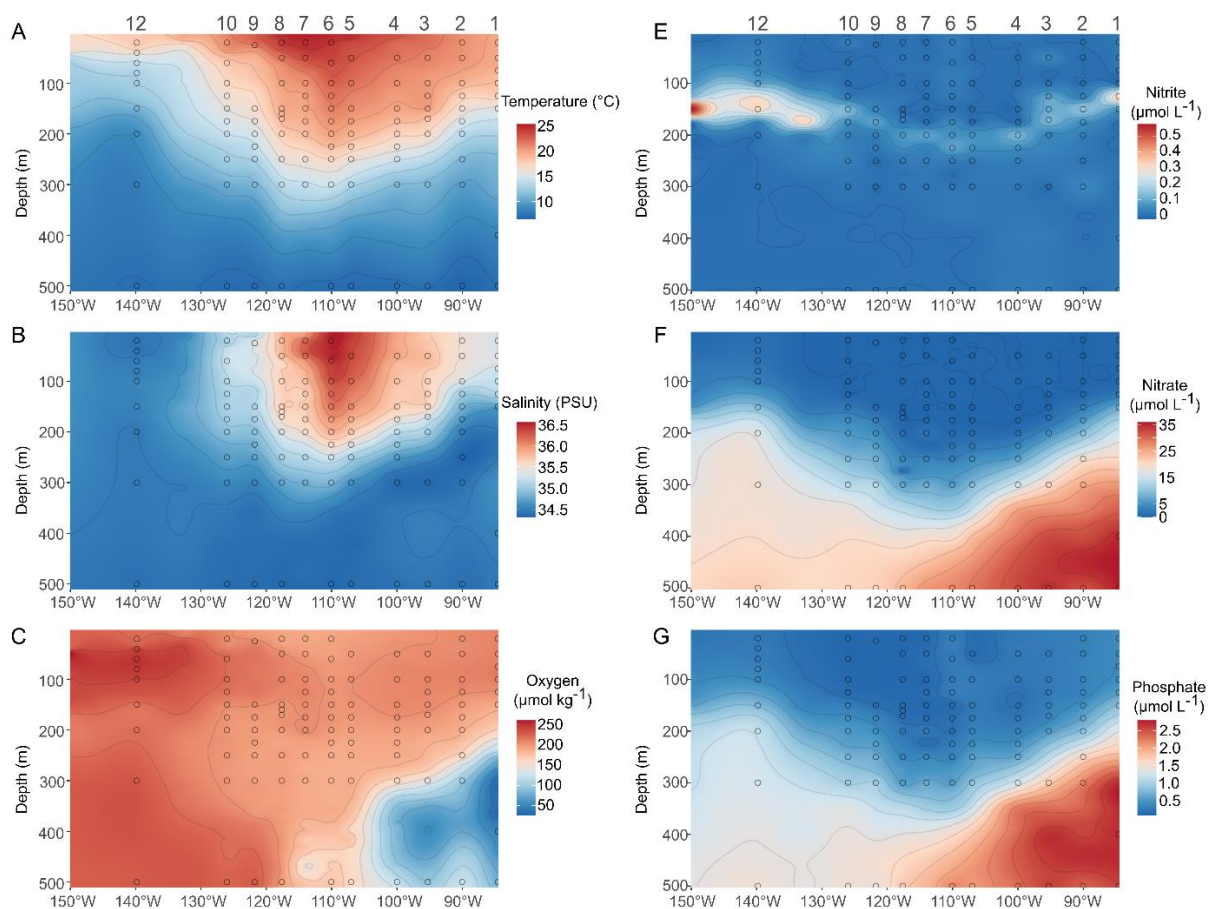
All statistical analysis and visualizations were done in the R environment (v. 4.1.2; R Core Team, 2020) using packages 'phyloseq' (McMurdie and Holmes, 2013), 'vegan' (Oksanen et al., 2020), 'dplyr' (Wickham et al., 2023), 'ggplot2' (Wickham, 2016), 'ggVennDiagram' (Gao et al., 2021) and 'Pheatmap' (Kolde, 2012). The principal coordinate analysis (PCoA) on presence/absence and abundance values was based on Jaccard distance.

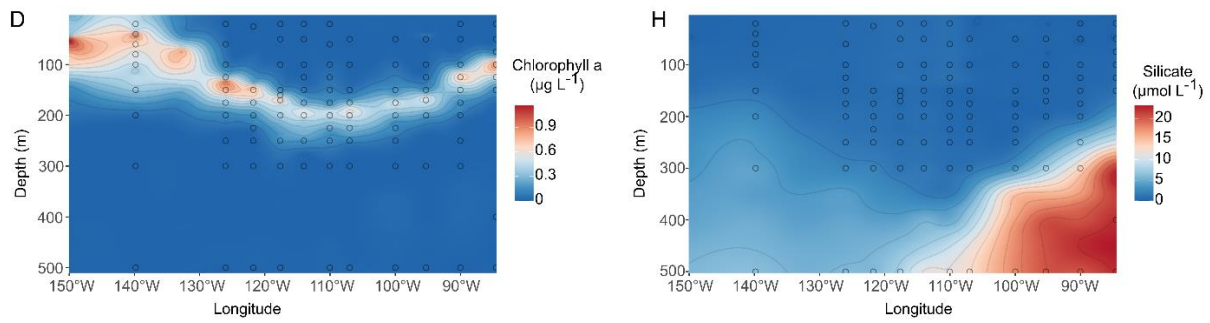
### 3. RESULTS

#### 3.1. Diversity patterns of protists and fungi in the water column of the ultra-oligotrophic South Pacific Gyre area

##### 3.1.1. Environmental characteristics of South Pacific Gyre

During the SO245 UltraPac cruise, the ship traversed through the oligotrophic region known as the "eye" of the Subtropical Pacific Gyre (SPG). The most significant variations in physicochemical conditions were observed within the top 500 meters of the SPG (**Figure 6**). In the central gyre region (stations 4 to 9; 100° W to 120° W), surface water temperatures were consistently high, ranging between 20 °C and 25 °C. Chlorophyll fluorescence measurements indicated extremely low levels of primary productivity in the surface waters down to a depth of 70 meters. At station 6 (110° W), located at the center of the gyre, the surface temperature peaked at 24.9 °C, gradually decreasing to 19.9 °C at a depth of 200 m. The deep chlorophyll maximum occurred between depths of 190 to 200 meters, with a fluorescence reading of 0.5  $\mu\text{g L}^{-1}$ .

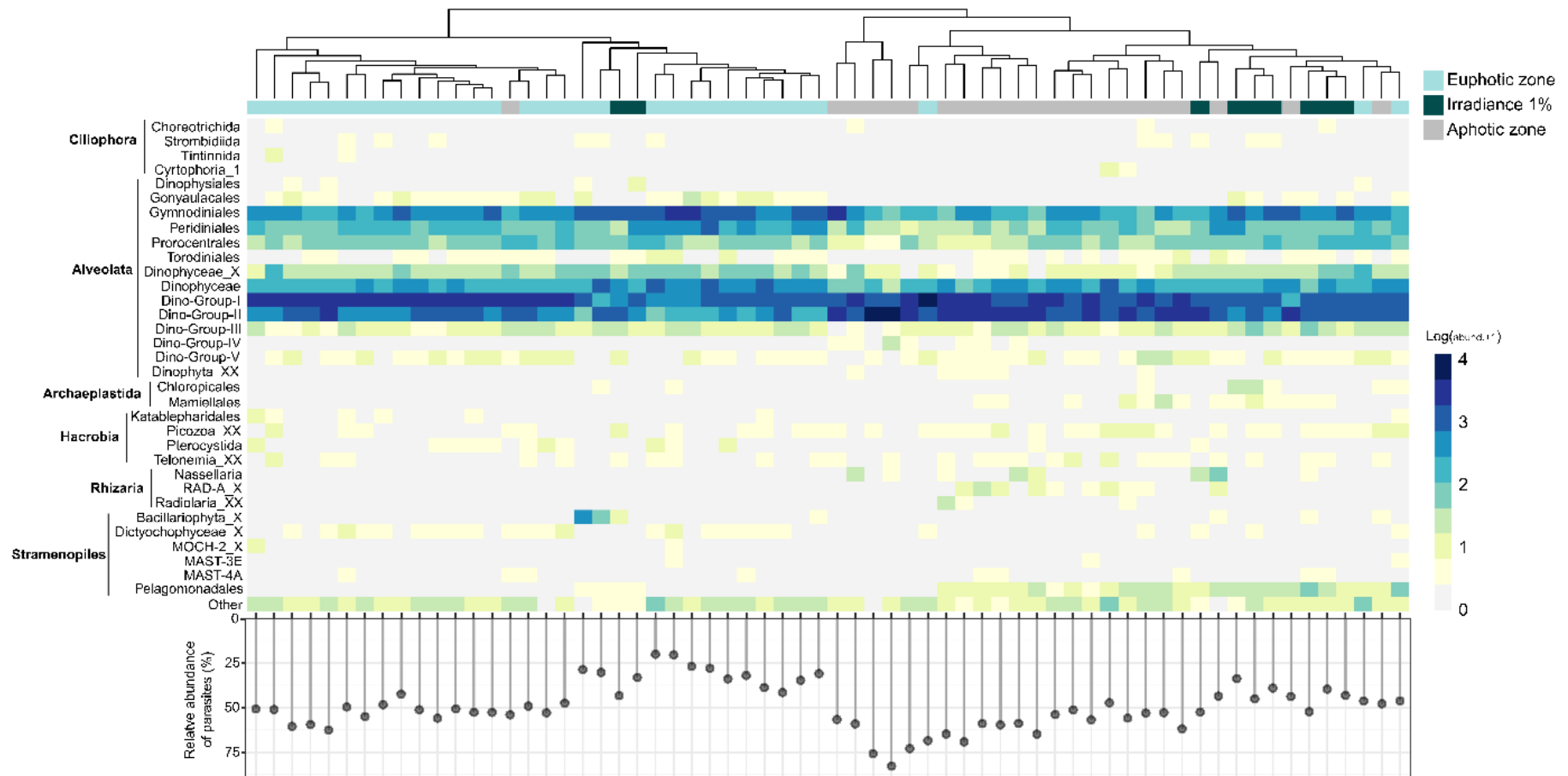




**Figure 6.** Distribution of physical and chemical parameters along the SO245 UltraPac transect. Transect distribution of (A) temperature, (B) salinity, (C) oxygen, (D) chlorophyll *a*, (E) nitrite, (F) nitrate, (G) phosphate, and (H) silicate concentration. Circles mark sampling and measurement depths.

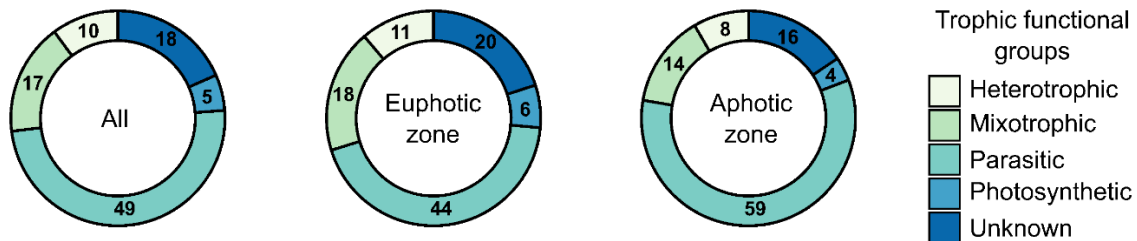
### 3.1.2. Community composition, diversity and assembly of protists along the SPG

Based on the 18S rRNA amplicon sequencing data analysis, the protists found at different depths and stations along the SPG were clustered into 1,288 ASVs. The final dataset included samples above 300 m (surface, DCM, and mesopelagic), along with samples collected during diel sampling at station 8 ( $n=84$ ). Remarkably, the relative read abundance of the protistan community at the supergroup level exhibited striking similarity across longitudinal scales of 5,500 km (**Figure S1**). Alveolata was found to dominate all analyzed samples, with an average relative read abundance of  $\sim 92 \pm 2\%$  of protistan community per sampling station (**Figure 7**). Other supergroups, such as Stramenopiles, did not exceed a relative read abundance of 18%. Within the Alveolata, the division Dinoflagellata contributed significantly to protist diversity, with 83% of assigned ASVs demonstrating relatively high phylogenetic diversity (total ASV  $n = 1,066$ ). The relative read abundances of Dinoflagellata showed a significant negative correlation with the abundance of Ciliophora and Chlorophyta ( $R=-0.48$ ,  $R=-0.54$ ,  $p<0.001$ ). These prevalent ASVs were taxonomically affiliated at the class level as Dinophyceae and parasitic Syndiniales, comprising 43% and 49% of the community, respectively (**Figure 7**). Dinophyceae were particularly abundant in the euphotic zone, exhibiting a negative correlation with depth (Pearson's correlation to depth,  $R=-0.63$ ,  $p<0.001$ ). In contrast, the relative read abundance of Syndiniales increased in the aphotic zone (Pearson's correlation to depth,  $R=0.62$ ,  $p<0.001$ ). These depth-related patterns were further supported by clustering the relative read abundance of the protistan community at the order level based on the different radiance zones (PERMANOVA,  $R^2=0.280$ ,  $p=0.001$ ; **Figure 7**).



**Figure 7.** Partitioning of protistan major taxonomic groups by radiance zone in South Pacific Gyre. Heatmap of relative read abundance of protistan community at the order level (orders with relative read abundance >1%). Columns were clustered based on Bray-Curtis distance with the top row colored by radiance zone. Abundances were log-transformed. Below the heatmap, the plot shows the relative read abundance of parasitic protists in clustered samples.

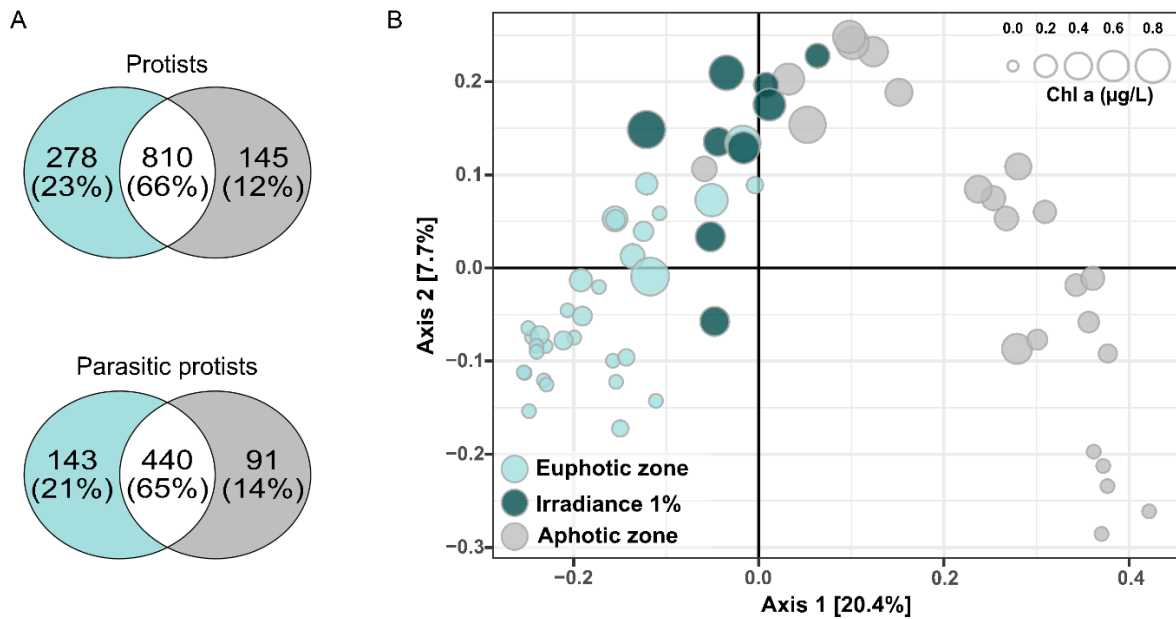
On average, the protistan community accounted for 49% parasitic, 17% mixotrophic, 10% heterotrophic, and 5% photosynthetic protists in terms of functional groups (**Figure 8**). Approximately 18% of the community had unknown functions, primarily assigned to the order Dinophyceae.



**Figure 8.** The average relative read abundance of protistan trophic functional groups in all samples, euphotic and aphotic zone.

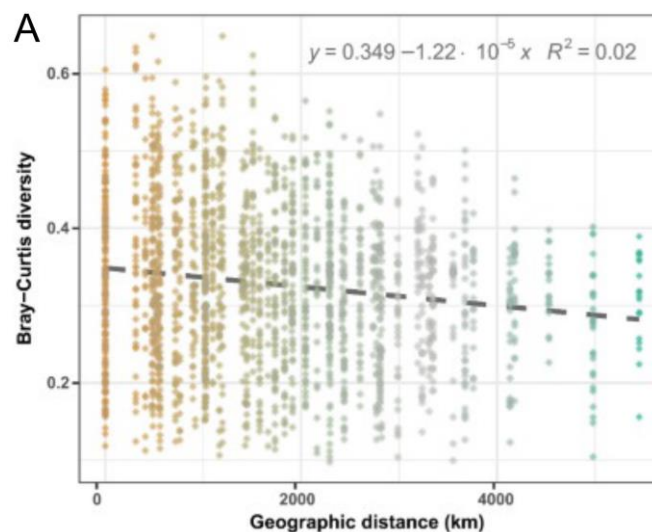
Among the parasitic protists, 66% of the ASVs were found in both the euphotic and aphotic zone (**Figure 9A**). However, a two-sample t-test revealed a significant difference in the relative read abundance of parasitic protists between the two zones (t-test,  $df=51.6$ ,  $p\text{-value} < 0.001$ ). The parasitic protists were represented by 667 ASVs assigned to the class Syndiniales, accounting for over 98% of total parasitic protists. Syndiniales encompassed five main groups at the order level: Dino-Groups I, II, III, IV, and V. The most abundant genera belonged to Dino-Groups I and II, exhibiting vertical variability along the depth profile and displaying consistent patterns among different sampling stations. In contrast, Dinophyceae had two-fold less ASVs and a lower contribution of highly dominant genera to the overall protistan community. At the order level, the most abundant were Gymnodiniales (15%), Peridinales (7%) and Procentrales (5%) (**Figure 7**).

Additionally, the PCoA conducted at the ASV level demonstrated that the entire protistan community inhabiting the SPG primarily clustered based on sampling depth, exhibiting a distinct separation between the euphotic and aphotic zone (**Figure 9B**). This result was further supported by PERMANOVA analysis, where sampling depth accounted for 42% of the variation of ASV composition, while the radiance zone and sampling station contributed 19% each (**Table S2**). Notably, similar to the overall protistan community, the differences in sampling depth had a more pronounced impact on the structure of parasitic protists compared to zonal differences, confirming the significant influence of marine vertical stratification on the overall composition of the protistan community.



**Figure 9.** (A) Number of unique, shared and ubiquitous ASVs of all protists and parasitic protists across the photic and aphotic zone. Color-coded categories by radiance zone (photic and aphotic zone). Color-coded categories of radiance zone (photic and aphotic zone). (B) PCoA of protistan community diversity color-coded by radiance zones, including irradiance zone of 1%. Each point represents an individual sample, and the size of the circle indicates the chlorophyll *a* concentration.

The distance decay model was applied to identify the factors influencing the protistan diversity. The analysis revealed a significant similarity decline within the entire protistan and parasitic community as geographic distance increased ( $R^2=0.019$ ,  $p<0.001$ , **Figure 10A**;  $R^2=0.036$ ,  $p<0.001$ ). Furthermore, linear regression models demonstrated that environmental differences had a more substantial impact on the diversity of the entire and parasitic protistan community compared to geographical distance ( $R^2=0.313$ ,  $p<0.001$ ;  $R^2=0.194$ ,  $p<0.001$ ).



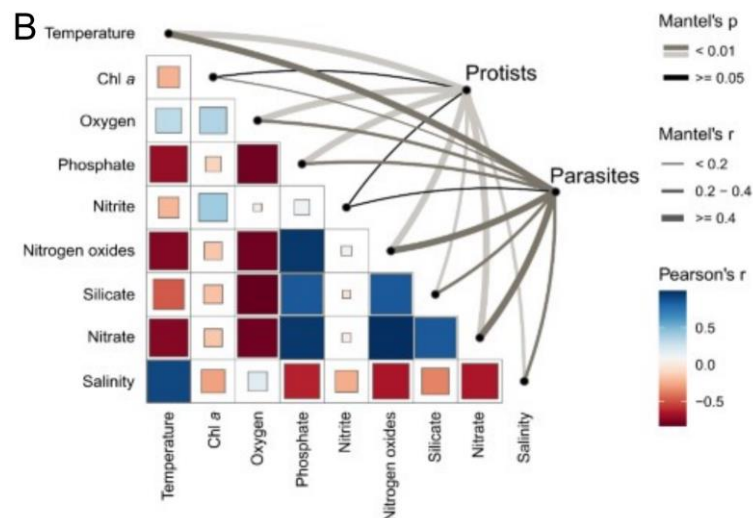


**Figure 10.** Factors driving variations of the protistan community. (A) Distance-decay relationship of Bray-Curtis and geographical distance (km) between sampling stations of the protistan community at the ASV level ( $p < 0.001$ ). The line represents a linear regression. (B) Mantel test correlation plot of protists and parasitic protists with environmental variables based on the Bray-Curtis distance.

The Mantel analysis was performed with various environmental factors to elucidate further the environmental drivers of protistan variation (Figure 10B, Table S3). Results showed that the entire protistan community was significantly affected by temperature, salinity, oxygen and nutrient concentrations, while the parasitic community additionally included chlorophyll *a* concentration.

Whether the interplay of assembly processes governing the protistan community turnover varies in the euphotic and aphotic zone, the null model was applied. The ecological processes across both zones of the SPG were dominated by dispersal limitation together with a higher influence of homogenizing dispersal and homogeneous selection in the euphotic zone (Figure 11). A significant proportion of the processes were undominated (51-63%).

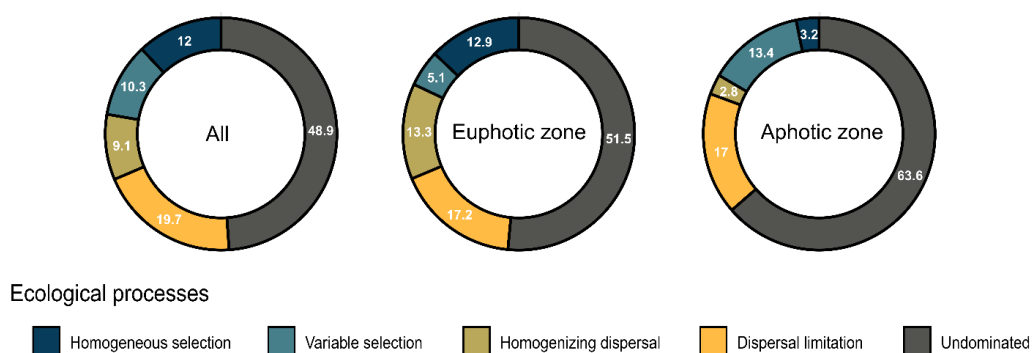


**Figure 11.**  $\beta$ NTI and relative importance of ecological processes driving the protistan assembly in SPG across entire, euphotic and aphotic zone.

Evaluating the diel variation of protistan community within the vertical profile of 300 m at the oligotrophic station (Station 8), the results have shown that samples collected at the same depth at different time points still have similar diversity while also showing the difference in radiance zones (PERMANOVA, **Table S4**). The overall protistan community was predominantly composed of Dinoflagellata across all samples and showed a significant negative correlation with the abundance of Metazoa (**Figure S2**; Pearson's correlation  $R=-0.99$ ,  $p<0.001$ ). To further distinguish vertical distribution and diel patterns, the average diversity of the protistan community at the order level was assessed (**Figure 12**).

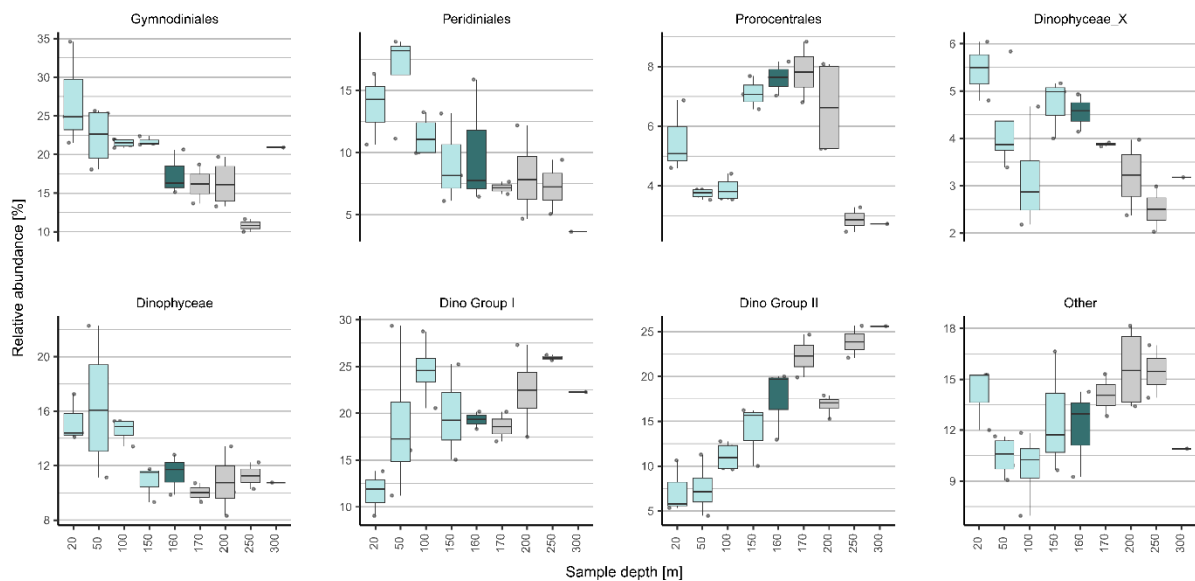


**Figure 12.** Diel variation in the relative read abundance of protistan community at order level at sampling station 8. Boxplots represent the 1st and 3rd quartiles, the line represents the median, and the points are the established data. Boxplots are color-coded by radiance zone (photic, irradiance 1% and aphotic zone). Orders with relative read abundance  $<2\%$  were aggregated into the group reported as ‘Other’.

A high negative correlation was shown between the read abundance of Syndiniales and Dinophyceae (Pearson's correlation  $R=-0.97$ ,  $p<0.001$ ). At station 8, Syndiniales were highly represented by Dino-Group I and Dino-Group II. Within Dino-group I, clades 1 and 5 accounted for higher proportions than others, while clades 10 and 11, and 22 were the predominant clades in Dino-Group II. The relative read abundance of Dino-Group II exhibited a sharp increase in depth (Pearson's correlation  $R=0.88$ ,  $p<0.001$ ). Dinophyceae were highly represented with Gymnodiniales and Peridinales with the highest abundance at the surface. The trophic strategies exhibited contrasting distribution in diel depth variation (**Figure 13**). The abundance

of heterotrophic, mixotrophic and photosynthetic protists reached the maximum in the euphotic zone, while parasitic communities in the aphotic zone.

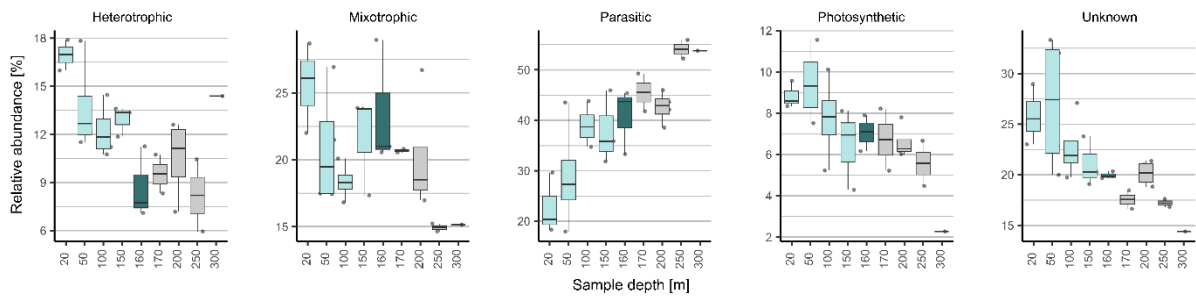


**Figure 13.** Diel variation in the relative read abundance of protistan trophic functional groups at sampling station 8. Boxplots represent the 1st and 3rd quartiles, the line represents the median, and the points are the established data. Boxplots are color-coded by radiance zone (photic, irradiance 1% and aphotic zone).

### 3.1.3. Community composition and diversity of fungi along the SPG

Based on the ITS2 region, the relative abundance of Fungi was comparatively low in contrast to the abundance of unidentified, unclassified and Metazoans in all samples, except for station 6 (**Figure S3**). At station 6, the relative abundance of Fungi exceeded over 75% with vertical distribution across the mesopelagic and bathypelagic zone (**Figure 14**). For further analyses of fungal community, a dataset comprising 51 samples and 69 ASVs was used (constitutes 62% of total ASVs assigned to Fungi).

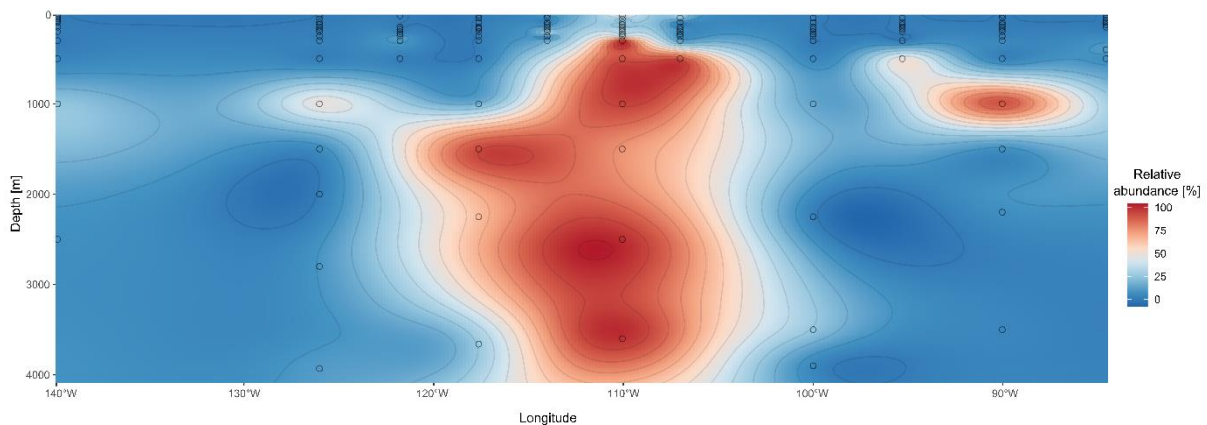


**Figure 14.** Relative abundance of Fungi based on the total ITS relative abundance.

The main phyla contributing to the fungal diversity of the SPG were Ascomycota, Basidiomycota and Mortierellomycota with 20, 47 and 2 ASVs, respectively (**Figure 15**). Basidiomycota exhibited high relative abundances in most samples, while Ascomycota had

higher dominance at sampling stations 7, 8, 10 and 12. In contrast to the majority of samples, the fungal community in the central part of SPG (station 6) was present in all depths dominated by the taxon *Rhodotorula* (Microbotryomycetes). A considerable fraction of the phylotypes assigned using FUNguild were classified as phototrophs, while 37% of ASVs represented saprotrophs, symbiotrophs (**Figure S4**).

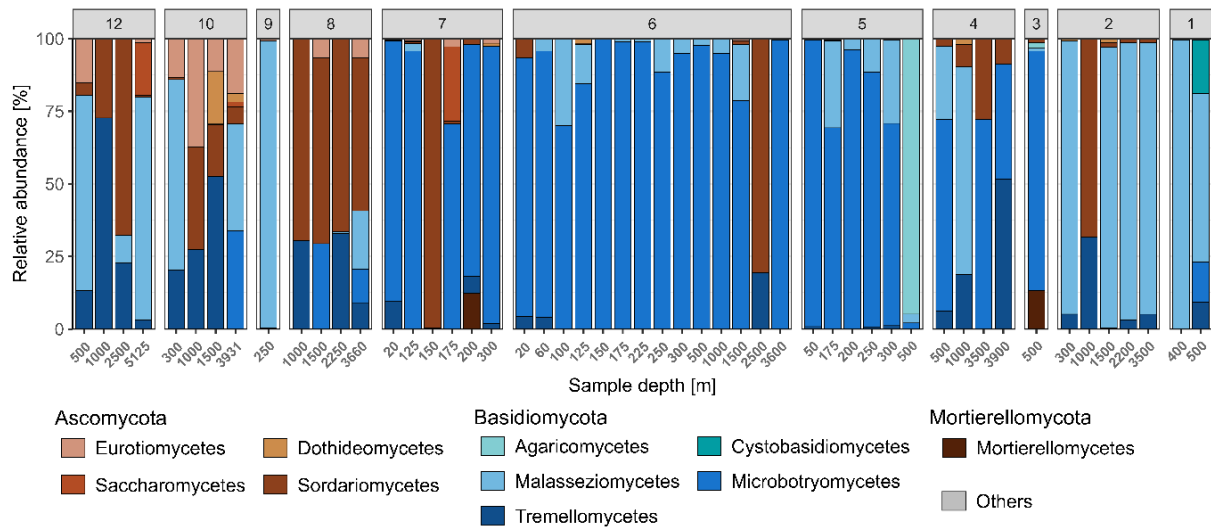


**Figure 15.** Relative abundance of fungal classes per depth and sampling station. Classes with relative abundance <1% were aggregated into the group reported as ‘Others’.

In contrast to the protistan community, PCoA analysis showed that the fungal community along the SPG primarily clustered based on the sampling station and pelagic zones (**Figure 16, Table S5**).

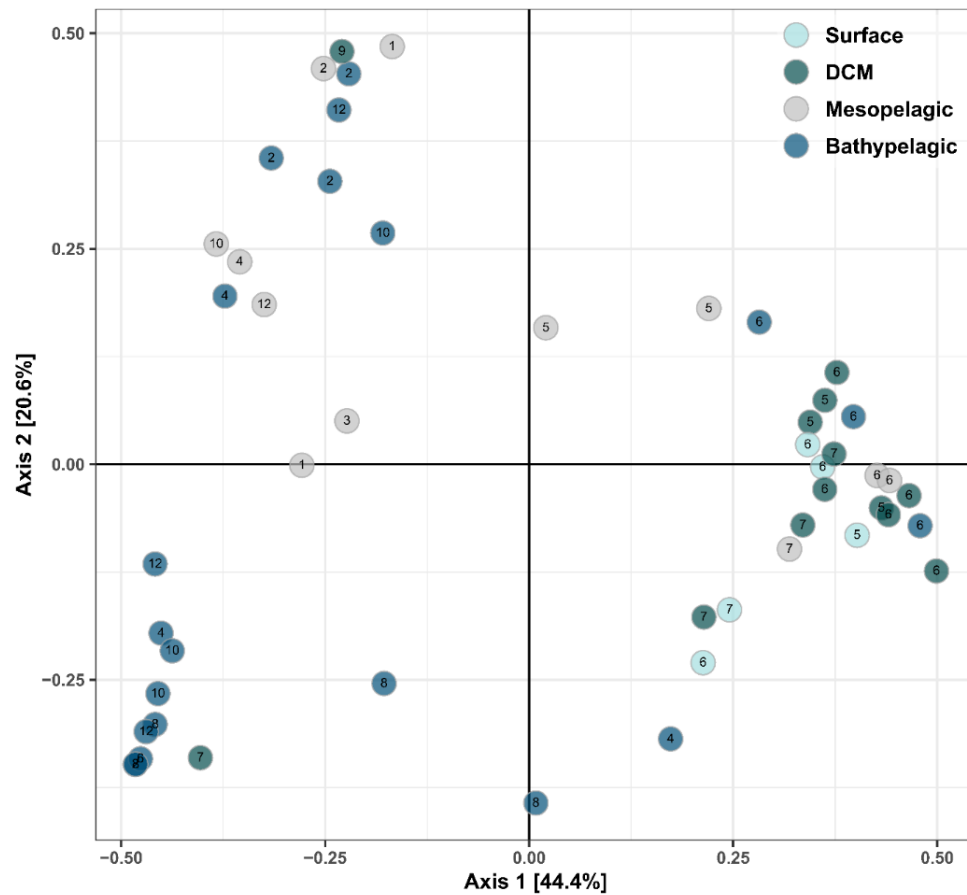


**Figure 16.** PCoA of fungal community diversity color-coded by pelagic zones and number coded by the station. Pelagic zones: epipelagic (surface: 20 - 80 m, DCM: 100 - 250 m), mesopelagic: 300 - 500 m, and bathypelagic: 1,000 – 5,125 m.

The station-to-station diversity was confirmed with a higher distance decay relationship of fungal diversity and geographical distance in comparison to the protistan community ( $R^2=0.166$ ,  $p<0.001$ ; **Figure 17A**). Conversely, the linear regression model demonstrated low environmental differences contributing to fungal diversity ( $R^2=0.018$ ,  $p<0.001$ ). Nevertheless, parameters such as oxygen, nitrates, phosphates and temperature, unlike salinity and chlorophyll a, strongly affected the fungal diversity (**Figure 17B**, **Table S6**).

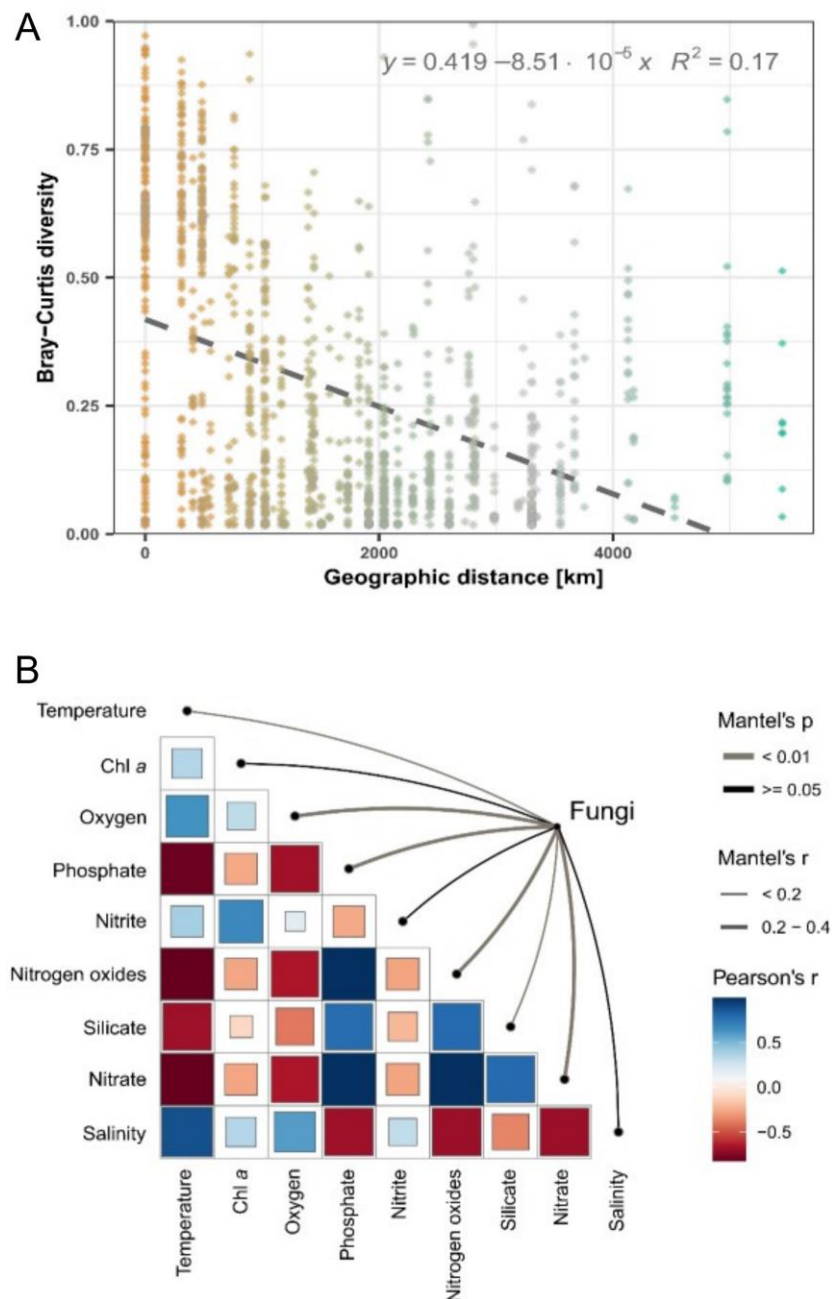


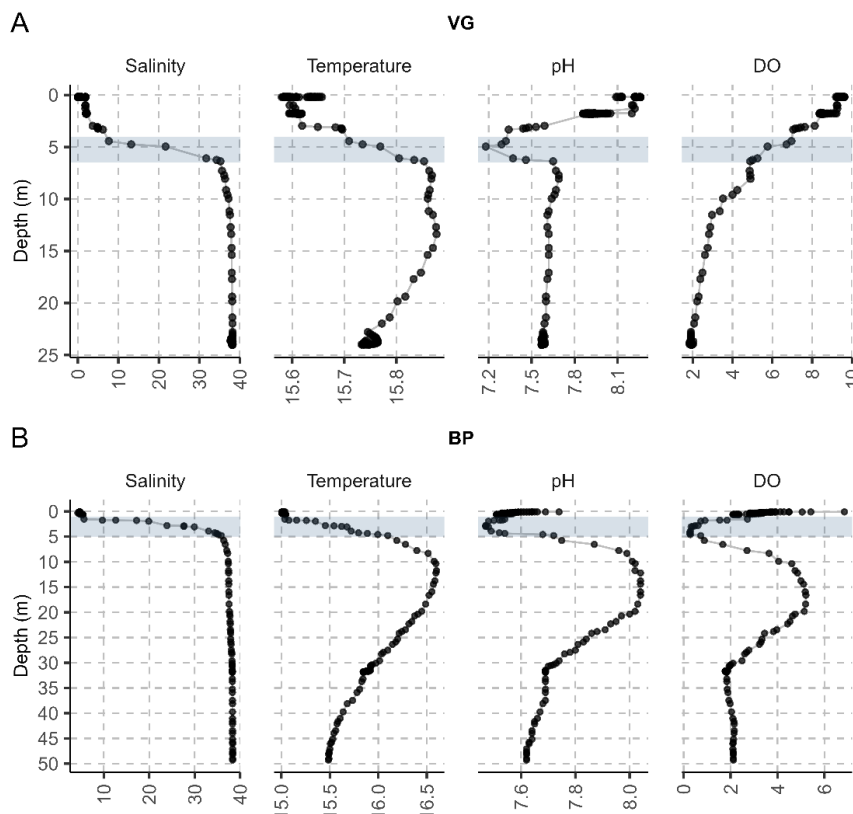
**Figure 17.** Factors driving variations of the fungal community. **(A)** Distance-decay relationship of Bray-Curtis and geographical distance (km) between sampling stations of fungal community at the ASV level ( $p < 0.001$ ). The line represents a linear regression. **(B)** Mantel test correlation plot of fungi with environmental variables based on the Bray-Curtis distance.

Further analysis of fungal diversity and environmental parameters at station 6 revealed no significant correlations. Due to the relatively low abundance of fungal ASVs, the diel variation of the community based on the ITS2 region was not further analyzed (**Figure S5**).

## 3.2. Diversity patterns of prokaryotes and protists in the water column of anchialine pits and caves in the area of National Park Kornati

### 3.2.1. Environmental characteristics of anchialine water columns

During the sampling, the water in all speleological objects was heavily stratified due to a strong salinity gradient (**Figure 18**). Salinity varied from an average of 3.98 ‰ at the surface (min. 1.88 ‰ in Vjetruša (VG), 5.93 ‰ max. in Gravrnjača (GKV)) and 37.87 ‰ in the bottom layer of the anchialine speleological object (min. 36.65 ‰ in Živa Voda (ZVP), 38.34 ‰ max. in Blitvica (BP)). A well-defined halocline was detected in all objects at a depth of approximately 3 m (min. 2.2 m (ZVP), max. 3.8 m (BP)). In contrast to salinity, temperature and pH varied in smaller intervals ( $16.03 \pm 0.53$  °C;  $\text{pH } 7.77 \pm 0.22$ ). In VG and ZVP speleological objects, pH and temperature decreased with depth, while in BP and GKV, the highest pH values were recorded directly below the halocline. DO steadily decreased with depth from normoxic to hypoxic condition in all speleological objects except BP. A decrease of DO was recorded in the halocline area of BP anchialine speleological object with a subsequent rapid increase below the halocline, reaching a maximum at ~16 m ( $0.29$ - $5.21$  mg L<sup>-1</sup>). The highest TN at the surface was measured in VG anchialine speleological object ( $7$  mg L<sup>-1</sup>) and the lowest in BP ( $0.39$  mg L<sup>-1</sup>; **Table S7**). The lowest TOC amounts were detected below the halocline in all anchialine speleological objects ( $0.56 \pm 0.21$  mg L<sup>-1</sup>).



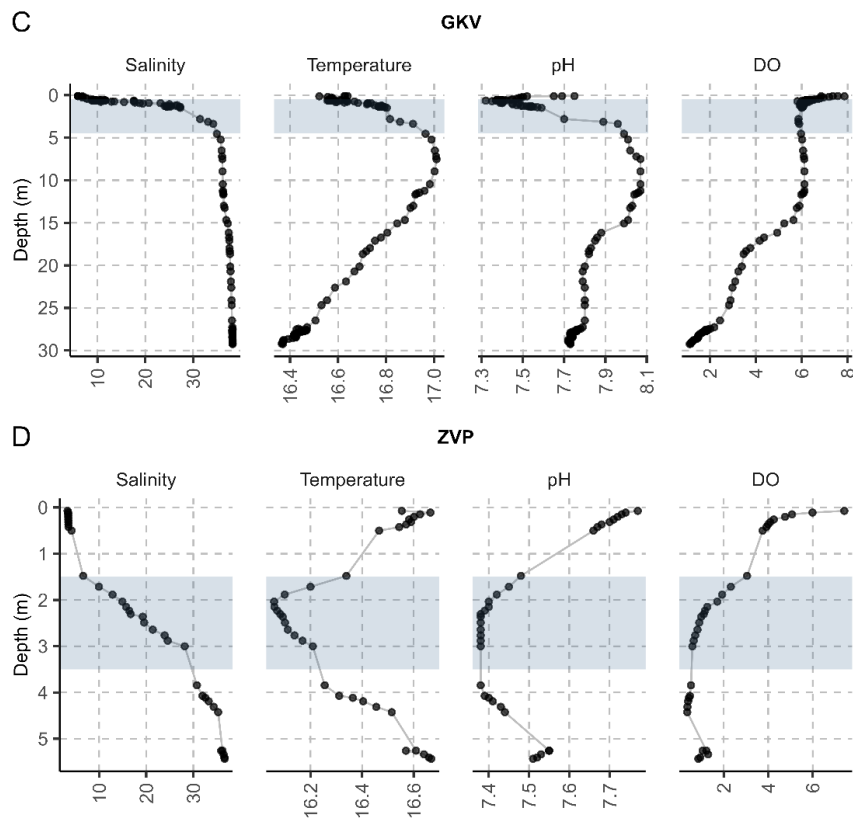


**Figure 18.** Hydrographical profile in a depth profile of anchialine speleological objects in June 2016. (A) Vjetruša (VG), (B) Blitvica (BP), (C) Gravnjača (GKV) and (D) Živa Voda (ZVP). From left to right: salinity (‰), temperature (°C), pH and dissolved oxygen (DO; mg L<sup>-1</sup>). Blue-colored rectangles highlight the halocline area.

### 3.2.2. Taxonomic composition and diversity of the prokaryotic community

Sequencing of V4 SSU rRNA resulted in a total of 1,992,407 reads of which 1,271,717 reads were clustered and classified into 12,088 target prokaryotic Operational Taxonomic Units (OTUs). The lowest number of target reads was recorded above the halocline in BP anchialine speleological object (n= 36,528) followed by the sample below the halocline of VG anchialine speleological object (n=46,722). In contrast to BP anchialine speleological object, the sample above the halocline in GKV anchialine speleological object was presented with the highest number of reads (n= 222,403), while below the halocline with the highest number of OTUs (n= 2,974). The prokaryotic community richness showed a similar pattern in both the VG and BP anchialine speleological object with the highest richness recorded in the halocline, while in the ZVP anchialine speleological object, the greatest richness was recorded below the halocline (n= 3,033; **Figure S6**). Shannon-Wiener index showed the highest diversity in samples below the halocline in anchialine speleological objects GKV (5.7) and BP (5.9), while in anchialine speleological object VG the highest diversity was recorded in halocline (5.3).

Altogether, 68 prokaryotic phyla were detected, from which nine were archaeal. The most abundant prokaryotes in all four anchialine speleological objects were affiliated with the phyla Proteobacteria, with the highest average of Gammaproteobacteria (22.9%), followed by Alphaproteobacteria (15.1%) and Deltaproteobacteria (4.3%; **Figure 19**). VG, BP and ZVP anchialine speleological object, on average, were dominated by Gammaproteobacteria (24%, 19.5%, 22.4%), respectively, while GKV anchialine speleological object was dominated by Alphaproteobacteria (27.8%), followed by Gammaproteobacteria (25.7%).

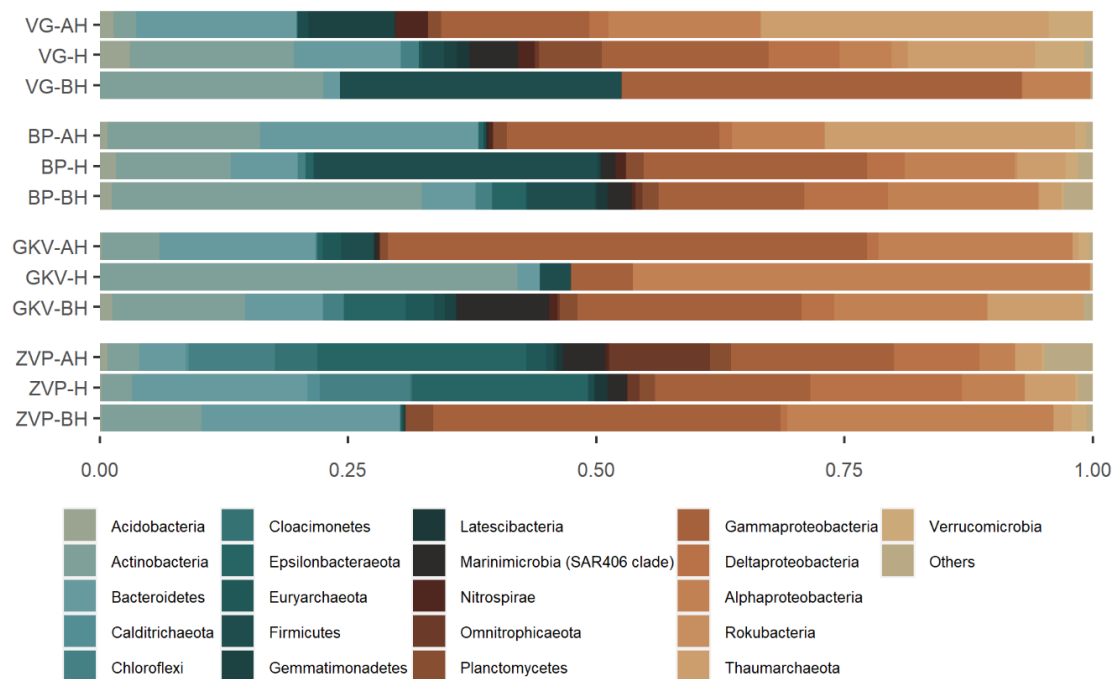


**Figure 19.** Taxonomic composition of the prokaryotic community in anchialine speleological objects based on the relative abundance of the most abundant phylum or classes (for Proteobacteria) ( $\geq 0.01$ ). Phyla with relative abundance  $< 0.01$  were aggregated into the group reported as ‘Others’. Above halocline (AH), halocline (H) and below halocline (BH).

Archaea were numerous in anchialine speleological object VG and BP in the surface area above the halocline with Thaumarchaeota (29%, 25.2%), of which in total Nitrososphaeria contributed (29%, 25.2%). The bacterial community of the VG also consisted of Bacteroidetes and Gemmatimonades with the contribution above and in the area of the halocline, and Actinobacteria and Firmicutes with the highest contribution below the halocline (22.4%, 28.3%). Actinobacteria were also present, with the highest amount below the halocline in BP (22.5%) and at the halocline in the GKV (42%). A higher amount of Epsilonbacteraeota was recorded in the ZVP anchialine speleological object in the halocline area and below (17.7%, 21.1%), while Bacteroides were recorded above and in the area of the halocline (20%, 17.6%).

The halocline in GKV anchialine speleological object was dominated by Actinobacteria (42%) with the clade PeM15 (39.1%). Based on the genus level, the prokaryotic community was dominant with the highest contribution of Gammaproteobacteria, Bacteroidetes, Alphaproteobacteria and Actinobacteria (**Figure 20**). The prokaryotic community shared only 2% of the target prokaryotic OTUs between anchialine speleological objects, showing a high contribution of unique OTUs in BP, GKV and ZVP, respectively (**Figure S7**).

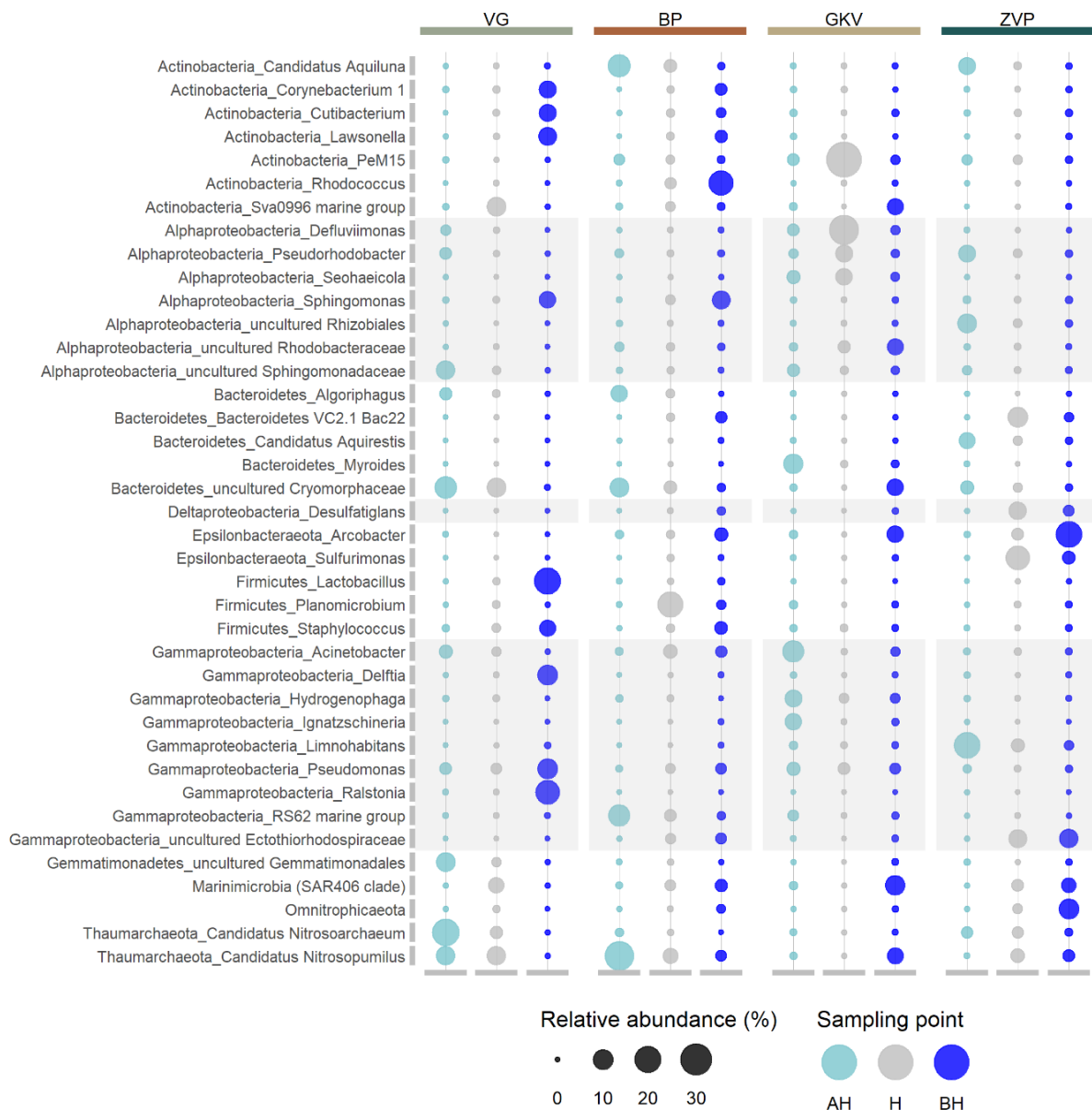


**Figure 20.** Prokaryotic community at the genus level with the relative abundance  $\geq 5\%$  in at least one sample. The bubble size represents the relative abundance of the genera, and the color represents the sampling point (above halocline (AH), halocline (H) and below halocline (BH)). Gray-colored rectangles highlight the genera of Proteobacteria.

### 3.2.3. Taxonomic composition and diversity of the protistan and fungal community

Illumina-sequencing of three depths within the four anchialine speleological objects resulted in a total of 31,045,886 V9 SSU rRNA reads, of which 3,931,978 reads were assigned to 2,991 target OTUs (protistan and fungal). The majority of clean reads were not assigned (~27%) or were assigned to the nontarget OTUs (metazoans, embryophytes and Bacteria; ~54%). The total number of assigned reads ranged between 57,334 (BP1, above halocline) and 979,181 (GKV2, halocline). Taxonomic richness varied notably along the salinity gradient with the lowest number of OTUs detected below the halocline in anchialine speleological object VG (n= 463) and the greatest richness above the halocline in BP anchialine speleological object (n= 1,093), followed by the richness of the halocline in ZVP (n= 914) (**Figure S8**). The highest protistan diversity, according to the Shannon-Wiener index, was recorded in the area of the halocline in BP anchialine speleological object (4.04) and VG anchialine speleological object (4.02), while the lowest was in the halocline of GKV anchialine speleological object (1.57).

Altogether, 22 higher taxonomical levels were recorded wherein an average protistan community of anchialine speleological objects consisted of Alveolata (44.4%), Fungi (29%), Stramenopiles (21.9%), Rhizaria (1.3%) and Chloroplastida (Viridiplantae; 1.3%) (**Figure 21**; **Figure 22**). On average, the ZVP anchialine speleological object was dominated by 56.7 % of Alveolata reads, of which the majority were affiliated with Ciliophora (45.6%).

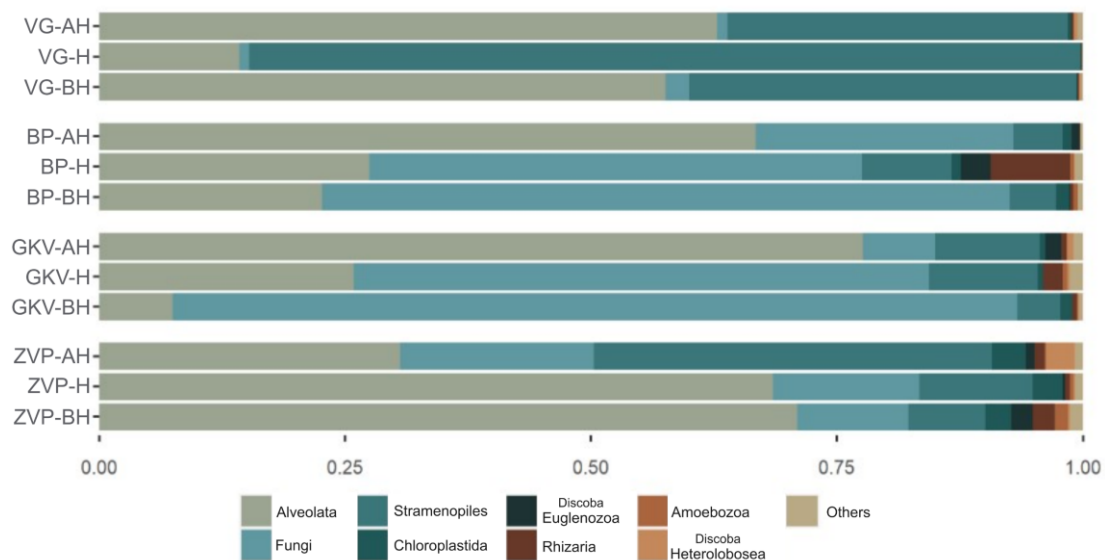


**Figure 21.** Taxonomic composition of the protistan and fungal community in anchialine speleological objects based on the relative abundance of the most abundant assigned higher taxonomic rank ( $\geq 0.01$ ). Higher taxonomic ranks with relative abundance  $< 0.01$  were aggregated into ‘Others’. Above halocline (AH), halocline (H) and below halocline (BH).

Fungi were recorded in 15.3% of average reads in the ZVP anchialine speleological object, with the highest contribution of Dikarya (19.6%) in the marine-like sample. An average of 20% of the reads belonged to Stramenopiles, with Chrysophyceae as the dominant group (17.3% of the reads; the highest above the halocline with 35.42% of reads). In contrast to the shallowest sampled anchialine speleological object, the GKV anchialine speleological object was dominated by Stramenopiles (52.8%) and Alveolata (44.9%). A high number of Chrysophyceae reads were found in the halocline of GKV (83.5%), with Chromulinales as the main lineage.

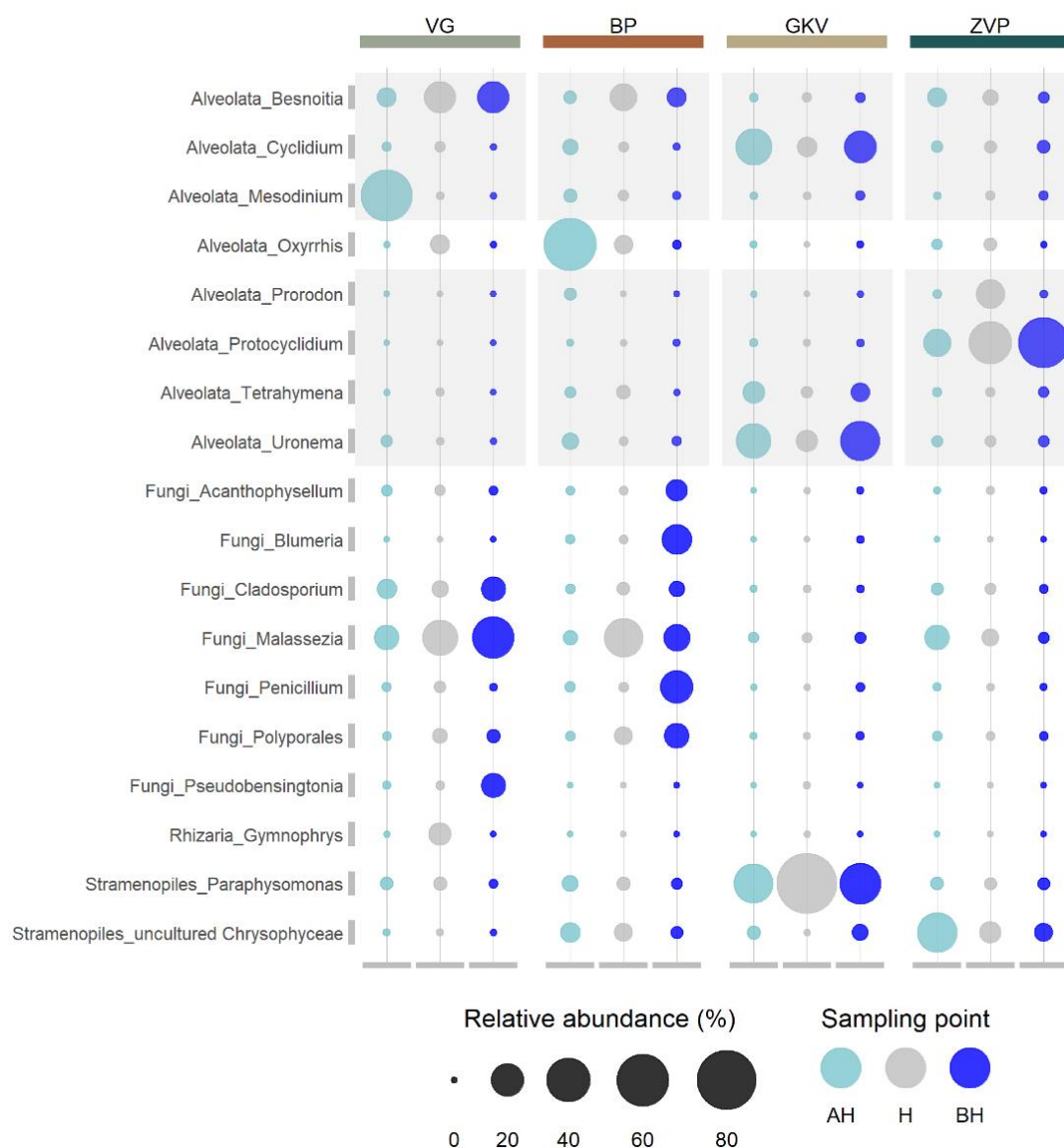


**Figure 22.** Protistan and fungal community at the genus level with a relative abundance  $\geq 5\%$  in at least one sample. The bubble size represents the relative abundance of the genera, and the color represents the sampling point (above halocline (AH), halocline (H), and below halocline (BH)). Gray-colored rectangles highlight the genera of Ciliophora.

The shift of Alveolata and Fungi was recorded in the salinity gradient of BP anchialine speleological object, with the domination of Alveolata reads in the surface area (77.6%; Ciliophora (12.2%) and Dinophyceae (64.1%)) and with Fungi reads in the marine-like area (85.8%; Dikarya (84.7%)). A similar composition to BP anchialine speleological object was identified in VG anchialine speleological object with Alveolata dominating above the halocline (66.7%; Ciliophora (60.6%) and Fungi dominating below the halocline (69.9%; Dikarya (69.1%)). The average reads of Rhizaria and Chloroplastida were relatively low, with 1.3%. The Venn diagram showed the overlap between the anchialine speleological objects with a total of 8.1% shared target protistan and fungal OTUs (**Figure S9**).

### 3.2.4. Co-occurrence patterns of microbial communities

The VG anchialine speleological object presents the deepest sampled anchialine speleological object of 60 m with a water depth of 24 m, characterized decreasing DO with increasing depth, ranging from 9.3 to 1.9 mg L<sup>-1</sup>. Within the salinity gradient, the relative abundance of Alveolata also decreased with increasing depth, ranging from 66.7% to 22.6% and shifting from Ciliophora (60.6%) above halocline to Apicomplexa (18.6%) below the halocline. The opposite trend was observed in the relative abundance of Fungi, with genera assigned to Dikarya subkingdom ranging from 26.3% to 69.9% with increasing depth. Commonly found in marine and brackish water, ciliates affiliated to the taxon *Mesodinium* were the major contributor to the protistan community above the halocline with 58.7%. In and below the halocline, Alveolata was represented with the highest relative abundance of OTUs affiliated to the apicomplexan parasite *Besnoitia*. The highest OTU richness and diversity was recorded in the halocline, varying from OTUs affiliated to heterotrophic dinoflagellate *Oxyrrhis* (5%), cercozoan taxon *Gymnophrys* with 8.1%, kinetoplastid flagellates Bodonidae (3%) to Stramenopiles (9.1%) with OTUs affiliated to Bacillariophyta and Chrysophyceae. Fungi were numerous in all layers with the highest abundance (69.1%) in the hypoxic marine-like area, dominated by genera *Malassezia*, *Cladosporium* and *Pseudobersingtonia*.

The co-occurrence of prokaryotic phyla with a higher abundance was recorded, showing a similar salinity gradient pattern. The abundance of Thaumarchaeota, Bacteroidetes, Gemmatimonadetes and Nitrospirae decreased with the increasing salinity gradient, while the abundance of Gammaproteobacteria, Firmicutes and Actinobacteria was greatest below the halocline. The ammonia-oxidizing archaea Nitrososphaeria from phyla Thaumarchaeota, which relies solely on the energy generated from the oxidation of ammonia, was recorded in high

abundance above (29%) and in the area of halocline (12.8%), corresponding with the highest concentration of ammonium with organic nitrogen ( $4.3 \text{ mg L}^{-1}$ ). Above the halocline, high nitrate and low nitrite concentrations were also recorded resulting from the activity of chemolithoautotrophic aerobic nitrite-oxidizing bacteria *Nitrospira* (3.3%) from phylum Nitrospirae. Bacteroidetes, together with a polyphosphate accumulating Gemmatimonadaceae (8.7%), were also abundant in the surface area, contributing to the chemoheterotrophy with Flavobacteriales (12.8%). Marinimicrobia with SAR406 clade (4.9%) and Actinobacteria with Sva0996 marine group (16.5%) showed a clear preference for the halocline area where pH, DO and measured nutrients decreased. The halocline region had the highest OTU richness resulting from the relative abundance of Planctomycetes, Verrucomicrobia, Deltaproteobacteria, Acidobacteria, Chloroflexi and Latescibacteria. The lowest concentration of DO ( $1.9 \text{ mg L}^{-1}$ ) was measured below the halocline, where the Gammaproteobacteria, Firmicutes and Actinobacteria had the highest relative abundance, totaling 91.1%. These phyla were represented by gram-negative aerobic bacteria *Pseudomonas*, *Ralstonia*, *Delftia* together with *Sphingomonas* (Alphaproteobacteria), gram-positive bacteria with facultatively anaerobic *Staphylococcus*, *Corynebacterium*, and anaerobic *Lawsonella* and *Cutibacterium*, indicating the area below the halocline as an area of pathogenic bacteria known to cause a variety of infections. The only taxon contributing to the prokaryotic community below the halocline that is not corroborated as pathogenic was *Lactobacillus*.

The BP anchialine speleological object was the deepest sampled anchialine speleological object, reaching a water depth of 50 m. The lowest total nitrogen concentration ( $0.29 \text{ mg L}^{-1}$ ) throughout the entire salinity gradient and the hypoxic layer was recorded in the area of the halocline. A similar pattern to the VG anchialine speleological object was observed in the protistan and fungal community of BP anchialine speleological object, shifting the relative abundance of Alveolata and Fungi within the salinity gradient. Compared to VG anchialine speleological object, different genera related to Alveolata dominated the area with the lowest salinity concentration. Above the halocline, the highest OTU richness was recorded together with the highest relative abundance of OTUs affiliated to heterotrophic dinoflagellate *Oxyrrhis*, reaching 62.1%. The brackish water of 4.3‰ in the surface area of BP anchialine speleological object was also favorable for the ciliates *Uronema* and *Cyclidium* together with OTUs affiliated to Chrysophyceae and Kinetoplastida. In the hypoxic halocline area, with decreasing pH, the majority of fungal reads were assigned to taxon *Malassezia* and the order Polyporales from subkingdom Dikarya (58.4%). Oxygen levels were considered low ( $0.48 \text{ mg L}^{-1}$ ) yet high enough to support the growth of Apicomplexa (Besnoitia), Ciliophora (Tetrahymena),

Dinophyceae (Oxyrrhis), Chrysophyceae and Bacillariophyta (*Ulnaria*, *Gomphonema*). The highest taxonomic diversity and relative abundance of Fungi (85.8%) was recorded below the halocline and dominated by *Acanthophysellum*, *Blumeria*, *Cladosporium*, *Malassezia*, *Penicillium* and *Polyporales*.

In the prokaryotic community, the most prominent archaeal lineage was Thaumarchaeota, with a similar contribution to the relative abundance and decreasing by the increasing salinity as in the VG anchialine speleological object. The ammonia-oxidizing archaea, *Nitrosopumilus* and *Nitrosoarchaeum*, reached the relative abundance of 25.2% in the surface area despite the low concentration of ammonium with organic nitrogen ( $0.22 \text{ mg L}^{-1}$ ). Bacteroidetes, including the strictly aerobic and chemoorganotrophic family Cryomorphaceae and *Algoriphagus* (Cyclobacteriaceae), were abundant in the area above the halocline. The transition of genera in the salinity gradient was demonstrated by the relative abundance of Actinobacteria and Gammaproteobacteria. In the surface area, Candidatus *Aquilina* (Actinobacteria; 15.3%) and RS62 marine group (Gammaproteobacteria; 11.6%) dominated, while in the marine-like area, *Rhodococcus* (Actinobacteria; 31.3%) and order Pseudomonadales (Gammaproteobacteria; 14.5%). In contrast to the protistan and fungal community, the highest OTU richness of the prokaryotic community was in the hypoxic halocline. The remaining phyla and families, Gammaproteobacteria, Actinobacteria, Alphaproteobacteria, Bacteroidetes, Thaumarchaeota, Deltaproteobacteria, Planctomycetes, Acidobacteria, Marinimicrobia (SAR406 clade), Verrucomicrobia and Nitrospirae contributed to the halocline prokaryotic community with high diversity. Below the halocline recorded community was characterized as pathogenic with the majority of the genera related to *Rhodococcus*, *Sphingomonas*, *Arcobacter*, *Lawsonella* and *Staphylococcus*. The OTUs assigned to strictly anaerobic sulfur-oxidizing Desulfobacteraceae (8.4%) and halophilic phototrophic purple sulfur-oxidizing Ectothiorhodospiraceae (3.6%) contributed to the community below the halocline.

The GKV anchialine speleological object is geographically most distant from other sampled anchialine speleological objects, with a water depth of 30 m characterized by the decrease of DO in the salinity gradient ( $7.86 - 1.12 \text{ mg L}^{-1}$ ). The concentration of ammonium with organic nitrogen  $1.4 \text{ mg L}^{-1}$  was measured in the surface area where the most abundant protistan OTUs affiliated to Alveolata (62.8%) and Stramenopiles (34.6%). Alveolata were highly dominated by Ciliophora (59.4%) with a low contribution of Dinophyceae (3.2%). The area above the halocline was hosted by the genera *Uronema* (23.8%) and *Cyclidium* (26.3%) from the subclass Scuticociliatia and Tetrahymena (7.6%) from the subclass Tetrahymenina. The lowest OTU richness was recorded in the halocline, where the nonphotosynthetic phagotrophic

chryomonads *Paraphysomonas* contributed with a high relative abundance of 83.5%. In contrast to Alveolata, the relative abundance of fungal community in the GKV anchialine speleological object was almost negligent with the highest abundance recorded in the marine-like area affiliated to genera *Malassezia* (2.3%).

The main prokaryotic groups detected in the surface area, where the highest concentration of TN ( $1.4 \text{ mg L}^{-1}$ ) and TOC ( $1.2 \text{ mg L}^{-1}$ ) were recorded, were Gammaproteobacteria, Alphaproteobacteria and Bacteroidetes with a relative abundance of 48.3%, 19.5% and 15.7%, respectively. High diversity of Gammaproteobacteria was comprised of diverse orders such as Pseudomonadales, Betaproteobacteriales, Cardiobacteriales, Oceanospirillales and SAR86 clade. Ubiquitous gram-negative and non-fermenting coccobacilli *Acinetobacter* (11.5%) had the highest relative abundance among other Gammaproteobacteria together with ubiquitous gram-negative and aerobic or facultatively anaerobic *Myroides* (9.1%) from phyla Bacteroidetes. The lowest OTU richness of the prokaryotic community in GKV anchialine speleological object was recorded also in the area of halocline with the highest abundance Actinobacteria (42.1%) and Rhodobacteraceae (Alphaproteobacteria; 46.1%). Family Rhodobacteraceae was presented by fundamentally aquatic bacteria *Defluviimonas*, *Pseudorhodobacter* and *Seohaecicola*. Genera *Defluviimonas* and *Pseudorhodobacter* are chemoorganotrophic bacteria, whereas *Defluviimonas* is also a facultative anaerobe growing anaerobically by denitrification. The prokaryotic community in the hypoxic marine-like area contributed to the microbial diversity with the highest recorded richness in GKV anchialine speleological object. Of the total community above halocline, Gammaproteobacteria, Alphaproteobacteria and Actinobacteria contributed with the highest relative abundance of 22.6%, 15.4% and 13.4%, respectively. A strong increasing pattern of relative abundance within the salinity gradient was recorded in phyla Thaumarchaeota, Marinimicrobia (SAR406 clade), Epsilonbacteraeota, Chloroflexi, Planctomycetes, Acidobacteria and Gemmatimonadetes. Compared to other anchialine speleological objects, phyla Euryarchaeota was detected only in GKV and ZVP anchialine speleological object with a relative abundance of 2%.

The ZVP anchialine speleological object is the shallowest sampled anchialine speleological object with a water depth of 6 m characterized by the sharp decrease of DO in the halocline area with a continued decrease by the salinity gradient ( $7.42 - 0.36 \text{ mg L}^{-1}$ ). In comparison to other sampled anchialine speleological objects, the highest protist diversity based on the higher taxon groups was established in the ZVP anchialine speleological object with the dominance of Stramenopiles, Alveolata, Chloroplastida, Heterolobosea and Rhizaria, together with Fungi in

the surface area. The relative abundance of Stramenopiles and Fungi has followed the decrease by the depth within the salinity gradient, whereas the relative abundance of Alveolata increased, ranging from 30.6% to 71.0%. Above the halocline, OTUs affiliated to Chrysophyceae and Synurophyceae reached a total relative abundance of 40.5% with the highest contribution of uncultured Chrysophyceae (32%) and *Poterioochromonas* (4.6%). The fungal community within the salinity gradient shifted the dominance of genera from *Malassezia* (Basidiomycota) to *Verrucoconiothyrium* (Ascomycota), with relative abundance ranging from 19.7% to 11.3%. In the area above halocline, *Besnoitia* (Apicomplexa), *Protocyclidium* (Ciliophora) and *Gymnodinium* (Dinophyceae) were the most abundant genera affiliated to Alveolata. Ciliates dominated in the low-nutrient conditions in and below the halocline. The most abundant OTUs in the halocline were affiliated with the scuticociliate taxon *Protocyclidium* and holotrichous ciliate *Prorodon*, while the taxon *Protocyclidium* increased with increasing depth, reaching 56.6% in the hypoxic marine-like area. Chloroplastida were present at every sampled depth with the relative abundance of 3% affiliated to marine colonial flagellate green algae taxon *Oltmannsiellopsis*.

The highest concentration of ammonium with organic nitrogen and TOC in the ZVP anchialine speleological object was measured in the surface area. The relative abundance of Gammaproteobacteria, Alphaproteobacteria, Bacteroidetes and Actinobacteria decreased with the increasing salinity gradient, while Epsilonbacteraeota, Omnitrophicaeota and Marinimicrobia (SAR406 clade) were most abundant in the marine-like area. Ubiquitous freshwater genera differing in many aspects of their lifestyles, *Limnohabitans*, *Methylothera*, *Polynucleobacter* and *Acidovorax* affiliated to Betaproteobacteriales, had a relative abundance of 28.8% in the area above the halocline. The taxon *Limnohabitans* had the greatest relative abundance (18.8%) compared to other detected Betaproteobacteriales. The remaining OTUs with a relative abundance greater than 5% in the surface area were affiliated to Candidatus Aquilina (Actinobacteria), uncultured Rhizobiales (Alphaproteobacteria), *Pseudorhodobacter* (Alphaproteobacteria) and Candidatus *Aquirestis* (Bacteroidetes). OTUs affiliated to *Sulfurimonas* (Epsilonbacteraeota), Ectothiorhodospiraceae (Gammaproteobacteria) and *Desulfatiglans* (Deltaproteobacteria) had relative abundances of 15.7%, 7.3% and 7.1%, respectively. Within this area, the obligate anaerobic taxon *Thermomarinilinea* (Chloroflexi; 9.2%) was detected in conjunction with the anaerobic and chemoorganoheterotrophic phylum Calditrichaeota (1.3%). In the depth with the highest salinity and lowest DO, archaeal phylum Epsilonbacteraeota with taxon *Arcobacter*, Omnitrophicaeota and Gammaproteobacteria with

family Ectothiorhodospiraceae contributed with relative abundances of 18.5%, 10% and 7.8%, respectively.

The PCoA plot revealed the differences between the anchialine speleological objects within the prokaryotic and protistan community, generally clustering samples in line with their anchialine speleological object origin (**Figure 23**). This result was confirmed by two-way PERMANOVA analysis, showing that both the protistan and prokaryotic community of the anchialine speleological objects differed significantly from each other ( $P < 0.001$ ).

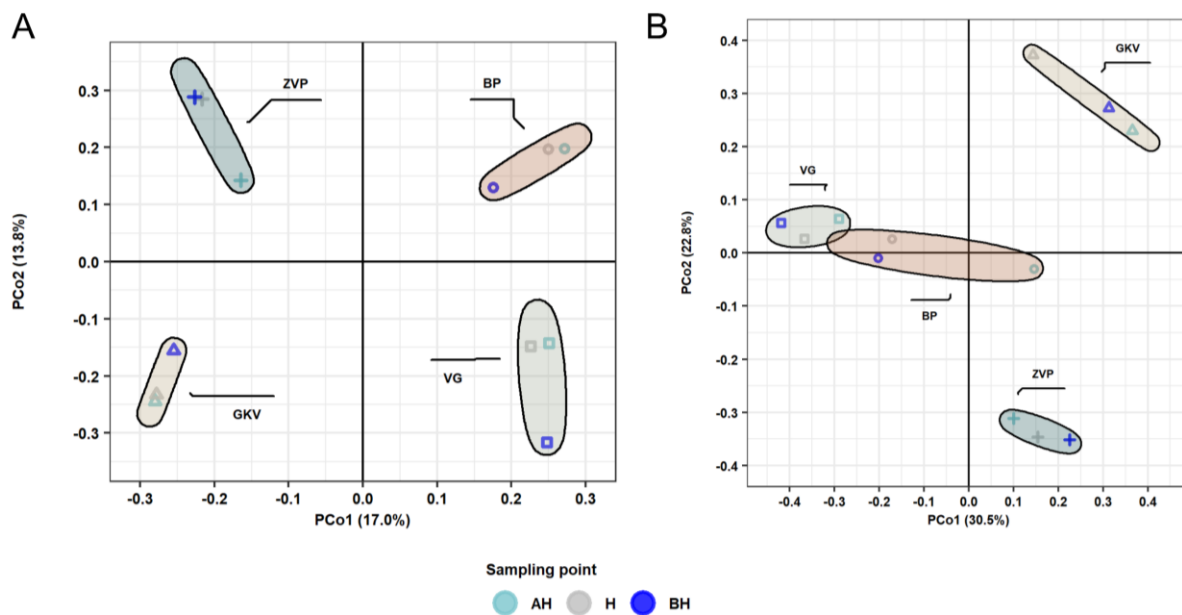


**Figure 23.** Principal coordinate analysis (PCoA) of (A) prokaryotic and (B) protistan community in anchialine speleological objects using Bray-Curtis distances on the level of OTUs. The plot is color-coded by the sampling point (above halocline (AH), halocline (H) and below halocline (BH)) and shape-coded by the anchialine speleological object. Groups are color-coded by the sample origin.

The diversity of communities was only affected by temperature, while no correlation was observed with other measured environmental parameters on the OTU level. Co-Inertia Analysis (CIA) resulted in a high significant correlation of prokaryotic and protistan communities of anchialine speleological objects ( $RV = 0.8369$ ,  $P < 0.001$ ; **Figure 24**).

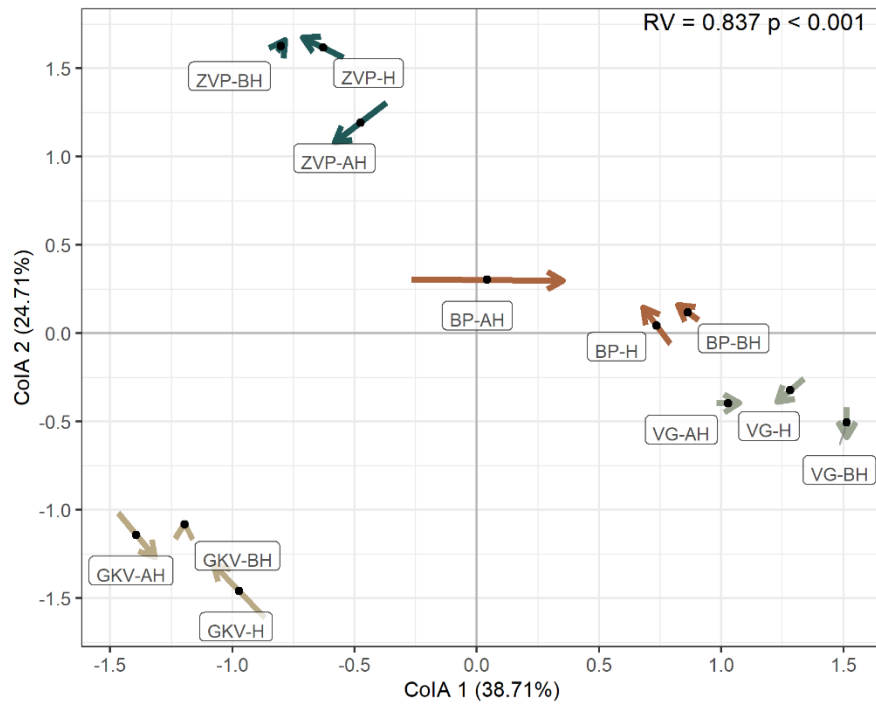


**Figure 24.** Comparison of the protistan and prokaryotic community diversity based on Co-Inertia Analysis (CIA). The beginning of the arrow presents the theoretical position of the protistan sample and the end of the arrow presents the prokaryotic sample. Arrows are color-coded by the anchialine speleological object indicating two connected projections, whereby the line length indicates the divergence between the two datasets. Significant RV value ( $p < 0.001$ ) is marked on the plot. Sample name abbreviations refer to the area of a sampling point: above the halocline (AH), in the halocline (H), and below the halocline (BH).

### 3.3. Diversity patterns of prokaryotes in the water column of the anchialine speleological object in the Martinska area

#### 3.3.1. Environmental characteristics of anchialine speleological object

The anchialine speleological object studied in the Martinska area exhibits a stable oxygen and salinity gradient along the depth, developing specific niches regarding different physical and chemical parameters (**Figure 25, Table S8**). While the top layer is practically freshwater, along the depth, salinity increases to brackish in the middle depths and finally reaches the salinity of marine ecosystems as it approaches the deeper layers (**Figure 25**). Physical parameters show similar trends in all three sampling time points (i.e., March, April, and August 2021). Depending on the month, halocline and oxycline develop at 2 to 3 meters of water depth. Anoxia occurred from the 3 m depth of the water column and continued to the bottom of the anchialine speleological object (12 m; including sampling points SC3, SC4, SC5, and SC6). The pH levels declined as depth increased, consistently remaining within the range of 7.0 to 7.3 in anoxic depths. Temperature fluctuations exhibited minimal variation, showing a gradual increase with the depth in March and April, while in August, the freshwater layer reached a peak of 15.8 °C.

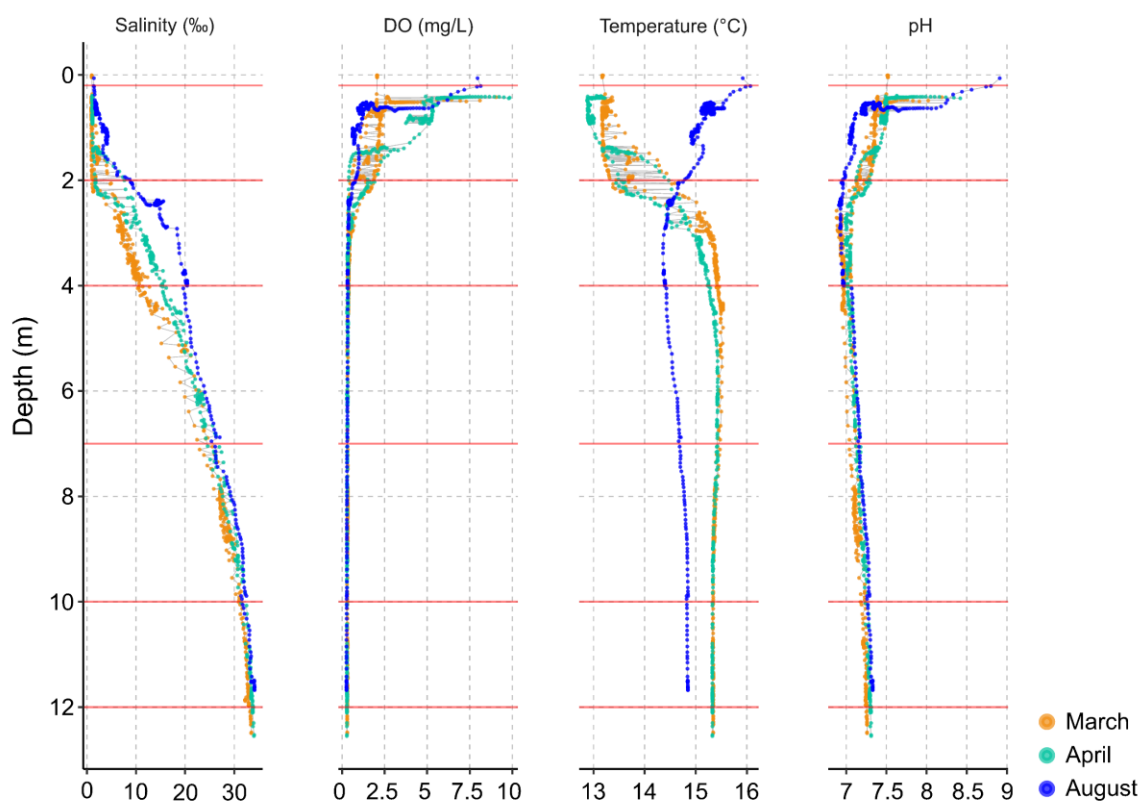


**Figure 25.** Vertical profile of parameters obtained in March, April, and August with a multi-parameter data sonde in anchialine speleological object: salinity (‰), dissolved oxygen (DO;  $\text{mg L}^{-1}$ ), temperature ( $^{\circ}\text{C}$ ) and pH. Red lines indicate the sampled depth.

Throughout all sampling time points, multiple peaks in dissolved organic carbon (DOC), ammonia ( $\text{NH}_3^+$ ), nitrate ( $\text{NO}_3^-$ ), nitrite ( $\text{NO}_2^-$ ), sulfide ( $\text{HS}^-$ ), and phosphate ( $\text{PO}_4^-$ ) were observed along the water column. The measured concentrations of  $\text{HS}^-$  peaked below the halocline, reaching a maximum of  $13,393 \mu\text{g L}^{-1}$  in April (SC4). Sulfate concentrations exhibited an upward trend with depth (April and August) and reached their highest levels in August at a depth of 12 meters, measuring  $3,200 \text{ mg L}^{-1}$ .

### 3.3.2. Prokaryotic diversity, activity and community structure

The 16S rRNA gene amplicon sequencing was used to assess the overall prokaryotic community composition of the anchialine speleological object. A preliminary overview of the microbial community by 16S rRNA amplicon analysis showed the temporal development and stabilization of oxycline from March to August (**Figure 26**). In total, 5,064 ASVs were assigned to 64 different phyla during the studied period, with the highest diversity of phyla present in the layers of halocline (app. 54 phyla; SC3 and SC4).

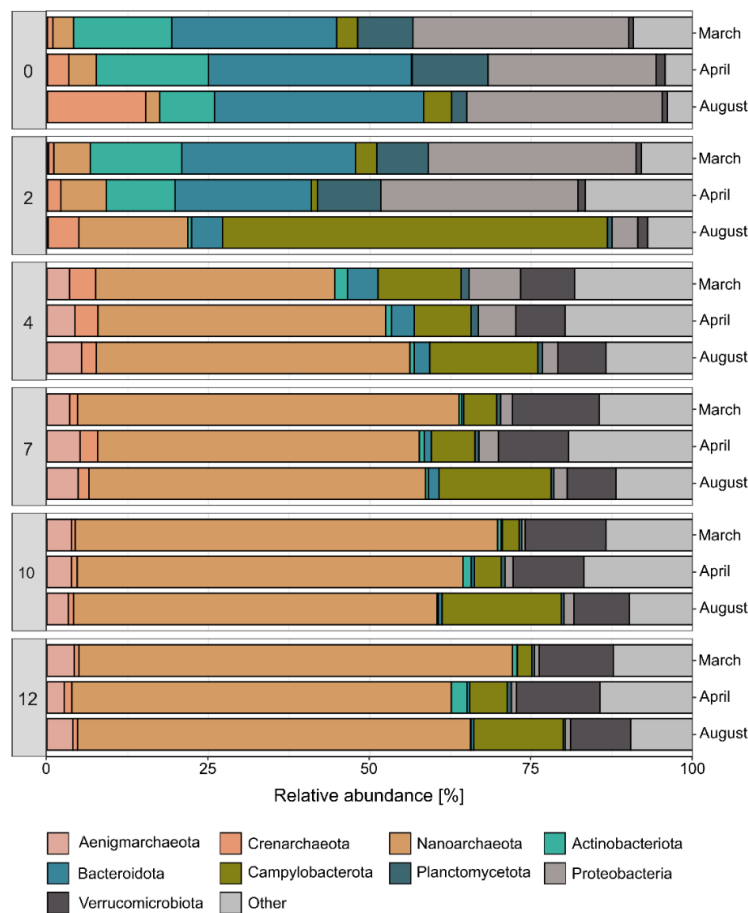


**Figure 26.** Dynamics of archaeal and bacterial phyla per depth along the salinity and oxygen gradient assessed by 16S rRNA data analysis in three sampling timepoints (March, April, and August). Phyla with relative abundance lower than 5% were grouped into ‘Other’.

A higher percentage of ASVs were classified as bacterial in the oxic upper layers (> 80%; SC1, SC2), whereas archaea dominated in the anoxic deeper layers (60-78%; SC3 to SC6). The majority of the 5,230 recovered ASVs were recorded from the deeper layers, with 60% assigned to 11 different archaeal phyla. In general, higher alpha diversity (richness) was recorded in the deeper samples (SC3-SC6) than in the surface layers (**Figure S10**), with the most abundant archaeal phyla Nanoarchaeota (Woesearchaeales) followed by Aenigmarchaeota and Crenarchaeota reaching up to 72% of total relative abundance in March (SC6).

Prior to the stabilization of oxy- and thermocline, Bacteroidota (*Pseudarcicella*) dominated the freshwater layers with a bloom of a single ASV in April (19%) (**Figure 27**). By stabilization of the oxycline and thermocline in August, the community of this layer experienced a bloom of Campylobacterota, comprising 7 ASVs, with a single ASV accounting for ca. 42% (Arcobacteraceae) of the community, along with Sulfurimonadaceae (*Sulfurimonas*, *Sulfurovum*, and *Sulfuricurvum*) cumulatively accounting for 59% of the community. Above the stable clines, individual ASV of *Nitrosarchaeum* dominated, making up 13% of the community. In the anoxic layers, Campylobacterales continued to dominate with Arcobacteraceae at 4 to 7 m depth, and *Sulfurovum* (Sulfurivaceae) and *Sulfurimonas* (Sulfurimonadaceae) in the layers below 7 m.

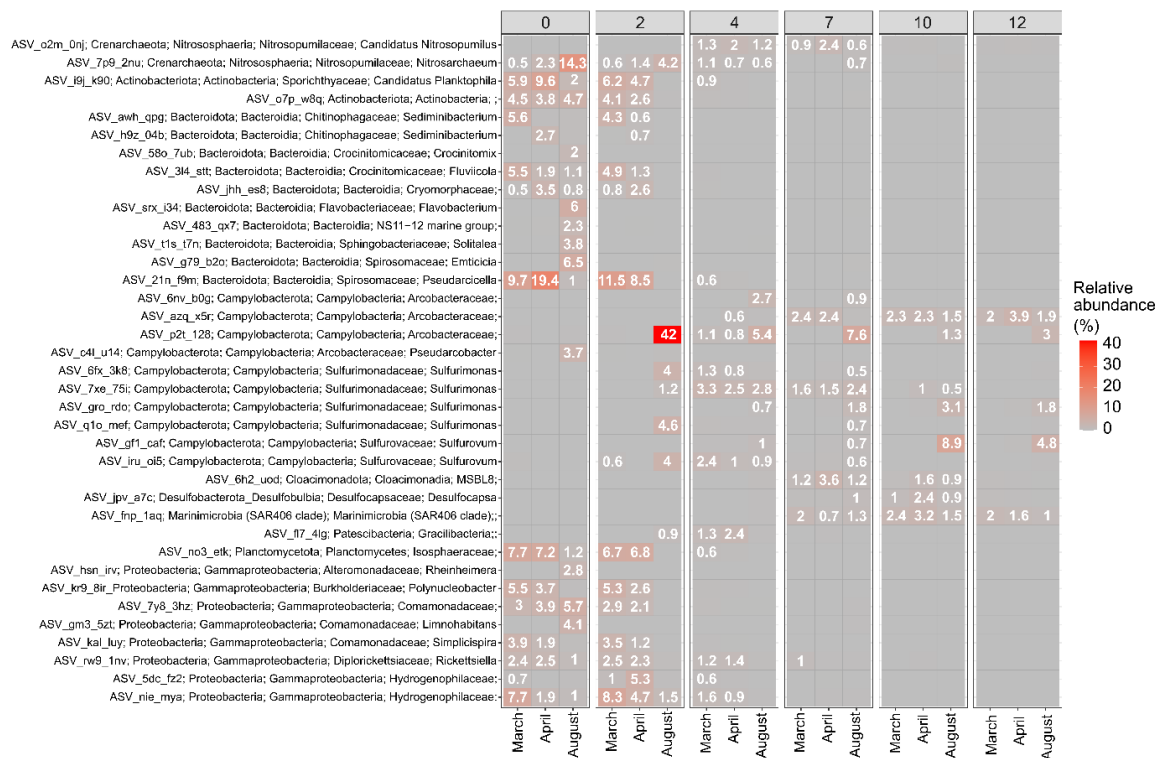


**Figure 27.** Heatmap of most abundant ASVs in anchialine speleological object per depth and month based on the 16S amplicon analysis.

To assess the activity and identity of the prokaryotic community, the combination of CARD-FISH and BONCAT was applied to the water samples collected in April and August (**Figure S11**). The total number of cells, the number of active cells and the number of EUB positive cells all peaked in the upper layers (SC1 and SC2), reaching their maximum of  $5.64 \times 10^6$ ,  $3.75 \times 10^6$  and  $2.95 \times 10^6$  cells  $\text{mL}^{-1}$  in the freshwater layer (SC1 in August), respectively (**Table S9**). The relative abundance of active and EUB-positive cells exhibited similar patterns in both April and August (**Figure 28**). A higher activity level and abundance of bacterial community was observed in the upper freshwater to brackish water layers, gradually declining with depth in anoxic layers. The highest relative abundance of active cells was counted in the freshwater layer (SC1, August), constituting 66.4% of the total active cells.

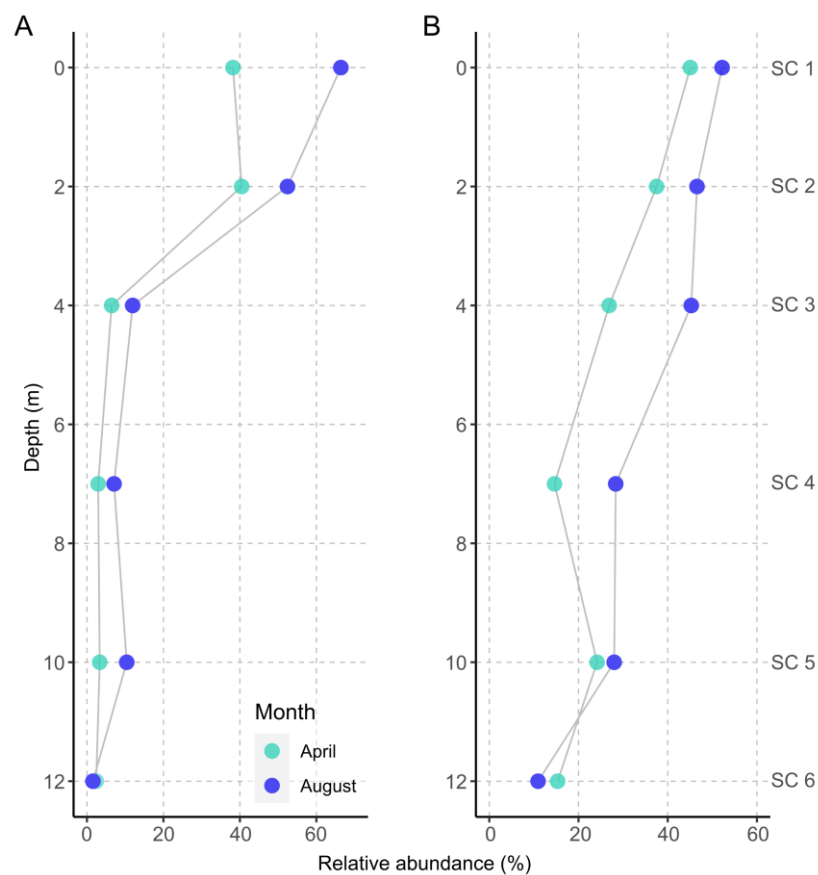


**Figure 28.** The relative abundance of active cells (**A**) and bacterial cells (**B**) per depth in April and August. Active cells present the BONCAT positive cells and bacterial cells present the CARD-FISH positive cell (probe EUBI-III).

To gain a genome-resolved view of the ecosystem and the functional profile of the stratified microbial community, the metagenomic datasets were generated from the depth profile samples collected in August at the peak of stratification. Applying automated binning, in total 418

Metagenome Assembled Genomes (MAGs) were reconstructed from these datasets (CheckM completeness  $\geq 50\%$ , contamination  $\leq 10\%$ ), of which 119 were high-quality drafts (CheckM completeness  $\geq 90\%$ , contamination  $\leq 5\%$ ). MAGs were classified into 35 distinct phyla with the majority of reconstructed MAGs affiliated to Patescibacteria (79 MAGs; 18.9%), Nanoarchaeota (74 MAGs; 17.7%), Omnitrophota (59 MAGs; 14.1%), and Proteobacteria (49 MAGs; 11.7%; **Figure 29A**). The highest number of MAGs was found in the SC4 sample at a depth of 7 meters (n=307) with the highest richness of Nanoarchaeota (22.2%), Patescibacteria (19.2%) and Omnitrophota (16.6%). In contrast to the MAG richness, the highest relative abundance of MAGs was observed in the layers transitioning from freshwater to brackish, with a cumulative abundance totaling 6,608 (**Figure 29B**).

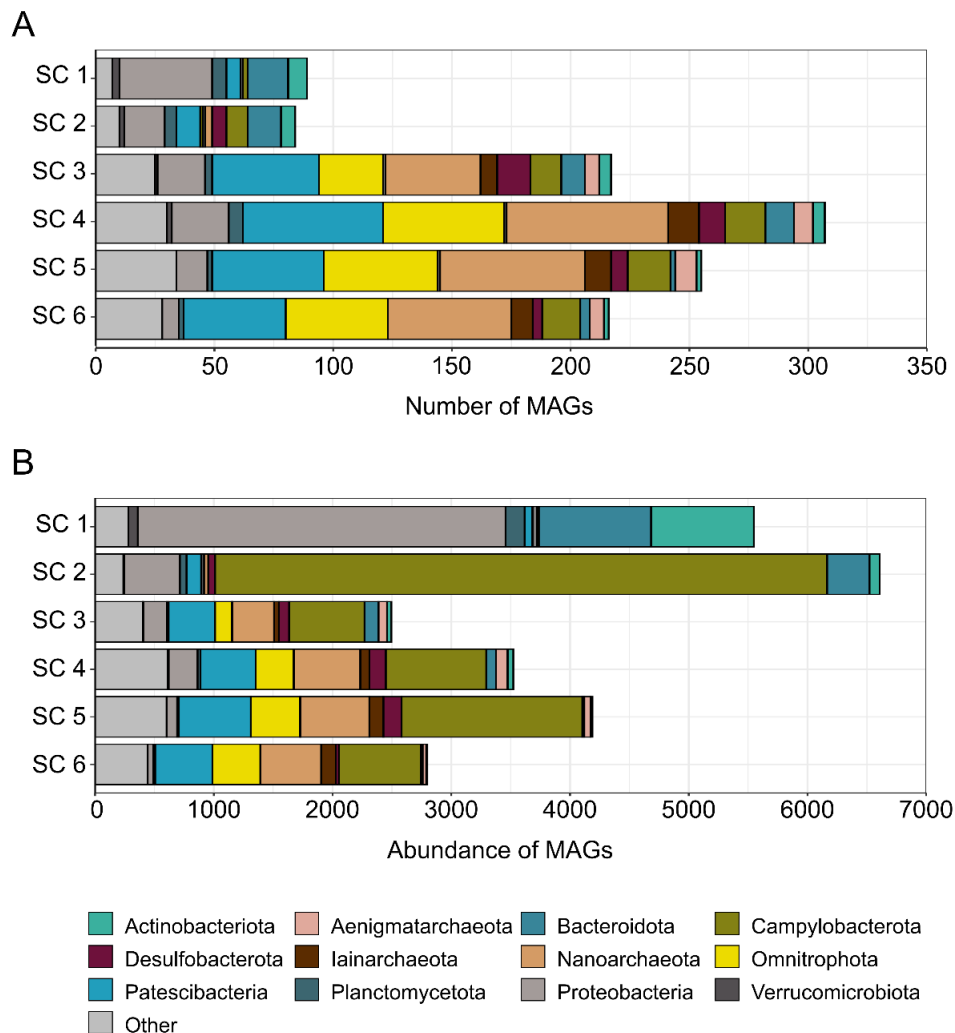


**Figure 29.** (A) Number of Metagenome Assembled Genomes (MAGs) and (B) their cumulative abundance on the phylum level per depth in anchialine speleological object.

There is only a relatively small overlap in the community across all different depths represented by a total of 11 representative MAGs (3% of all reconstructed MAGs) that are affiliated to Thermoproteota (*Nitrosarchaeum*), Nanopelagicales (S36-B12), Ilumatobacteraceae (BACL27), Bacteroidales (UBA6244 sp002440885), Arcobacteraceae (CAIJNA01), Phycisphaerales (F1-60-MAGs104), Burkholderiales (*Gallionella*, *Limnohabitans*, *Limnohabitans\_A*, and Thiobacillaceae) and Diplorickettsiales (*Rickettsiella\_A*; **Figure 30**).

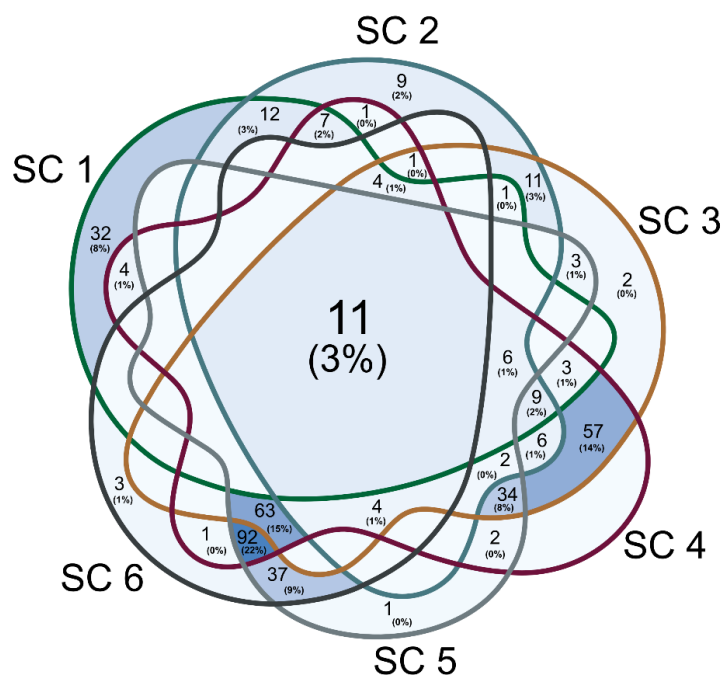


**Figure 30.** Venn diagram of shared and unique Metagenome Assembled Genomes (MAGs) per depth in August.

Different datasets originating from different depths along the water column of anchialine speleological object represented a strong stratification in their community composition as expected. The uppermost layer has a hallmark epilimnetic freshwater community dominated by *Limnohabitans* and Nanopelagicales (**Figure 31**). Around 8% of reconstructed MAGs (accounting for ca. 35% of MAGs present in SC1) were exclusively present in this strata and were not present in the other sampled depths (**Figure 30**).

The second sampling layer (SC2), coinciding with the thermocline and oxycline, represents a slightly higher alpha diversity compared to the top layer based on the ASV analysis. Despite its slightly higher alpha diversity, relative abundances extracted from the MAG analysis corroborate with the ASV abundance analysis and highlight a bloom of sulfur-oxidizing bacteria affiliated to families Arcobacteraceae, Sulfurimonadaceae, and Thiobacillaceae (**Figure 31**). The sample SC2 contained 9 MAGs exclusively present in this layer of the anchialine speleological object belonging to taxa Bacteroidales (F082, Paludibacteraceae,

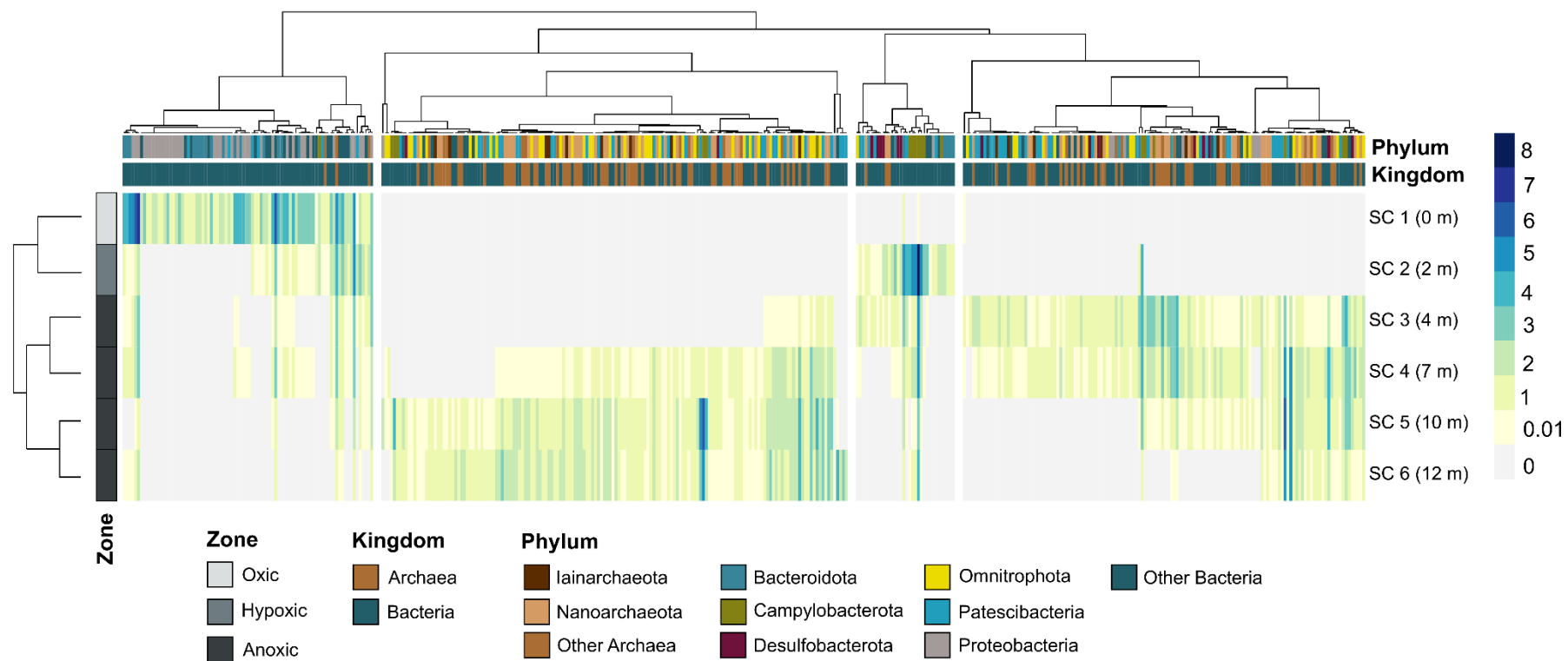


**Figure 31.** Overview of the distribution of metagenomic abundances in oxygen and salinity gradient of anchialine speleological object per depth.

UBA12481 and UBA1556), Campylobacterota (Sulfurimonadaceae), Chloroflexota (EnvOPS12), Patescibacteria (BM507) and Proteobacteria (Magnetaquicocccaceae).

The anoxic lower layers (SC3 to SC6) represent a higher overlap in their community composition apart from 2, 1, and 3 MAGs that are exclusively present in SC3 (Omnitrophota (Koll11) and Patescibacteria (Paceibacterales)), SC5 (Proteobacteria (Alteromonas)), and SC6 (Patescibacteria (two representatives of family UBA2163 and GCA-2747515)), respectively. Along the depth in these three datasets, the community gradually shifts with 57 MAGs shared between SC3 and SC4, 92 MAGs shared between SC4, SC5, and SC6, 37 MAGs shared between SC5 and SC6, and 63 MAGs that are shared across all these four datasets (**Figure 30, Figure 31**).

Furthermore, the PCoA carried out at the ASV level revealed a distinct clustering pattern of the entire prokaryotic community within the anchialine speleological object based on sampling depth. This clustering pattern consistently showed a clear separation between the oxic and anoxic zones in all three months (**Figure 32A**). Notably, in August, the SC2 sample exhibited a significant separation from the other samples collected at a depth of 2 meters. This finding was corroborated by the clustering analysis of the cumulative abundance of the MAGs, where the samples grouped into two primary clusters, distinguishing the freshwater to brackish oxic community from the saline anoxic community (**Figure 31, Figure 32B**). In total, 69.4% of the variation in the prokaryotic community structure accounted by the two axes of the PCoA ordination at the ASV level, while the diversity based on the cumulative abundance of MAGs explained 20% of the variation.

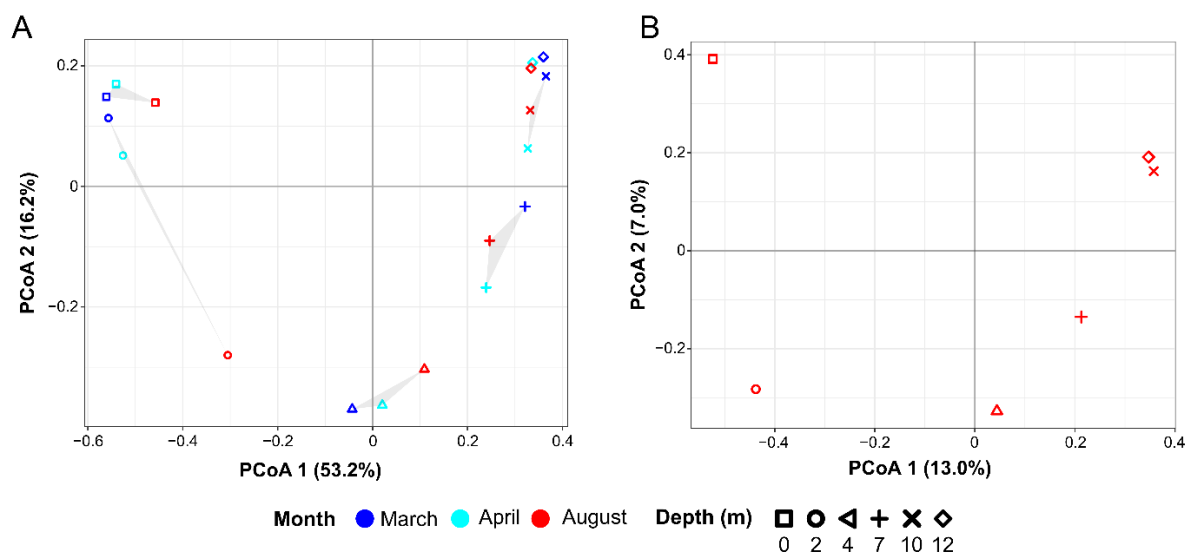


**Figure 32.** Diversity of microbial community in anchialine speleological object based on the level of (A) ASV abundance and (B) MAG cumulative abundance per depth.

### 3.3.3. Functional gene diversity and metabolic potential of the prokaryotic community

While the community composition varies considerably among different depths (sharing only 11 common MAGs comprising only 3% of all reconstructed MAGs, **Figure 30**), the overall combined profile of annotated genes in all MAGs present in each depth seems to be very similar. From the total of 7,535 KEGG KO annotated genes, 4,911 were detected in all 6 depths, comprising ca. 65% of all annotated genes without considering the taxonomy of the genome containing these genes in each depth (**Figure 33**).

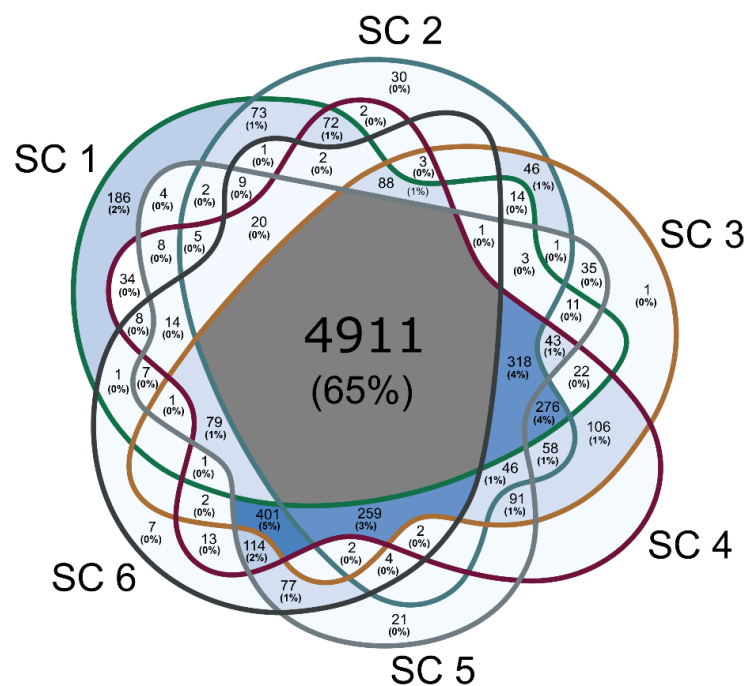
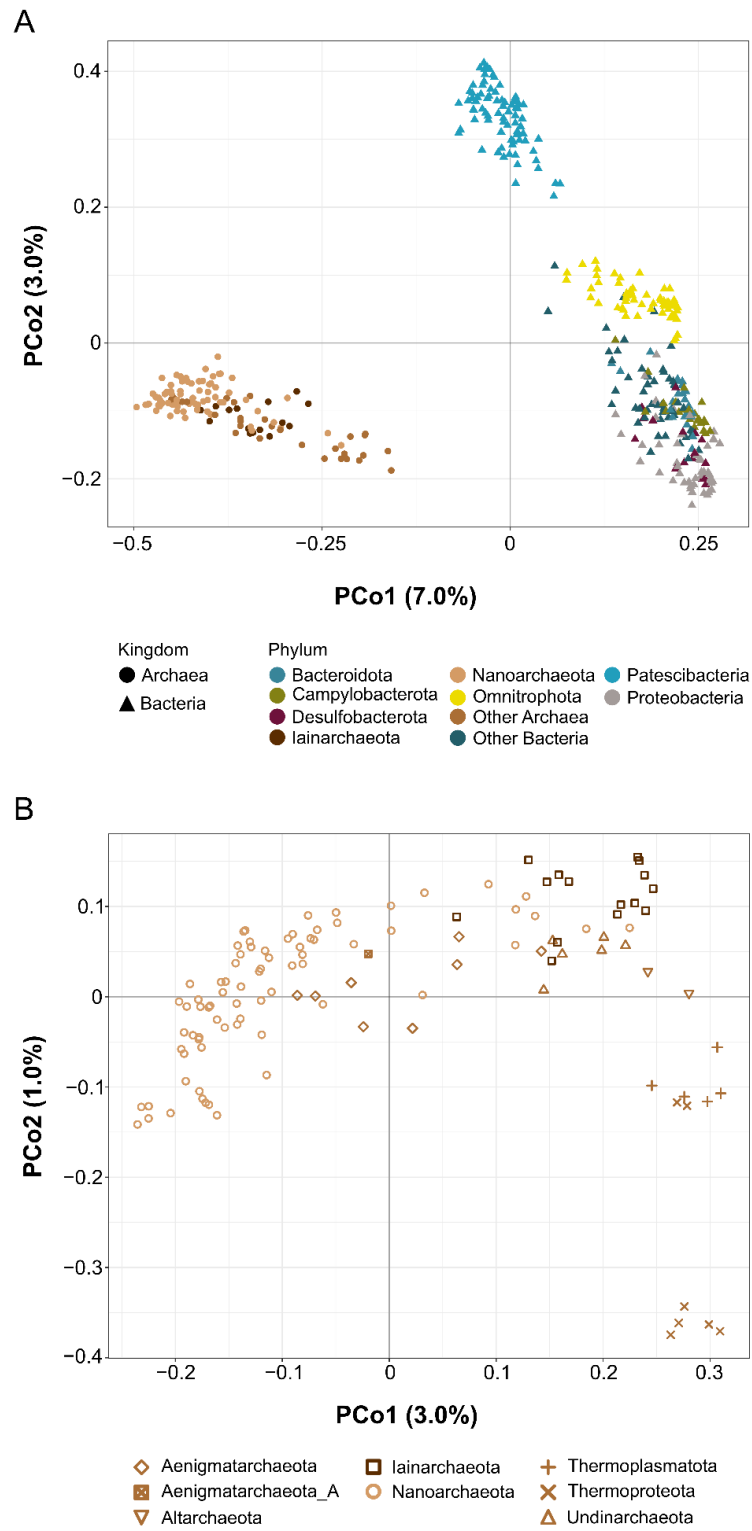


**Figure 33.** Venn diagram of shared and unique KEGG KO annotated genes per depth present in Metagenome Assembled Genomes (MAGs).

Interestingly, only 186 KEGG KO were exclusively present in the metabolic profile of the SC1 community, while 8% of MAGs were exclusively present in this sample. However, they are evidently contributing only a minor metabolic novelty (2% of all detected KOs) to the community. These 186 KOs encode for functions related to KEGG categories metabolism, genetic information processing, and signaling and cellular processes.

Comparing the profile of annotated genes in reconstructed MAGs shows a strong clustering that differentiates between Bacteria and Archaea (**Figure 34A**). However, this is not reflected in the overall metabolic profile of the community at each depth despite the higher diversity of Archaea at the deeper strata (**Figure 34B**). Based on PCoA analyses, a different profile is

evident at higher taxonomic resolution for representatives of Patescibacteria and Omnitrophota compared to other bacterial taxa (**Figure 34C**).



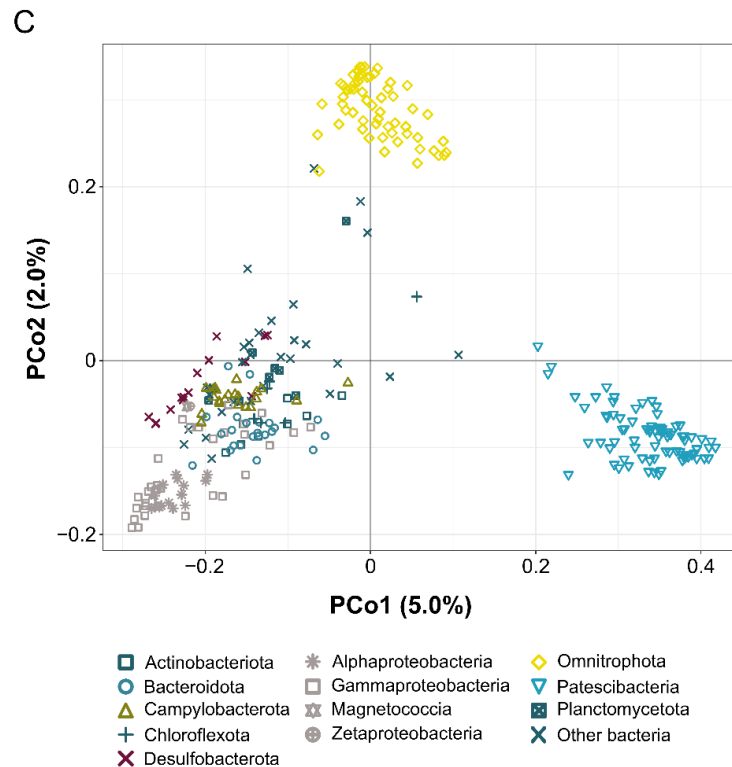


**Figure 34.** Diversity of Metagenome Assembled Genomes (MAGs) in anchialine speleological object based on the present KEGG KO annotated genes. PCoA conducted on the (A) whole community, (B) Archaeal MAGs and (C) Bacterial MAGs.

Initially, functional diversity in the anchialine speleological object was differentiated between the core genes (i.e., present in most bacterial and archaeal MAGs; **Figure 35A**) versus the less prevalent auxiliary genes (**Figure 35B**) that are most likely involved in environmental adaptations. The cumulative abundance of the MAGs containing each annotated KO was assigned as the abundance of that KO in each depth. The annotated KOs were further separated into abundant and rare based on the sum of their abundance in all depths (arbitrary threshold of 2000 cumulative abundance). Taking the abundance of each KO into account adjusted the view of the community's metabolic profile, revealing differences in the prevalence of functions at each depth (**Figure 35**). Overall, the annotated KOs were categorized into the following dominant groups: protein families related to genetic information processing (with a maximum of 12% in SC1), carbohydrate metabolism (10.5% in SC1), genetic information processing within the translation (10.2% in SC6), and signaling and cellular processes (9% in SC2, **Table S10**, **Table S11**), respectively.

The predominant metabolic pathway modules in the first and second layer (SC1 and SC2; clusters 2, 4, 5, and 7) were related to various metabolic processes, including carbohydrate metabolism, energy metabolism, lipid metabolism, nucleotide metabolism, amino acid

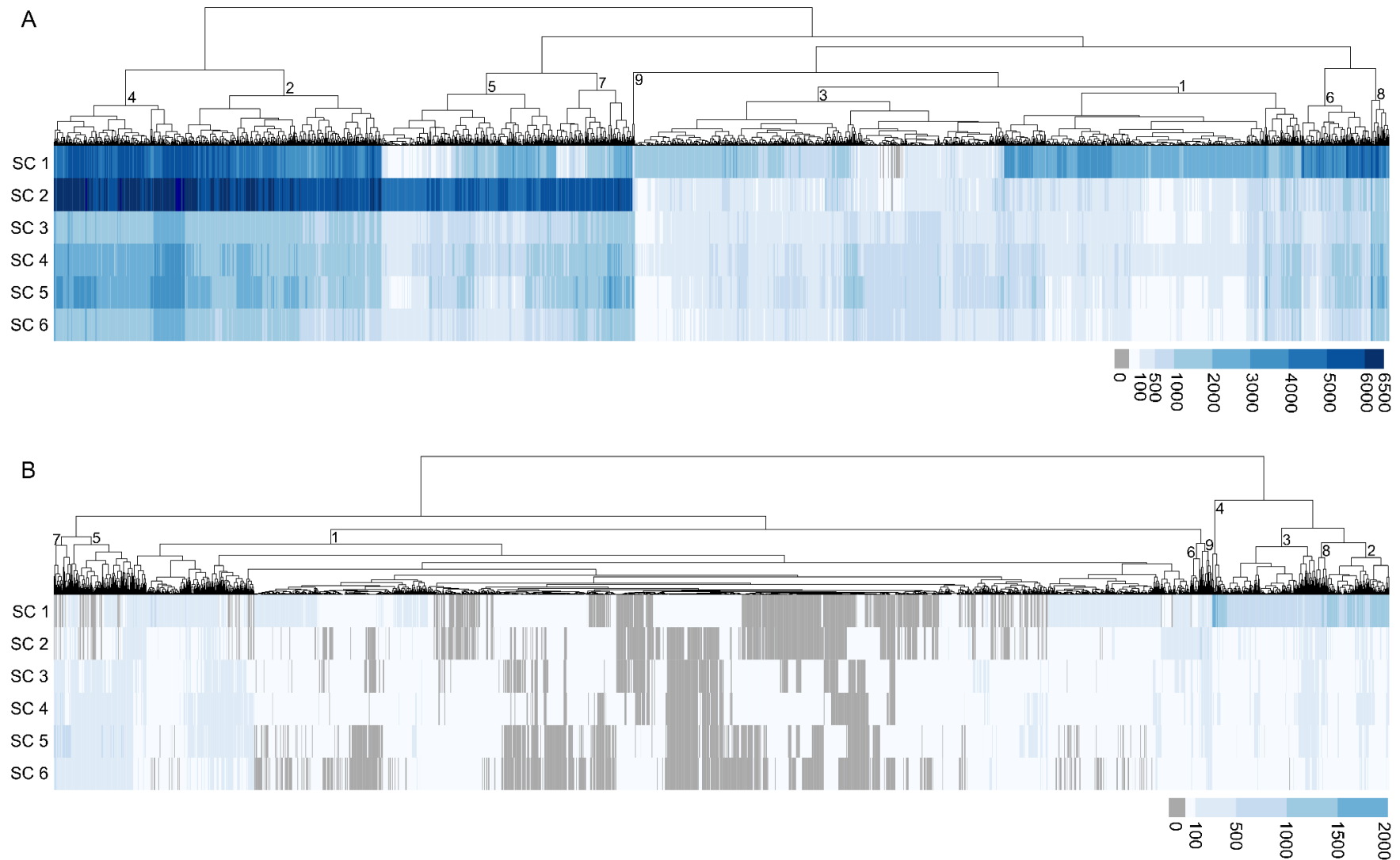


**Figure 35.** Heatmaps displaying the cumulative abundance of KEGG KO annotated genes per depth within the Metagenome Assembled Genomes (MAGs). (A) Representing the abundant genes and (B) representing the rare genes in each sample. The numbers on the dendrogram of each heatmap correspond to the clusters.

metabolism, glycan metabolism, and metabolism of cofactors and vitamins. Several important pathways were identified within the pathway modules of central carbohydrate metabolism, including gluconeogenesis, pyruvate oxidation, the citrate cycle (also known as the TCA cycle), pentose phosphate pathway, and PRPP biosynthesis.

Results highlighted the relevance of several key chemolithotrophic pathways in the anchialine ecosystem. Specifically, the thiosulfate oxidation pathway, which is catalyzed by the SOX complex and converts thiosulfate to sulfate; the nitrogen fixation pathway, which converts atmospheric nitrogen into ammonia, and the carbon fixation pathway, which includes the reductive citrate cycle (also known as the Arnon-Buchanan cycle) and the phosphate acetyltransferase-acetate kinase pathway.

#### 3.3.3.1. The carbon cycle

A range of carbon pathways was identified in the prokaryotic community with incomplete pathways for methanogenesis and methanotrophy (**Figure 36**). Carbon fixation pathways observed were the Calvin–Benson Cycle, acetogenesis via the Wood–Ljungdahl pathway (reductive acetyl-CoA), 3-hydroxypropionate cycle (3HP), 4-hydroxybutyrate pathway (4HB), as well as a low abundance of reverse TCA (rTCA) cycle genes (**Figure 36, Figure 37**). Reverse TCA cycle genes (*aclA*, *aclB*) were most abundant in the depth SC2 present mainly in Campylobacteria MAGs. Conversely, genes for the Calvin–Benson cycle (*rbcL*) were abundant in the freshwater layer present in bacterial Gammaproteobacteria (Burkhoderiales) and in layers below SC2 in the high number of MAGs ( $n=45$ ) assigned to Nanoarchaeota and Ianarchaeota adapted to anoxygenic conditions (**Figure 37**). Genes involved in C1 metabolism, methanol and formaldehyde oxidation, together with methane monooxygenase, were rare with low relative abundance. Anoxygenic photosystem I (*pufLM*) pathway was found in two MAGs associated with Alpha- and Gammaproteobacteria abundant in the SC1, while anoxygenic photosystem II was found only in one MAG associated with Chlorobia abundant in SC3.

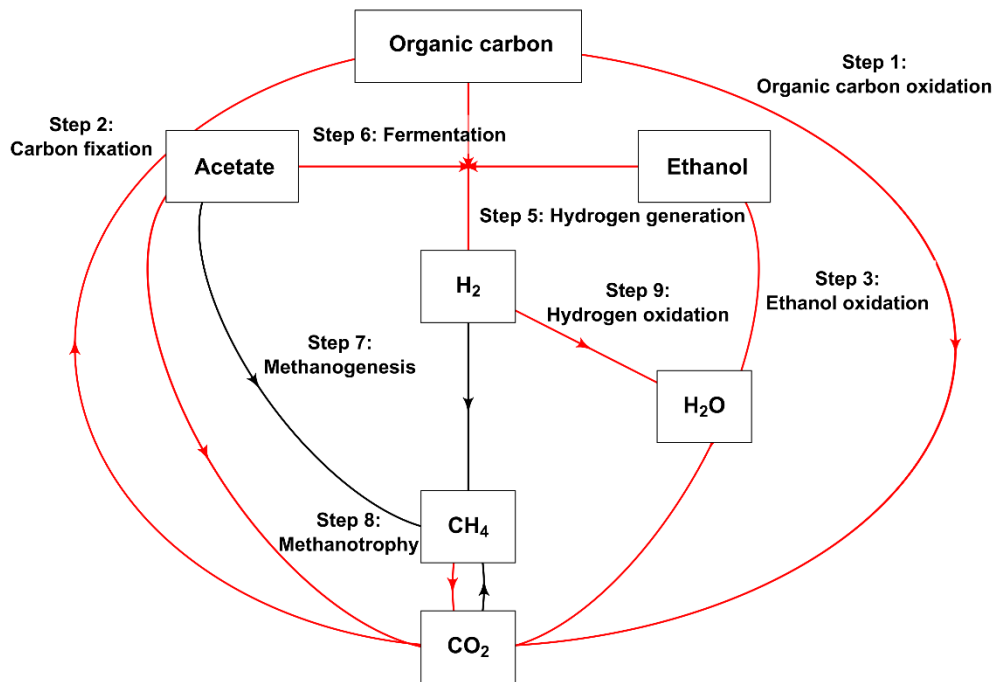


**Figure 36.** Diverse microbial-mediated sub-pathways of carbon metabolism in anchialine speleological object. Red arrows denote the presence of sub-pathways, while their absence is indicated with black arrows.

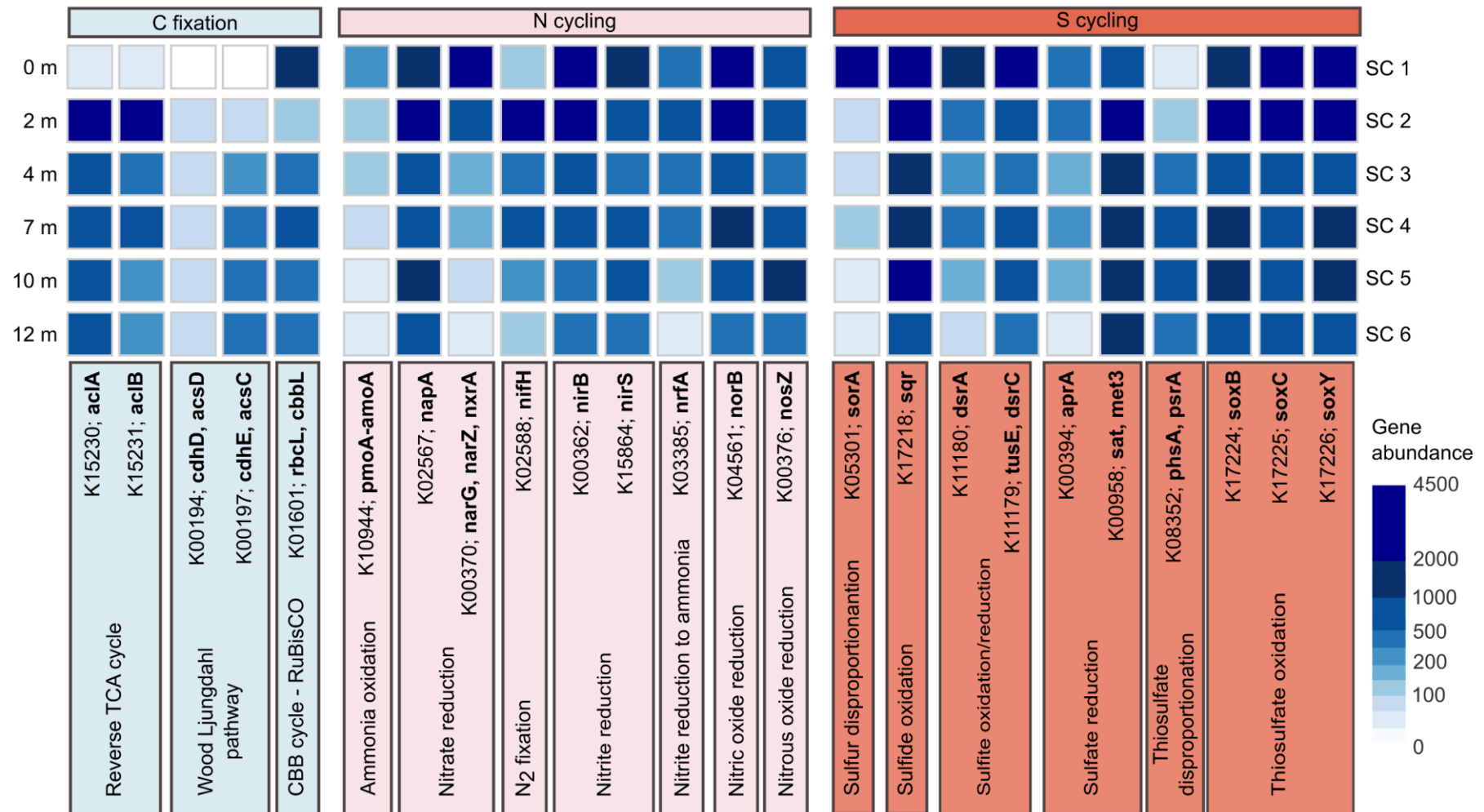


**Figure 37.** Heatmap depicting the abundance of key functional genes involved in carbon fixation, nitrogen cycling, and sulfur cycling across depths within the anchialine speleological object.

### 3.3.3.2. The sulfur cycle

Across the salinity gradient, complete sets of genes associated with both assimilatory and dissimilatory sulfate reduction, and thiosulfate oxidation by SOX complex were identified in all depths (**Figure 38**). Assimilatory sulfate reduction genes were mostly affiliated with Gammaproteobacteria (n=16). In total, 40 MAGs encoded complete assimilatory sulfate reduction, while partial assimilatory sulfate reduction pathways were present in the majority of MAGs. The complete dissimilatory sulfate reduction pathway (aprAB, dsrAB, and sat) was found in 19 MAGs assigned to Desulfobacterota (Desulfobaccia, Desulfobulbia, Desulfobacteria; n=14), Gammaproteobacteria (Burkholderiales; n=3) and AABM5-125-24 (n=2). Genes encoding the thiosulfate oxidation by SOX complex were annotated in 20 MAGs belonging to phyla Campylobacterota (n=7) and Proteobacteria (n=13).

Abundant genes were involved in sulfur oxidation (sor), sulfide oxidation (sqr), and thiosulfate oxidation pathways. The genes encoding thiosulfate oxidation (SOX) were found in 23 MAGs assigned mainly to Campylobacteria and Gammaproteobacteria (Burkholderiales) (**Figure 37**).

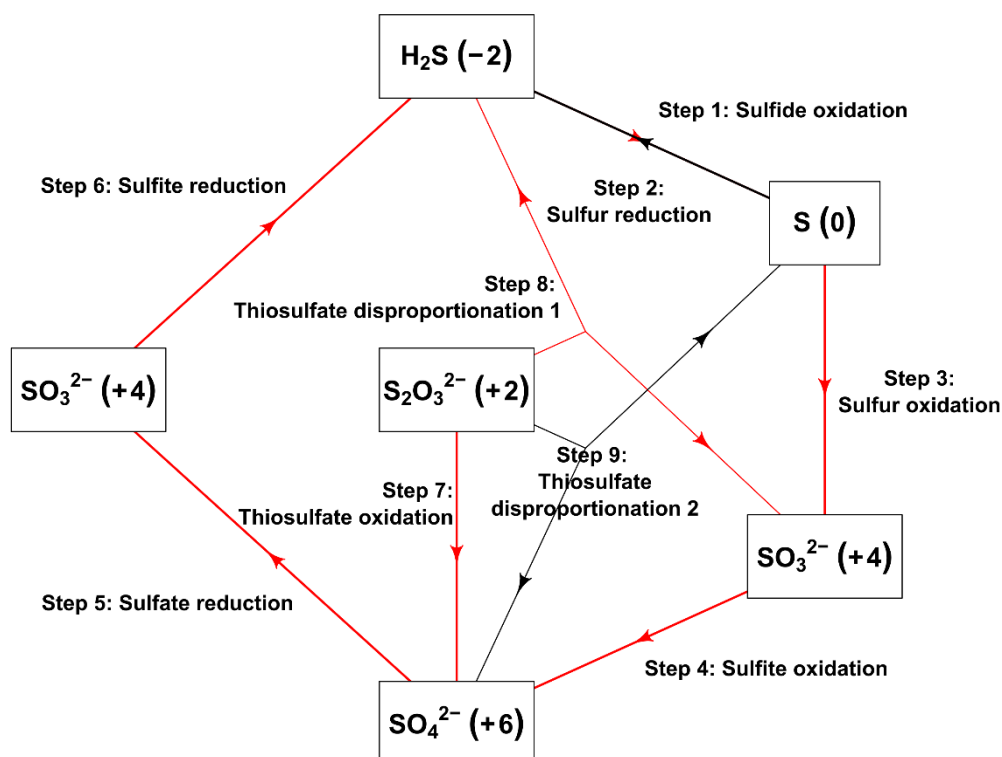


**Figure 38.** Diverse microbial-mediated sub-pathways of sulfur metabolism in anchialine speleological object. Red arrows denote the presence of sub-pathways, while their absence is indicated with black arrows.

### 3.3.3.3. The nitrogen cycle

In the anchialine speleological object, complete pathways of dissimilatory nitrate reduction to ammonium (DNRA), assimilatory nitrate reduction (Step 4), denitrification (Step 4-7), and nitrogen fixation (Step 1) were identified (**Figure 39**). Nitrate reductase (narG) was more enriched in SC1 together with nitrite reductase (nirBS), whereas the nitrous-oxide reductase (nosZ) was more abundant in anoxic layers SC5 (**Figure 37**). Nitrogen fixation genes (nifDHK) were abundant in the sample SC2 and were affiliated with Desulfobacterota, Campylobacterota, and Brukhorderiales (Gammaproteobacteria) (**Figure 37**). Most of the MAGs had partial dissimilatory nitrate reduction to ammonium and denitrification pathways.

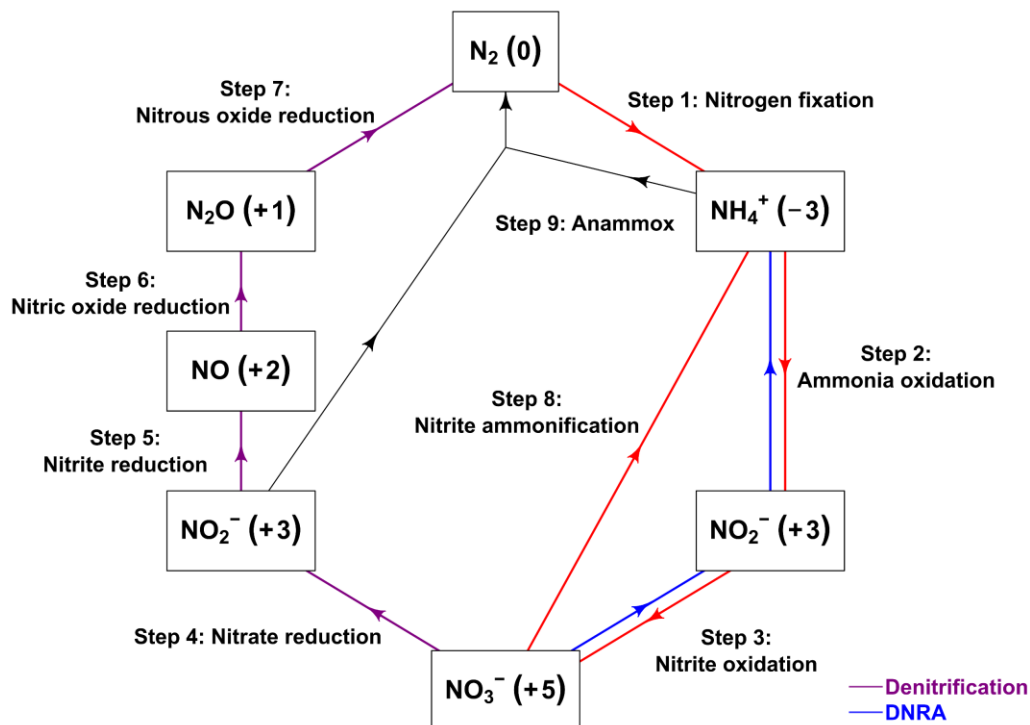


**Figure 39.** Diverse microbial-mediated sub-pathways of nitrogen metabolism in anchialine speleological object. Black arrows denote the absence of sub-pathways. DNRA - dissimilatory nitrate reduction to ammonium.

## 4. DISCUSSION

### 4.1. Diversity patterns of protists and fungi in the water column of the ultra-oligotrophic south Pacific Gyre area

Conducted research along the subtropical South Pacific Gyre (SPG) encompassing epipelagic, mesopelagic and bathypelagic zones, provides new insights into the vertical and longitudinal distribution of taxonomic and functional composition of protists and fungi. Taking place during the Australian summer, the research cruise covered a vast geographical area of 7,000 km along the SPG, comprising samples within the longitudinal scale of 5,5000 km in which the diversity and composition of the protistan and fungal community was analyzed using 18S and ITS region, respectively.

The similarity analysis revealed significant differences in the oceanic protist community regarding water depth. Depth was identified as a major driver of protist community composition, which aligns with previous studies (Countway et al., 2007; Giner et al., 2019; Ollison et al., 2021; Schnetzer et al., 2011; Yeh and Fuhrman, 2022). The distribution pattern of protists closely resembled that of the bacterial community diversity studied in the same period within the SPG (Reintjes et al., 2019). Notably, the composition of the bacterial community exhibited substantial changes with increasing depth, primarily driven by variation in light variability (Reintjes et al., 2019). The most pronounced shifts in bacterial composition occurred in the 1% irradiance zone, characterized by a decline in the abundance of mesopelagic clades (Reintjes et al., 2019). A prior study on photosynthetic microbial communities found that the photosynthetic community primarily comprised *Prochlorococcus*, aerobic anoxygenic phototrophs, and a diverse community of small photosynthetic eukaryotes. Surprisingly, photosynthetic activity spanned the euphotic zone rather than concentrated solely at the deep chlorophyll maximum (DCM), with 68-79% of primary productivity occurring above DCM (Duerschlag et al., 2022) aligning with the observation in this study.

In this study, the significant correlations was identified between environmental variables and protistan diversity, highlighting the impact of abiotic factors on community dynamics within the upper 300 m of the water column. The results indicate that protistan diversity is primarily influenced by temperature and nitrogen availability rather than other environmental factors or geography. These results are consistent with the vertical stratification of microbial communities, which respond to changes in physicochemical parameters, such as light, temperature, and nutrient availability (Sunagawa et al., 2015). Notably, the extremely low concentrations of inorganic nitrogen throughout the euphotic zone indicate the importance of

nutrient recycling for primary production in the SPG. This emphasizes the crucial role of heterotrophic activities responsible for the breakdown and recycling of organic matter (Duerschlag et al., 2022). Protists exhibit diverse metabolic capabilities, including photosynthetic, mixotrophic and heterotrophic (parasitic). This versatility allows protists to contribute to the export of organic matter through their photosynthetic activities in the euphotic zone and the remineralization processes within the mesopelagic zone within the same regional environment (Cohen et al., 2021).

A high proportion of Alveolata was recorded in the western North Pacific (Sogawa et al., 2022). The aphotic zone of the SPG exhibited a greater prevalence of parasitic communities, indicating their heightened contribution to the overall ecosystem. However, despite the differences in relative read abundances, there was also a notable similarity between the communities. This similarity suggests that ecologically and morphologically similar species have likely partitioned their ecological niches, allowing for their coexistence in the region. A high prevalence of parasitic protists was also recorded in the diel sampling, with the highest contribution of Syndiniales. Previous studies confirmed their wide distribution and genetic diversity due to their ability to colonize a wide range of ecological niches, which was also represented in the results (Clarke et al., 2019; Rizos et al., 2023; Sehein et al., 2022; Yan et al., 2023; Zamora-Terol et al., 2021). Parasitism is an important source of mortality within marine protist communities, though it is seldom accounted for in ecosystem and biogeochemical models (Guillou et al., 2008). Previous studies have revealed the presence of distinct communities of heterotrophic protists in both the photic and aphotic layers of the water column on a global scale.

Additionally, previous research has shown that the mesopelagic zone exhibits high metabolic activity among protists and approximately 90% of carbon is respired in this particular layer. Syndiniales, highly abundant in studied samples, appear to have a significant role as parasites in SPG food webs, although this interaction has been overlooked. This suggests a potential feedback mechanism between parasitic infections, the release of organic matter, and prokaryotic assimilative activity. The capacity of these parasitoids to control their hosts is highly dependent on the parasitic fitness and mechanisms underlying the parasitic specificity (Anderson and Harvey, 2020; Chambouvet et al., 2008). Host density is thought to be the main determinant of parasite abundance and infection rates, with increased host encounters and infections occurring under conditions of a plankton bloom. Other factors may influence Syndinial population dynamics, such as temperature, nutrients, water column depth, and degree of physical mixing, although these factors have not been studied extensively (Jephcott et al.,

2016). In addition, zoosporic parasites likely play a significant role in maintaining genetic polymorphism and biodiversity in host populations and regulating phytoplankton succession. They can infect several types of plankton including protozoan, such as dinoflagellates or ciliates, and metazoans, such as crustaceans and copepods as endoparasites. Because of their short generation times and abundant progeny, zoosporic parasitoids exert important top-down control that significantly influences entire aquatic food webs, especially phytoplankton population dynamics. The limited diel resolution in this study makes it difficult to identify reliable factors influencing Syndiniales populations under different ecological and biological conditions (Hu et al., 2018).

The global planktonic marine fungal community has been found to cluster by the ocean, suggesting that fungal dispersal occurs in oceans (Ettinger et al., 2021; Hassett et al., 2019). Results in this study have shown the clustering of fungal communities among the site and confirmed that site-to-site variation was a stronger factor in explaining fungal community structure, suggesting that local environmental filtering may play a critical role in assembling the fungal community in SPG (Ettinger et al., 2021). The homogeneous fungal community patterns observed in ultra-oligotrophic sampling station 6 the "oligotrophic eye" reflect surprisingly stable community composition across the vertical depth profile from 20 to 3600m. Along the transect, high abundance of potentially labile unsaturated aliphatic molecular formula with a low degradation index for the dissolved organic matter of likely marine microbial origin (Osterholz et al., 2021). In a previous study, at sampling station 6, bacterial community considerable external hydrolysis as well as extensive selfish substrate uptake-imply that these organisms are capable of both mechanisms of polysaccharide processing (Reintjes et al., 2020). The typically oligotrophic conditions would suggest low environmental abundances of pelagic fungi, which may increase under eutrophication or dissolved organic carbon enrichment, as observed for copiotrophic bacteria. Although few studies have tried to quantify their actual biomass, it seems this can even exceed that of bacteria, particularly in habitats rich in organic carbon (Bochdansky et al., 2017; Richards et al., 2012). The fungal community in the SPG, specifically inhabiting the aphotic realm, revealed that environmental factors, especially oxygen and nitrate, were closely related to fungal diversity. The prevalent taxon *Rhodotula* is predominant basidiomycetes in the marine environment, where they have been sourced from seawater, sediment, and hydrothermal vent, but also as symbionts of marine invertebrates and seaweeds (Buedenbender et al., 2021; Nagahama et al., 2001; Richards et al., 2012). New studies of deep-sea sediment fungi isolates in SPG have shown their metabolic capability of

degradation of aromatic compounds, lignin, lignocellulose, carbonate, and carboxylic acids (Sobol et al., 2023).

The following study provides evidence of the previously unrecognized occurrence of parasitic protists and fungi in the nutrient-limited South Pacific Gyre. In this work, the protistan community was analyzed focusing on the significant presence of parasitic protists, which were found to be particularly abundant in the upper 300 m of the aphotic zone in the SPG. Additionally, this study of fungal communities revealed their distinct presence in the aphotic zone at the central part of the SPG, suggesting their substantial contribution to yet insufficiently described microbial food web. To draw broader conclusions, additional samplings are required to ensure significant reliability and enhance the applicability of the presented findings. Exploring the diversity of fungi and their interactions with protistan and prokaryotic communities will enable us to understand open ocean ecosystems comprehensively.

## **4.2. Diversity patterns of prokaryotes and protists in the water column of anchialine pits and caves in the area of Kornati National Park**

Anchialine speleological objects represent an understudied subterranean environment, especially at the microbiological level (Hoffman et al., 2020). In this context, this study provides an overview of the microbial life (protistan together with fungal, and prokaryotic community) in the water column throughout the halocline of this enigmatic karstic environment in the Mediterranean region. Investigated caves and pits are located on nearby islands and connected to the same marine basin. The surface area of anchialine speleological object is influenced by different anthropological or non-anthropological interventions (birds or bat nests, Roman amphorae). These specific inland environments characterized by a salinity-stratified water column and saltwater exchange with the sea, specific physical and chemical parameters, depth, and isolated position represent the appropriate study sites for allopatric speciation processes. The observed microbial biodiversity is comparable with different anchialine ecosystems in other environments (Addesso et al., 2021). The conducted Co-Inertia Analysis (CIA) resulted in a strong statistically significant correlation between protistan and prokaryotic communities in the different caves (V. Edgcomb, 2016). This site-specific adaptation is a very rare case in marine environments (Stock et al., 2013).

Another interesting point of results is the low percentage of shared Operational Taxonomic Units (OTUs) between the caves (only 2% in the prokaryotic and 8.1% in the protistan community) and the lack of the distance-decay relationships, which can be explained by only one sampling date per cave. OTUs analysis on high taxonomic levels demonstrated that the taxon composition shifted markedly by anchialine speleological object and sampling depth both in the protistan and prokaryotic communities (Campbell and Kirchman, 2013). The difference can be governed by some physical or chemical data that has not been measured or by the mass effect and dispersal, but all this has to be studied in more depth (Zhu et al., 2019).

Only in the BP cave, the richness and the Shannon index of the protistan community had not followed a similar pattern. This cave is the deepest among other sampled caves and the most branched with speleothems in the submerged part. The highest protistan richness was detected in the area below the halocline in Gravnjača (GKV) and Živa Voda (ZVP) cave, while the lowest in the area above and below the halocline in the Vjetruša (VG) cave. Alveolata and Stramenopiles were the most diverse and abundant groups, as observed in other ecosystems (Adl et al., 2012; Gong et al., 2015). A decrease in Alveolata with depth was detected in two caves (Blitvica (BP) and GKV), where an increase of Fungi with depth was recorded.

Commonly found in marine and brackish water, ciliates affiliated to the taxon *Mesodinium* were the major contributor to the protistan community above the halocline in the VG cave (Nishitani and Yamaguchi, 2018). In and below the halocline, Alveolata was represented with the highest relative abundance of OTUs affiliated to the apicomplexan parasite *Besnoitia* (Y. Zhang et al., 2022). Compared to the VG cave, different Alveolata genera (*Oxyrrhis*) dominated the area with the lowest salinity concentration in the BP cave. Despite being known as globally distributed euryhaline and eurythermal dinoflagellate taxon with prevalence in intertidal pools and estuaries, it was reported that reduced salinity, caused by freshwater inflow, may stimulate blooms of this taxon (Guo et al., 2013).

In the GKV cave, the geographically most distant cave that during the Roman time was used as a freshwater source, Alveolata were highly dominated by Ciliophora. The area above the halocline was dominated by the subclass Scuticociliatia. This subclass gathers free-living ciliates in fresh, brackish and marine water together with opportunistic or facultative parasitic ciliates of aquatic animals (T. Zhang et al., 2019). Parasitic ciliate *Uronema* (Scuticociliatia) produces proteases responsible for the digestion of the host's tissues and proteins responsible for the high mortality rates of fish (Cardoso et al., 2017). However, fishes were not recorded in any of the investigated cave. The lowest OTU richness was recorded in the halocline, where the nonphotosynthetic phagotrophic chrysomonads *Paraphysomonas* contributed with a high relative abundance (83.5%). Usually known as important feeders on bacteria, *Paraphysomonas* can be found as a freely swimming cell and also occurring attached to bacterial mats or other surfaces (Scoble and Cavalier-Smith, 2014).

Compared to other sampled caves, the highest protistan diversity based on the higher taxon groups was established in the ZVP cave, the shallowest sampled cave, with the dominance of Stramenopiles, Alveolata, Fungi, Chloroplastida, Heterolobosea and Rhizaria in the surface area. The relative abundance of Stramenopiles and Fungi has followed the decrease by the depth within the salinity gradient, whereas the relative abundance of Alveolata increased, ranging from 30.6% to 71.0%. Above the halocline, OTUs affiliated to Chrysophyceae and Synurophyceae reached a total relative abundance of 40.5%, with the highest contribution of uncultured Chrysophyceae (32%) and *Poterioochromonas* (4.6%; Moser and Weisse, 2011). The fungal community within the salinity gradient shifted the dominance of genera from *Malassezia* (Basidiomycota) to *Verrucoconiothyrium* (Ascomycota). Ciliates (scuticociliate *Protocyclidium* and holotrichous ciliate *Prorodon*) dominated in the low-nutrient conditions in and below the halocline. Fungi were numerous in all layers with the highest abundance (69.1%) in the hypoxic marine-like area, dominated by genera *Malassezia*, *Cladosporium* and

*Pseudobersingtonia*. Species of this genera often have pathogenic or saprophytic lifestyles, e.g., *Malassezia* is a lipid-dependent basidiomycetous yeast accounting for the majority of the eukaryotic diversity in deep-sea subsurface sediments (Amend, 2014; V. P. Edgcomb et al., 2011).

The prokaryotic community was partially dominated in all the investigated caves by Gammaproteobacteria, and it was not possible to identify a partially similar pattern in richness and alpha diversity as it was in the protistan community. In the shallowest cave (ZVP), where the sunlight enters into the surface layers of the cave, the highest richness was detected. Although this cave was not the richest in nutrients, this is the only cave where the influence of the light could have an impact on the community. In the VG cave, the abundance of Thaumarchaeota, Bacteroidetes, Gemmatimonadetes and Nitrospirae decreased with the increasing salinity gradient, while the abundance of Gammaproteobacteria, Firmicutes and Actinobacteria was greatest below the halocline. The ammonia-oxidizing archaea Nitrososphaeria, which relies solely on the energy generated from the oxidation of ammonia, was recorded in high abundance above (29%) and the area of halocline (12.8%), corresponding with the highest concentration of ammonium with organic nitrogen (4.3 mg L<sup>-1</sup>; Wang et al., 2019). Bacteroidetes, together with a polyphosphate accumulating Gemmatimonadaceae (DeBruyn et al., 2011), were also abundant in the surface area, contributing to chemoheterotrophy. The lowest DO concentration (1.9 mg L<sup>-1</sup>) was measured below the halocline, where the Gammaproteobacteria, Firmicutes and Actinobacteria had the highest relative abundance. The common kestrel nests and bats were detected in this cave that could have a possible contribution to the source of pathogenic bacterial strains below the halocline. The only taxon contributing to the prokaryotic community below the halocline that is not corroborated as pathogenic was *Lactobacillus*.

In the prokaryotic community of the BP cave, the most prominent archaeal lineage was Thaumarchaeota, with a similar contribution to the relative abundance and decreasing by the increasing salinity as in the VG cave. The ammonia-oxidizing archaea, *Nitrosopumilus* and *Nitrosoarchaeum*, reached a relative abundance of 25.2% in the surface area despite the low concentration of ammonium with organic nitrogen (0.22 mg L<sup>-1</sup>). Bacteroidetes, including the strictly aerobic and chemoorganotrophic family Cryomorphaceae and *Algoriphagus* (Cyclobacteriaceae), were abundant in the area above the halocline. Although previous studies showed their prevalence in the productive ocean and coastal regions, no specific associations with organic matter of Cryomorphaceae are known (Bowman, 2020). The transition of genera in the salinity gradient was demonstrated by the relative abundance of Actinobacteria and Gammaproteobacteria. In the surface area, Candidatus *Aquilina* and RS62 marine group

dominated, while in the marine-like area, *Rhodococcus* and order Pseudomonadales. The highest OTU richness of the prokaryotic community in this cave was determined in the hypoxic halocline. This could be correlated to the higher bacterial activity in this layer (Korlević et al., 2016). Below the halocline recorded community was characterized as pathogenic with the majority of the genera related to *Rhodococcus*, *Sphingomonas*, *Arcobacter*, *Lawsonella* and *Staphylococcus*. The source of this pathogenic bacteria remains unclear.

The main prokaryotic groups detected in the surface area of the GKV cave were Gammaproteobacteria, Alphaproteobacteria and Bacteroidetes. Ubiquitous gram-negative and non-fermenting coccobacilli *Acinetobacter* (11.5%) had the highest relative abundance among other Gammaproteobacteria together with ubiquitous gram-negative and aerobic or facultatively anaerobic *Myroides* (9.1%) from phyla Bacteroidetes. *Acinetobacter* species are widely distributed in nature and their growth may be enhanced by the contaminated environment such as hydrocarbon contaminated areas, activated sludge, sewage (Al Atrouni et al., 2016), whereas relatively little is known of pathogenic taxon *Myroides* with proven high multi-drug resistance (Meyer et al., 2019). The lowest OTU richness of the prokaryotic community in GKV cave was recorded in the area of halocline with the highest abundance of Actinobacteria and Rhodobacteraceae. Marine actinobacterial lineage PeM15 (39.1%) is identified in various habitats from aerobic to anaerobic environments and is very sensitive to nutrient enrichment (Arocha-Garza et al., 2017). Heterotrophic Marine Group II (Thermoplasmata) has reached the highest relative abundance above and below the halocline known to reside mostly in the photic zone with unique organic carbon degradation pattern (C. L. Zhang et al., 2015).

The highest concentration of ammonium with organic nitrogen and TOC was measured in the surface area of the ZVP cave, potentially contributing to the development of the prokaryotic community. The relative abundance of Gammaproteobacteria, Alphaproteobacteria, Bacteroidetes and Actinobacteria decreased with the increasing salinity gradient, while Epsilonbacteraeota, Omnitrophicaeota and Marinimicrobia (SAR406 clade) were most abundant in the marine-like layer. The taxon *Limnohabitans* had the greatest relative abundance (18.8%) compared to other detected Betaproteobacteriales. This taxon is characterized by a high growth rate and metabolic flexibility with a notably tight relationship to algae-derived organic substances (Šimek et al., 2013). Decreased DO and low nutrient concentration contributed to the diversity of the prokaryotic community in and below the halocline, with the highest OTU richness recorded below the halocline. Genera associated with chemically distinct environments enriched with sulfur compounds were detected in the halocline *Sulfurimonas*

(Epsilonbacteraeota), Ectothiorhodospiraceae (Gammaproteobacteria) and *Desulfatiglans* (Deltaproteobacteria). In depth with the highest salinity and lowest DO, archaeal phylum Epsilonbacteraeota, Omnitrophicaeota and Gammaproteobacteria were detected (Baricz et al., 2021; Glöckner et al., 2010).

This study identifies specific transitional boundaries for protistan and prokaryotic communities in the salinity gradient of anchialine speleological objects. Each anchialine speleological object had a unique protistan and prokaryotic community, indicating that anchialine niches play an important role in determining the microbial diversity of anchialine speleological objects. This result also confirms the highly endemic character of anchialine environments and targeted studies should therefore be carried out to reveal the extent of the diversity and the ecological roles of the protistan and prokaryotic communities.

### **4.3. Diversity patterns of prokaryotes in the water column of the anchialine speleological object in the Martinska area**

Salinity is often considered to be the major factor shaping prokaryote community composition in diverse habitats acting as a critical environmental filter (Lozupone and Knight, 2007; Thompson et al., 2017). Previous study conducted in anchialine caves and pits in the National park Kornati area has shown a high diversity of prokaryotic communities within the salinity and oxygen gradient (Kajan et al., 2022). To advance the prior research, a comprehensive study encompassing three distinct methodological approaches has been employed to elucidate the taxonomic composition, activity, and functional capabilities of the prokaryotic community within the anchialine speleological object in the Martinska area. Firstly, the study used 16S rRNA gene amplicon sequencing to evaluate the general composition of the prokaryotic community. Secondly, a combination of CARD-FISH and BONCAT was utilized to investigate the prokaryotic community's activity and identity. Thirdly, metagenomic datasets were generated to obtain a comprehensive view of the ecosystem and the functional profile of the stratified microbial community at the genome level.

In order to capture the temporal variation of the prokaryotic community, sampling was conducted in three months (March, April, and August). The sampling within the anchialine speleological object in the Martinska area was limited to a depth of 12 meters due to the cave's passage geometry. Throughout the sampling period, the studied anchialine speleological object maintained stable both in oxygen and salinity gradients along the depth. This particular anchialine speleological object serves as an illustrative example of an environment characterized by numerous pronounced gradients, resembling a miniature underground natural Winogradsky column for liquid substances. For this study, a larger number of samples than in the previous study by Kajan et al. (2022) was used to observe the community niche dispersion and transition.

A preliminary overview of the microbial community by 16S rRNA amplicon analysis showed the temporal development and stabilization of oxycline from March to August. Overall, differences in prokaryotic community compositions were detected between the samples in oxic and anoxic regions. In the freshwater layer, the most abundant were bacteria, accounting for lower diversity but higher cell abundance and activity. High taxonomic variability was detected in the anoxic saline layers with a high diversity of DPANN, Omnitrochota and Patescibacteria. Similar pattern of high abundance of DPANN affiliated Metagenome Assembled Genomes (MAGs) was observed in the anoxic strata of meromictic ice-capped Lake A in the Canadian

High Arctic (Vigneron et al., 2022). Within the meromictic community, thiosulfate oxidation potential was detected in aerobic Woesearchaeota, whereas diverse metabolic functions were identified in anaerobic DPANN archaea, including degradation and fermentation of cellular compounds, and sulfide and polysulfide reduction (Vigneron et al., 2022).

The diversity of prokaryotic community detected in anchialine speleological object has showed high similarities to diverse extreme ecosystems, i.e. hypersaline Arctic spring (Macey et al., 2020; Magnuson et al., 2023), hydrothermal sediments (Krukenberg et al., 2021), deep-sea hydrothermal vent sulfide chimneys (Hou et al., 2020).

Interestingly, only 3 MAGs contained genes indicating photosynthetic capabilities. Within the freshwater strata, two distinct Proteobacterial taxa, *Aestuariivirga* and SYFN01 were observed (Padilla Crespo et al., 2020). Conversely, in the anoxic strata, the presence of green sulfur bacteria *Chlorobium* was detected (Berg et al., 2019; Vigneron et al., 2021).

Prior to the stabilization of oxy- and thermocline in August, the freshwater layers were dominated by Bacteroidota (*Pseudarcicella*), a typical freshwater microorganism (Zwirgmaier et al., 2015). Clearly and as shown based on the community composition data, a bloom of a MAG affiliated to the phylum Campylobacterota (Arcobacteraceae; CAIJNA01) was detected at the SC2 stratum that coincided with the oxycline in August. Based on the MAG abundance results, it was detected as present in all depths and represented the most abundant MAG in layers SC2, SC3 and SC4, however, it remains unclear as to whether this bacterium is active in the anoxic layers (SC3 and SC4) or its abundance in these layers is due to sedimentation of the intense bloom developed at SC2. Previous study in the tropical subterranean estuary detected that microbial community within the chemocline was dominated by *Sulfurimonas* and *Sulfurovum* of the Campylobacteria likely responsible for sulfide oxidation coupled with nitrate reduction (Aronson et al., 2023; Huang et al., 2021). Campylobacterota are usually a predominant bacterial primary producer in hydrothermal mixing zones (Campbell et al., 2006; Nakagawa et al., 2005; Oren & Garrity, 2021). Among the deep-sea vent Campylobacterota genera including both free-living forms and epi- or endosymbionts of invertebrates, intraspecific variability in energy metabolism along with available redox couples is observed (Yoshida-Takashima et al., 2022).

Prevalence of dissimilatory metabolisms such as SOX complex, dissimilatory sulfate reduction and nitrogen fixation have been shown to be directly connected to environmental gradient (oxygen gradient specifically). Inspecting the distribution of different KOs along the depth profile highlights some dissimilatory metabolic modules that are more prevalent at certain depths. Abundance-corrected profiles of KOs show the peak abundance of dissimilatory

functions related to thiosulfate oxidation by SOX complex and nitrogen fixation at the SC2 layer. As previously shown, the whole anoxic gradient of anchialine speleological object was dominated by sulfur-oxidizing bacteria, contrasting to the community detected in the Australian anchialine cave, where thiosulphate disproportionation was driven by diverse bacterial phyla (Ghaly et al., 2023). Furthermore, unlike the findings in this research, the Australian anchialine cave exhibited the presence of C1 metabolism in conjunction with a fully functional nitrogen and sulfate pathway (Ghaly et al., 2023).

The complete dissimilatory sulfate reduction pathway was annotated in MAGs assigned to Desulfobacterota (*Desulfobaccia*, *Desulfobulbia*, *Desulfobacteria*), Gammaproteobacteria (Burkholderiales), and AABM5-125-24. Desulfobacterota were found to be the main drivers for the sulfate reduction process and production of the toxic hydrogen sulfide in the lake water column (Cabello-Yeves et al., 2023; Diao et al., 2018). The analyses show that MAGs containing the core dissimilatory metabolism of each niche seem to have dissimilar metabolic profiles that allow them to furnish their niches further.

This study identifies specific transitional boundaries of prokaryotic communities in the salinity gradient of an anchialine speleological objects. In addition to their diverging metabolic profile, these MAGs represent different patterns of stratification along the water column that further rebuts their functional redundancy at a community and ecosystem level as well (Louca and al., 2016, 2018).

## 5. CONCLUSIONS

The overall research and results presented within this doctoral dissertation provide insight into the biodiversity and ecological roles of the microbial communities present in marine oligotrophic ecosystems. The final remarks of this dissertation can be summarized in the following points:

1. Physicochemical gradients, including light penetration, oxygen concentration and salinity, along with nutrient limitation, play a crucial role in defining the community composition and dynamics within the studied oligotrophic marine ecosystems.
2. The first hypothesis, „*The presence of protist and fungal communities in the ultra-oligotrophic South Pacific Gyre depends on the depth of light penetration (photic zone).*“ was confirmed by the following:
  - The presence of protistan communities in the ultra-oligotrophic South Pacific Gyre reflect the environment and is associated with the depth of light penetration. This is evident from the inability to detect the 18S sequences of protists below the 1% irradiance zone. In addition to light penetration, temperature and nitrogen availability significantly influence protistan diversity. Moreover, diel sampling revealed a significant prevalence of parasitic protists in the central part of South Pacific Gyre, with Syndiniales contributing the most with relative read abundance.
  - The results illustrate the clustering of fungal communities based on the sampling site, underscoring that site-specific variation is a more prominent factor in explaining the structure of fungal communities. This implies that local environmental filtering likely plays a crucial role in shaping the fungal community in the South Pacific Gyre.
3. The second hypothesis, „*The composition of protistan and prokaryotic communities in anchialine pits and caves changes with the salinity gradient.*“ was confirmed by the following:
  - Distinct transitional boundaries exist for protistan and prokaryotic communities within the salinity gradient of anchialine speleological objects in National park Kornati. The composition of protistan and prokaryotic communities in anchialine pits and caves changes along the salinity gradient within the water column, demonstrating a notable degree of niche specialization. When analyzing each speleological object individually,

it becomes apparent that salinity primarily influences the variation in community composition. Nevertheless, when studying communities across all four objects, as illustrated in the halocline samples case, it is challenging to exclusively attribute diversity to salinity, given the significant differences observed among the communities.

- Each anchialine speleological object hosts a unique protistan and prokaryotic community, emphasizing the substantial role of niches within speleological objects in shaping microbial diversity.
4. The third hypothesis, „*The diversity, activity and function of the prokaryotic community in anchialine speleological object depends on the availability of oxygen and the salinity gradient.*“ was confirmed by the following:
- The microbial community structure in the anchialine speleological object near Martinska is significantly influenced by salinity and oxygen gradients, resulting in shifts among dominant prokaryotic groups. Notably, there are significant differences in community composition between the freshwater and anoxic saline layers, underscoring the profound impact of environmental conditions on microbial distribution.
  - Various dissimilatory metabolic pathways, such as thiosulfate oxidation, sulfate reduction, and nitrogen fixation, exhibit depth-dependent variations within the anchialine speleological object near Martinska. Specific metabolic modules are more prevalent at distinct depths in the water column.
  - Despite sharing a high percentage of metabolic traits, Metagenome Assembled Genomes (MAGs) represent diverse niches within the ecosystem and are not functionally redundant. They display unique metabolic profiles and exhibit distinct stratification patterns along the water column.

The doctoral dissertation results provide the basis for further research on the functional characteristics of microbial communities in marine oligotrophic ecosystems, particularly in ocean gyres and coastal anchialine ecosystems.

The dissertation underscores the critical role of physicochemical gradients, including light penetration, oxygen concentration, salinity, and nutrient limitation, in shaping the composition and dynamics of the microbial community. Understanding these drivers can aid in predicting how microbial communities may respond to environmental changes.

Overall, this research provides a foundation for future studies in this field and emphasizes the importance of considering site-specific conditions and environmental drivers when studying microbial diversity and function.

## 6. LITERATURE

- Adesso, R., Gonzalez-Pimentel, J. L., D'Angeli, I. M., De Waele, J., Saiz-Jimenez, C., Jurado, V., Miller, A. Z., Cubero, B., Vigliotta, G., & Baldantoni, D. (2021). Microbial Community Characterizing Vermiculations from Karst Caves and Its Role in Their Formation. *Microbial Ecology*, *81*(4), 884–896. <https://doi.org/10.1007/s00248-020-01623-5>
- Adl, S. M., Bass, D., Lane, C. E., Lukeš, J., Schoch, C. L., Smirnov, A., Agatha, S., Berney, C., Brown, M. W., Burki, F., Cárdenas, P., Čepička, I., Chistyakova, L., del Campo, J., Dunthorn, M., Edvardsen, B., Eglit, Y., Guillou, L., Hampl, V., ... Zhang, Q. (2019). Revisions to the Classification, Nomenclature, and Diversity of Eukaryotes. *Journal of Eukaryotic Microbiology*, *66*(1), 4–119. <https://doi.org/10.1111/jeu.12691>
- Adl, S. M., Simpson, A. G. B., Lane, C. E., Lukeš, J., Bass, D., Bowser, S. S., Brown, M. W., Burki, F., Dunthorn, M., Hampl, V., Heiss, A., Hoppenrath, M., Lara, E., le Gall, L., Lynn, D. H., McManus, H., Mitchell, E. A. D., Mozley-Stanridge, S. E., Parfrey, L. W., ... Spiegel, F. W. (2012). The Revised Classification of Eukaryotes. *Journal of Eukaryotic Microbiology*, *59*(5), 429–514. <https://doi.org/10.1111/j.1550-7408.2012.00644.x>
- Al Atrouni, A., Joly-Guillou, M.-L., Hamze, M., & Kempf, M. (2016). Reservoirs of Non-baumannii Acinetobacter Species. *Frontiers in Microbiology*, *7*(FEB), 49. <https://doi.org/10.3389/fmicb.2016.00049>
- Altschul, S. F., Gish, W., Miller, W., Myers, E. W., & Lipman, D. J. (1990). Basic local alignment search tool. *Journal of Molecular Biology*, *215*(3), 403–410. [https://doi.org/10.1016/S0022-2836\(05\)80360-2](https://doi.org/10.1016/S0022-2836(05)80360-2)
- Amann, R. I., Ludwig, W., & Schleifer, K. H. (1995). Phylogenetic identification and in situ detection of individual microbial cells without cultivation. *Microbiological Reviews*, *59*(1), 143–169. <https://doi.org/10.1128/mr.59.1.143-169.1995>
- Amend, A. (2014). From Dandruff to Deep-Sea Vents: Malassezia-like Fungi Are Ecologically Hyper-diverse. *PLoS Pathogens*, *10*(8), e1004277. <https://doi.org/10.1371/journal.ppat.1004277>
- Amend, A., Burgaud, G., Cunliffe, M., Edgcomb, V. P., Ettinger, C. L., Gutiérrez, M. H., Heitman, J., Hom, E. F. Y., Ianiri, G., Jones, A. C., Kagami, M., Picard, K. T., Quandt, C. A., Raghukumar, S., Riquelme, M., Stajich, J., Vargas-Muñiz, J., Walker, A. K., Yarden, O., & Gladfelter, A. S. (2019). Fungi in the Marine Environment: Open Questions and Unsolved Problems. *MBio*, *10*(2). <https://doi.org/10.1128/mBio.01189-18>
- Anderson, S. R., & Harvey, E. L. (2020). Temporal Variability and Ecological Interactions of Parasitic Marine Syndiniales in Coastal Protist Communities. *MSphere*, *5*(3). <https://doi.org/10.1128/mSphere.00209-20>
- Apprill, A., McNally, S., Parsons, R., & Weber, L. (2015). Minor revision to V4 region SSU rRNA 806R gene primer greatly increases detection of SAR11 bacterioplankton. *Aquatic Microbial Ecology*, *75*(2), 129–137. <https://doi.org/10.3354/ame01753>

- Arocha-Garza, H. F., Canales-Del Castillo, R., Eguiarte, L. E., Souza, V., & De la Torre-Zavala, S. (2017). High diversity and suggested endemism of culturable Actinobacteria in an extremely oligotrophic desert oasis. *PeerJ*, 5(5), e3247. <https://doi.org/10.7717/peerj.3247>
- Aronson, H. S., Clark, C. E., LaRowe, D. E., Amend, J. P., Polerecky, L., & Macalady, J. L. (2023). Sulfur disproportionating microbial communities in a dynamic, microoxic-sulfidic karst system. *Geobiology*, August, 1–13. <https://doi.org/10.1111/gbi.12574>
- Azam, F., & Malfatti, F. (2007). Microbial structuring of marine ecosystems. *Nature Reviews Microbiology*, 5(10), 782–791. <https://doi.org/10.1038/nrmicro1747>
- Bailey, G. N., Harff, J., & Sakellariou, D. (2017). *Under the Sea: Archaeology and Palaeolandscapes of the Continental Shelf* (G. N. Bailey, J. Harff, & D. Sakellariou, Eds.; Vol. 20). Springer International Publishing. <https://doi.org/10.1007/978-3-319-53160-1>
- Baltar, F., Zhao, Z., & Herndl, G. J. (2021). Potential and expression of carbohydrate utilization by marine fungi in the global ocean. *Microbiome*, 9(1), 106. <https://doi.org/10.1186/s40168-021-01063-4>
- Baricz, A., Chiriac, C. M., Andrei, A., Bulzu, P., Levei, E. A., Cadar, O., Battes, K. P., Cîmpean, M., Şenilă, M., Cristea, A., Muntean, V., Alexe, M., Coman, C., Szekeres, E. K., Sicora, C. I., Ionescu, A., Blain, D., O'Neill, W. K., Edwards, J., ... Banciu, H. L. (2021). Spatio-temporal insights into microbiology of the freshwater-to-hypersaline, oxic-hypoxic-euxinic waters of Ursu Lake. *Environmental Microbiology*, 23(7), 3523–3540. <https://doi.org/10.1111/1462-2920.14909>
- Barton, L. L., Mandl, M., & Loy, A. (2010). *Geomicrobiology: Molecular and Environmental Perspective*. Springer Netherlands. <https://doi.org/10.1007/978-90-481-9204-5>
- Beaufort, L., Couapel, M., Buchet, N., Claustre, H., & Goyet, C. (2008). Calcite production by coccolithophores in the south east Pacific Ocean. *Biogeosciences*, 5(4), 1101–1117. <https://doi.org/10.5194/bg-5-1101-2008>
- Becking, L. E., Renema, W., Santodomingo, N. K., Hoeksema, B. W., Tuti, Y., & de Voogd, N. J. (2011). Recently discovered landlocked basins in Indonesia reveal high habitat diversity in anchialine systems. *Hydrobiologia*, 677(1), 89–105. <https://doi.org/10.1007/s10750-011-0742-0>
- Bender, M. L., & Jönsson, B. (2016). Is seasonal net community production in the South Pacific Subtropical Gyre anomalously low? *Geophysical Research Letters*, 43(18), 9757–9763. <https://doi.org/10.1002/2016GL070220>
- Benner, R. (2011). Biosequestration of carbon by heterotrophic microorganisms. *Nature Reviews Microbiology*, 9(1), 75–75. <https://doi.org/10.1038/nrmicro2386-c3>
- Benner, R., & Strom, M. (1993). A critical evaluation of the analytical blank associated with DOC measurements by high-temperature catalytic oxidation. *Marine Chemistry*, 41(1–3), 153–160. [https://doi.org/10.1016/0304-4203\(93\)90113-3](https://doi.org/10.1016/0304-4203(93)90113-3)
- Berg, J. S., Pjevac, P., Sommer, T., Buckner, C. R. T., Philippi, M., Hach, P. F., Liebeke, M., Holtappels, M., Danza, F., Tonolla, M., Sengupta, A., Schubert, C. J., Milucka, J., & Kuypers, M. M. M. (2019). Dark aerobic sulfide oxidation by anoxygenic phototrophs in anoxic waters. *Environmental Microbiology*, 21(5), 1611–1626. <https://doi.org/10.1111/1462-2920.14543>

- Bishop, R. E., Humphreys, W. F., Cukrov, N., Žic, V., Boxshall, G. A., Cukrov, M., Iliffe, T. M., Kršinić, F., Moore, W. S., Pohlman, J. W., & Sket, B. (2015). 'Anchialine' redefined as a subterranean estuary in a crevicular or cavernous geological setting. *Journal of Crustacean Biology*, 35(4), 511–514. <https://doi.org/10.1163/1937240X-00002335>
- Bochdansky, A. B., Clouse, M. A., & Herndl, G. J. (2017). Eukaryotic microbes, principally fungi and labyrinthulomycetes, dominate biomass on bathypelagic marine snow. *The ISME Journal*, 11(2), 362–373. <https://doi.org/10.1038/ismej.2016.113>
- Bonnet, S., Guieu, C., Bruyant, F., Prášil, O., Van Wambeke, F., Raimbault, P., Moutin, T., Grob, C., Gorbunov, M. Y., Zehr, J. P., Masquelier, S. M., Garczarek, L., & Claustre, H. (2008). Nutrient limitation of primary productivity in the Southeast Pacific (BIOSOPE cruise). *Biogeosciences*, 5(1), 215–225. <https://doi.org/10.5194/bg-5-215-2008>
- Bowman, J. P. (2020). Out From the Shadows – Resolution of the Taxonomy of the Family Cryomorpaceae. *Frontiers in Microbiology*, 11(May), 1–12. <https://doi.org/10.3389/fmicb.2020.00795>
- Boyd, P. W., & Kennedy, F. (2021). Microbes in a sea of sinking particles. *Nature Microbiology*, 6(12), 1479–1480. <https://doi.org/10.1038/s41564-021-01005-8>
- Brankovits, D., Pohlman, J. W., Niemann, H., Leigh, M. B., Lewis, M. C., Becker, K. W., Iliffe, T. M., Alvarez, F., Lehmann, M. F., & Phillips, B. (2017). Methane- and dissolved organic carbon-fueled microbial loop supports a tropical subterranean estuary ecosystem. *Nature Communications*, 8(1), 1835. <https://doi.org/10.1038/s41467-017-01776-x>
- Bristow, L. A., Mohr, W., Ahmerkamp, S., & Kuypers, M. M. M. (2017). Nutrients that limit growth in the ocean. *Current Biology*, 27(11), R474–R478. <https://doi.org/10.1016/j.cub.2017.03.030>
- Browning, T. J., & Moore, C. M. (2023). Global analysis of ocean phytoplankton nutrient limitation reveals high prevalence of co-limitation. *Nature Communications*, 14(1), 5014. <https://doi.org/10.1038/s41467-023-40774-0>
- Bryant, D. A. (2003). The beauty in small things revealed. *Proceedings of the National Academy of Sciences*, 100(17), 9647–9649. <https://doi.org/10.1073/pnas.1834558100>
- Buedenbender, L., Kumar, A., Blümel, M., Kempken, F., & Tasdemir, D. (2021). Genomics- and Metabolomics-Based Investigation of the Deep-Sea Sediment-Derived Yeast, *Rhodotorula mucilaginosa* 50-3-19/20B. *Marine Drugs*, 19(1), 14. <https://doi.org/10.3390/md19010014>
- Bura-Nakić, E., Helz, G. R., Ciglenečki, I., & Čosović, B. (2009). Reduced sulfur species in a stratified seawater lake (Rogoznica Lake, Croatia); seasonal variations and argument for organic carriers of reactive sulfur. *Geochimica et Cosmochimica Acta*, 73(13), 3738–3751. <https://doi.org/10.1016/j.gca.2009.03.037>
- Cabello-Yeves, P. J., Picazo, A., Roda-Garcia, J. J., Rodriguez-Valera, F., & Camacho, A. (2023). Vertical niche occupation and potential metabolic interplay of microbial consortia in a deeply stratified meromictic model lake. *Limnology and Oceanography*, 1–20. <https://doi.org/10.1002/lno.12437>

- Calbet, A., & Landry, M. R. (2004). Phytoplankton growth, microzooplankton grazing, and carbon cycling in marine systems. *Limnology and Oceanography*, 49(1), 51–57. <https://doi.org/10.4319/lo.2004.49.1.0051>
- Calderón-Gutiérrez, F., Sánchez-Ortiz, C. A., & Huato-Soberanis, L. (2018). Ecological patterns in anchialine caves. *PLOS ONE*, 13(11), e0202909. <https://doi.org/10.1371/journal.pone.0202909>
- Callahan, B. J., Sankaran, K., Fukuyama, J. A., McMurdie, P. J., & Holmes, S. P. (2016). Bioconductor workflow for microbiome data analysis: from raw reads to community analyses. *F1000Research*, 5, 1492. <https://doi.org/10.12688/f1000research.8986.1>
- Campbell, B. J., Engel, A. S., Porter, M. L., & Takai, K. (2006). The versatile  $\epsilon$ -proteobacteria: key players in sulphidic habitats. *Nature Reviews Microbiology*, 4(6), 458–468. <https://doi.org/10.1038/nrmicro1414>
- Campbell, B. J., & Kirchman, D. L. (2013). Bacterial diversity, community structure and potential growth rates along an estuarine salinity gradient. *The ISME Journal*, 7(1), 210–220. <https://doi.org/10.1038/ismej.2012.93>
- Cantalapiedra, C. P., Hernández-Plaza, A., Letunic, I., Bork, P., & Huerta-Cepas, J. (2021). eggNOG-mapper v2: Functional Annotation, Orthology Assignments, and Domain Prediction at the Metagenomic Scale. *Molecular Biology and Evolution*, 38(12), 5825–5829. <https://doi.org/10.1093/molbev/msab293>
- Caporaso, J. G., Kuczynski, J., Stombaugh, J., Bittinger, K., Bushman, F. D., Costello, E. K., Fierer, N., Peña, A. G., Goodrich, J. K., Gordon, J. I., Huttley, G. A., Kelley, S. T., Knights, D., Koenig, J. E., Ley, R. E., Lozupone, C. A., McDonald, D., Muegge, B. D., Pirrung, M., ... Knight, R. (2010). QIIME allows analysis of high-throughput community sequencing data. *Nature Methods*, 7(5), 335–336. <https://doi.org/10.1038/nmeth.f.303>
- Caporaso, J. G., Lauber, C. L., Walters, W. A., Berg-Lyons, D., Lozupone, C. A., Turnbaugh, P. J., Fierer, N., & Knight, R. (2011). Global patterns of 16S rRNA diversity at a depth of millions of sequences per sample. *Proceedings of the National Academy of Sciences*, 108, 4516–4522. <https://doi.org/10.1073/pnas.1000080107>
- Cardoso, P. H. M., Balian, S. de C., Matushima, E. R., Pádua, S. B. de, & Martins, M. L. (2017). First report of scuticociliatosis caused by *Uronema* sp. in ornamental reef fish imported into Brazil. *Revista Brasileira de Parasitologia Veterinária*, 26(4), 491–495. <https://doi.org/10.1590/s1984-29612017031>
- Caron, D. A., Countway, P. D., Jones, A. C., Kim, D. Y., & Schnetzer, A. (2012). Marine Protistan Diversity. *Annual Review of Marine Science*, 4(1), 467–493. <https://doi.org/10.1146/annurev-marine-120709-142802>
- Carr, M. E., Friedrichs, M. A. M., Schmeltz, M., Noguchi Aita, M., Antoine, D., Arrigo, K. R., Asanuma, I., Aumont, O., Barber, R., Behrenfeld, M., Bidigare, R., Buitenhuis, E. T., Campbell, J., Ciotti, A., Dierssen, H., Dowell, M., Dunne, J., Esaias, W., Gentili, B., ... Yamanaka, Y. (2006). A comparison of global estimates of marine primary production from ocean color. *Deep-Sea Research Part II: Topical Studies in Oceanography*, 53(5–7), 741–770. <https://doi.org/10.1016/j.dsr2.2006.01.028>

- Chambouvet, A., Morin, P., Marie, D., & Guillou, L. (2008). Control of Toxic Marine Dinoflagellate Blooms by Serial Parasitic Killers. *Science*, 322(5905), 1254–1257. <https://doi.org/10.1126/science.1164387>
- Chaumeil, P.-A., Mussig, A. J., Hugenholtz, P., & Parks, D. H. (2020). GTDB-Tk: a toolkit to classify genomes with the Genome Taxonomy Database. *Bioinformatics*, 36(6), 1925–1927. <https://doi.org/10.1093/bioinformatics/btz848>
- Chenn, H. (2018). Generate High-Resolution Venn and Euler Plots. VennDiagram package. *R Package*, 33. <https://cran.r-project.org/web/packages/VennDiagram/VennDiagram.pdf>
- Chlebicki, A., & Jakus, N. (2019). Halotolerant and chaotolerant microfungi from littoral anchialine caves Golubinka and Medova Buza (Croatia). *Journal of Cave and Karst Studies*, 81(3), 153–161. <https://doi.org/10.4311/2016MB0149>
- Ciais, P., Sabine, C., Bala, G., Bopp, L., Brovkin, V., Canadell, J., Chhabra, A., DeFries, R., Galloway, J., Heimann, M., Jones, C., Le Quéré, C., Myneni, R. B., Piao, S., & Thornton, P. (2013). Carbon and Other Biogeochemical Cycles. In *Climate Change 2013: The Physical Science Basis. Contribution of Working Group I to the Fifth Assessment Report of the Intergovernmental Panel on Climate Change* (Vol. 58, Issue 12, pp. 7250–7257). Cambridge University Press, Cambridge, United Kingdom and New York, NY, USA. <https://doi.org/10.1128/AAC.03728-14>
- Clarke, L. J., Bestley, S., Bissett, A., & Deagle, B. E. (2019). A globally distributed Syndiniales parasite dominates the Southern Ocean micro-eukaryote community near the sea-ice edge. *The ISME Journal*, 13(3), 734–737. <https://doi.org/10.1038/s41396-018-0306-7>
- Claustre, H., Huot, Y., Obernosterer, I., Gentili, B., Tailliez, D., & Lewis, M. (2008). Gross community production and metabolic balance in the South Pacific Gyre, using a non intrusive bio-optical method. *Biogeosciences*, 5(2), 463–474. <https://doi.org/10.5194/BG-5-463-2008>
- Cohen, N. R., McIlvin, M. R., Moran, D. M., Held, N. A., Saunders, J. K., Hawco, N. J., Brosnahan, M., DiTullio, G. R., Lamborg, C., McCrow, J. P., Dupont, C. L., Allen, A. E., & Saito, M. A. (2021). Dinoflagellates alter their carbon and nutrient metabolic strategies across environmental gradients in the central Pacific Ocean. *Nature Microbiology*, 6(2), 173–186. <https://doi.org/10.1038/s41564-020-00814-7>
- Coleine, C., Stajich, J. E., & Selbmann, L. (2022). Fungi are key players in extreme ecosystems. *Trends in Ecology & Evolution*, 37(6), 517–528. <https://doi.org/10.1016/j.tree.2022.02.002>
- Countway, P. D., Gast, R. J., Dennett, M. R., Savai, P., Rose, J. M., & Caron, D. A. (2007). Distinct protistan assemblages characterize the euphotic zone and deep sea (2500 m) of the western North Atlantic (Sargasso Sea and Gulf Stream). *Environmental Microbiology*, 9(5), 1219–1232. <https://doi.org/10.1111/j.1462-2920.2007.01243.x>
- Cuculić, V., Cukrov, N., Željko Kwokal, & Mlakar, M. (2011). Distribution of trace metals in anchialine caves of Adriatic Sea, Croatia. *Estuarine, Coastal and Shelf Science*, 95(1), 253–263. <https://doi.org/10.1016/j.ecss.2011.09.011>
- Culver, D. C., & Pipan, T. (2019). *The Biology of Caves and Other Subterranean Habitats* (2nd ed.). Oxford University Press. <https://doi.org/10.1093/oso/9780198820765.001.0001>

- Cunliffe, M. (2023). Who are the marine fungi? *Environmental Microbiology*, 25(1), 131–134. <https://doi.org/10.1111/1462-2920.16240>
- Dai, M., Luo, Y., Achterberg, E. P., Browning, T. J., Cai, Y., Cao, Z., Chai, F., Chen, B., Church, M. J., Ci, D., Du, C., Gao, K., Guo, X., Hu, Z., Kao, S., Laws, E. A., Lee, Z., Lin, H., Liu, Q., ... Zhou, K. (2023). Upper Ocean Biogeochemistry of the Oligotrophic North Pacific Subtropical Gyre: From Nutrient Sources to Carbon Export. *Reviews of Geophysics*, 61(3). <https://doi.org/10.1029/2022RG000800>
- Daims, H., Brühl, A., Amann, R., Schleifer, K.-H., & Wagner, M. (1999). The Domain-specific Probe EUB338 is Insufficient for the Detection of all Bacteria: Development and Evaluation of a more Comprehensive Probe Set. *Systematic and Applied Microbiology*, 22(3), 434–444. [https://doi.org/10.1016/S0723-2020\(99\)80053-8](https://doi.org/10.1016/S0723-2020(99)80053-8)
- Daims, H., Lückner, S., & Wagner, M. (2006). daime, a novel image analysis program for microbial ecology and biofilm research. *Environmental Microbiology*, 8(2), 200–213. <https://doi.org/10.1111/j.1462-2920.2005.00880.x>
- de Vargas, C., Audic, S., Henry, N., Decelle, J., Mahé, F., Logares, R., Lara, E., Berney, C., Le Bescot, N., Probert, I., Carmichael, M., Poulain, J., Romac, S., Colin, S., Aury, J.-M., Bittner, L., Chaffron, S., Dunthorn, M., Engelen, S., ... Velayoudon, D. (2015). Eukaryotic plankton diversity in the sunlit ocean. *Science*, 348(6237), 1261605–1/11. <https://doi.org/10.1126/science.1261605>
- DeBruyn, J. M., Nixon, L. T., Fawaz, M. N., Johnson, A. M., & Radosevich, M. (2011). Global biogeography and quantitative seasonal dynamics of Gemmatimonadetes in soil. *Applied and Environmental Microbiology*, 77(17), 6295–6300. <https://doi.org/10.1128/AEM.05005-11>
- Devries, T. (2022). The Ocean Carbon Cycle. *Annual Review of Environment and Resources*, 47, 317–341. <https://doi.org/10.1146/annurev-enviro-120920-111307>
- Diao, M., Huisman, J., & Muyzer, G. (2018). Spatio-temporal dynamics of sulfur bacteria during oxic--anoxic regime shifts in a seasonally stratified lake. *FEMS Microbiology Ecology*, 94(4), 40. <https://doi.org/10.1093/femsec/fiy040>
- Dolan, J. R., Ritchie, M. E., & Ras, J. (2007). The “neutral” community structure of planktonic herbivores, tintinnid ciliates of the microzooplankton, across the SE Tropical Pacific Ocean. *Biogeosciences*, 4(3), 297–310. <https://doi.org/10.5194/bg-4-297-2007>
- Dray, S., & Dufour, A.-B. (2007). The ade4 Package: Implementing the Duality Diagram for Ecologists. *Journal of Statistical Software*, 22(4), 1–20. <https://doi.org/10.18637/jss.v022.i04>
- Ducklow, H., Steinberg, D., & Buesseler, K. (2001). Upper Ocean Carbon Export and the Biological Pump. *Oceanography*, 14(4), 50–58. <https://doi.org/10.5670/oceanog.2001.06>
- Duerschlag, J., Mohr, W., Ferdelman, T. G., LaRoche, J., Desai, D., Croot, P. L., Voß, D., Zielinski, O., Lavik, G., Littmann, S., Martínez-Pérez, C., Tschitschko, B., Bartlau, N., Osterholz, H., Dittmar, T., & Kuypers, M. M. M. (2022). Niche partitioning by photosynthetic plankton as a driver of CO<sub>2</sub>-fixation across the oligotrophic South Pacific Subtropical Ocean. *The ISME Journal*, 16(2), 465–476. <https://doi.org/10.1038/s41396-021-01072-z>

- Duque, C., Michael, H. A., & Wilson, A. M. (2020). The Subterranean Estuary: Technical Term, Simple Analogy, or Source of Confusion? *Water Resources Research*, 56(2), 1–7. <https://doi.org/10.1029/2019WR026554>
- Edgar, R. C., Haas, B. J., Clemente, J. C., Quince, C., & Knight, R. (2011). UCHIME improves sensitivity and speed of chimera detection. *Bioinformatics*, 27(16), 2194–2200. <https://doi.org/10.1093/bioinformatics/btr381>
- Edgcomb, V. (2016). Marine protist associations and environmental impacts across trophic levels in the twilight zone and below. *Current Opinion in Microbiology*, 31, 169–175. <https://doi.org/10.1016/j.mib.2016.04.001>
- Edgcomb, V. P., Beaudoin, D., Gast, R., Biddle, J. F., & Teske, A. (2011). Marine subsurface eukaryotes: The fungal majority. *Environmental Microbiology*, 13(1), 172–183. <https://doi.org/10.1111/j.1462-2920.2010.02318.x>
- Ettinger, C. L., Vann, L. E., & Eisen, J. A. (2021). Global Diversity and Biogeography of the *Zostera marina* Mycobiome. *Applied and Environmental Microbiology*, 87(12), 1–19. <https://doi.org/10.1128/AEM.02795-20>
- Ferdelman, T. (2019). *Nutrient Data from CTD Niskin Bottles from Sonne Expedition SO-245 "UltraPac."* <https://doi.pangaea.de/10.1594/PANGAEA.899228>
- Field, C. B., Behrenfeld, M. J., Randerson, J. T., & Falkowski, P. (1998). Primary production of the biosphere: Integrating terrestrial and oceanic components. *Science*, 281(5374), 237–240. <https://doi.org/10.1126/science.281.5374.237>
- Filipčić, A. (1998). Climatic regionalization of Croatia according to W. Köppen for the standard period 1961 – 1990 in relation to the period 1931 – 1960. *Acta Geographica Croatica*, 33(1), 7–15.
- Flombaum, P., Gallegos, J. L., Gordillo, R. A., Rincón, J., Zabala, L. L., Jiao, N., Karl, D. M., Li, W. K. W., Lomas, M. W., Veneziano, D., Vera, C. S., Vrugt, J. A., & Martiny, A. C. (2013). Present and future global distributions of the marine Cyanobacteria *Prochlorococcus* and *Synechococcus*. *Proceedings of the National Academy of Sciences*, 110(24), 9824–9829. <https://doi.org/10.1073/pnas.1307701110>
- Follows, M., & Oguz, T. (2005). The Ocean carbon cycle and climate. In *NATO Science Series* (Vol. 42, Issue 07). <https://doi.org/10.5860/CHOICE.42-4041>
- Fuhrman, J. A. (2009). Microbial community structure and its functional implications. *Nature*, 459(7244), 193–199. <https://doi.org/10.1038/nature08058>
- Gao, C.-H., Yu, G., & Cai, P. (2021). ggVennDiagram: An Intuitive, Easy-to-Use, and Highly Customizable R Package to Generate Venn Diagram. *Frontiers in Genetics*, 12(September). <https://doi.org/10.3389/fgene.2021.706907>
- Gareth Jones, E. B., Ramakrishna, S., Vikineswary, S., Das, D., Bahkali, A. H., Guo, S. Y., & Pang, K. L. (2022). How Do Fungi Survive in the Sea and Respond to Climate Change? *Journal of Fungi*, 8(3). <https://doi.org/10.3390/jof8030291>
- Garritano, A. N., Song, W., & Thomas, T. (2022). Carbon fixation pathways across the bacterial and archaeal tree of life. *PNAS Nexus*, 1(5), 1–12. <https://doi.org/10.1093/pnasnexus/pgac226>

- Ghaly, T. M., Focardi, A., Elbourne, L. D. H., Sutcliffe, B., Humphreys, W., Paulsen, I. T., & Tetu, S. G. (2023). Stratified microbial communities in Australia's only anchialine cave are taxonomically novel and drive chemotrophic energy production via coupled nitrogen-sulphur cycling. *Microbiome*, *11*(1), 190. <https://doi.org/10.1186/s40168-023-01633-8>
- Giner, C. R., Pernice, M. C., Balagué, V., Duarte, C. M., Gasol, J. M., Logares, R., & Massana, R. (2019). Marked changes in diversity and relative activity of picoeukaryotes with depth in the world ocean. *The ISME Journal* *2019* *14*:2, *14*(2), 437–449. <https://doi.org/10.1038/s41396-019-0506-9>
- Giovannoni, S. J. (2017). SAR11 Bacteria: The Most Abundant Plankton in the Oceans. *Annual Review of Marine Science*, *9*(1), 231–255. <https://doi.org/10.1146/annurev-marine-010814-015934>
- Glöckner, J., Kube, M., Shrestha, P. M., Weber, M., Glöckner, F. O., Reinhardt, R., & Liesack, W. (2010). Phylogenetic diversity and metagenomics of candidate division OP3. *Environmental Microbiology*, *12*(5), 1218–1229. <https://doi.org/10.1111/j.1462-2920.2010.02164.x>
- Gómez, F. (2007). On the consortium of the tintinnid *Eutintinnus* and the diatom *Chaetoceros* in the Pacific Ocean. *Marine Biology*, *151*(5), 1899–1906. <https://doi.org/10.1007/s00227-007-0625-0>
- Gong, J., Shi, F., Ma, B., Dong, J., Pachiadaki, M., Zhang, X., & Edgcomb, V. P. (2015). Depth shapes  $\alpha$ - and  $\beta$ -diversities of microbial eukaryotes in surficial sediments of coastal ecosystems. *Environmental Microbiology*, *17*(10), 3722–3737. <https://doi.org/10.1111/1462-2920.12763>
- Gonzalez, B. C. (2010). *Novel bacterial diversity in an anchialine blue hole on Abaco Island, Bahamas. December*, 184.
- Gonzalez, B. C., Borda, E., Carvalho, R., & Schulze, A. (2012). Polychaetes from the Mayan underworld: phylogeny, evolution, and cryptic diversity. *Natura Croatica*, *21*, 51–53. <https://hrcak.srce.hr/87196>
- Gonzalez, B. C., Iliffe, T. M., Macalady, J. L., Schaperdoth, I., & Kakuk, B. (2011). Microbial hotspots in anchialine blue holes: Initial discoveries from the Bahamas. *Hydrobiologia*, *677*(1), 149–156. <https://doi.org/10.1007/s10750-011-0932-9>
- Gonzalez, B. C., Martínez, A., Borda, E., Iliffe, T. M., Fontaneto, D., & Worsaae, K. (2017). Genetic spatial structure of an anchialine cave annelid indicates connectivity within - but not between - islands of the Great Bahama Bank. *Molecular Phylogenetics and Evolution*, *109*, 259–270. <https://doi.org/10.1016/j.ympev.2017.01.003>
- Gonzalez, B., Martínez, A., Olesen, J., Truskey, S., Ballou, L., Allentoft-Larsen, M., Daniels, J., Heinerth, P., Parrish, M., Manco, N., Ward, J., Iliffe, T., Osborn, K., & Worsaae, K. (2020). Anchialine biodiversity in the Turks and Caicos Islands: New discoveries and current faunal composition. *International Journal of Speleology*, *49*(2), 71–86. <https://doi.org/10.5038/1827-806X.49.2.2316>
- Gray, C. J., & Engel, A. S. (2013). Microbial diversity and impact on carbonate geochemistry across a changing geochemical gradient in a karst aquifer. *The ISME Journal*, *7*(2), 325–337. <https://doi.org/10.1038/ismej.2012.105>

- Grob, C., Ulloa, O., Claustre, H., Huot, Y., Alarcón, G., & Marie, D. (2007). Contribution of picoplankton to the total particulate organic carbon concentration in the eastern South Pacific. *Biogeosciences*, 4(5), 837–852. <https://doi.org/10.5194/bg-4-837-2007>
- Grossart, H. P., Van den Wyngaert, S., Kagami, M., Wurzbacher, C., Cunliffe, M., & Rojas-Jimenez, K. (2019). Fungi in aquatic ecosystems. *Nature Reviews Microbiology*, 17(6), 339–354. <https://doi.org/10.1038/s41579-019-0175-8>
- Guidi, L., Chaffron, S., Bittner, L., Eveillard, D., Larhlimi, A., Roux, S., Darzi, Y., Audic, S., Berline, L., Brum, J. R., Coelho, L. P., Espinoza, J. C. I., Malviya, S., Sunagawa, S., Dimier, C., Kandels-Lewis, S., Picheral, M., Poulain, J., Searson, S., ... Gorsky, G. (2016). Plankton networks driving carbon export in the oligotrophic ocean. *Nature*, 532(7600), 465–470. <https://doi.org/10.1038/nature16942>
- Guillou, L., Bachar, D., Audic, S., Bass, D., Berney, C., Bittner, L., Boutte, C., Burgaud, G., De Vargas, C., Decelle, J., Del Campo, J., Dolan, J. R., Dunthorn, M., Edvardsen, B., Holzmann, M., Kooistra, W. H. C. F., Lara, E., Le Bescot, N., Logares, R., ... Christen, R. (2013). The Protist Ribosomal Reference database (PR2): A catalog of unicellular eukaryote Small Sub-Unit rRNA sequences with curated taxonomy. *Nucleic Acids Research*, 41(D1). <https://doi.org/10.1093/NAR/GKS1160>
- Guillou, L., Viprey, M., Chambouvet, A., Welsh, R. M., Kirkham, A. R., Massana, R., Scanlan, D. J., & Worden, A. Z. (2008). Widespread occurrence and genetic diversity of marine parasitoids belonging to Syndiniales (Alveolata). *Environmental Microbiology*, 10(12), 3349–3365. <https://doi.org/10.1111/j.1462-2920.2008.01731.x>
- Guo, Z., Zhang, H., Liu, S., & Lin, S. (2013). Biology of the Marine Heterotrophic Dinoflagellate *Oxyrrhis marina*: Current Status and Future Directions. *Microorganisms*, 1(1), 33–57. <https://doi.org/10.3390/microorganisms1010033>
- Gurevich, A., Saveliev, V., Vyahhi, N., & Tesler, G. (2013). QUAST: quality assessment tool for genome assemblies. *Bioinformatics*, 29(8), 1072–1075. <https://doi.org/10.1093/bioinformatics/btt086>
- Gutiérrez-Rodríguez, A., Lopes dos Santos, A., Safi, K., Probert, I., Not, F., Fernández, D., Gourvil, P., Bilewitch, J., Hulston, D., Pinkerton, M., & Nodder, S. D. (2022). Planktonic protist diversity across contrasting Subtropical and Subantarctic waters of the southwest Pacific. *Progress in Oceanography*, 206, 102809. <https://doi.org/10.1016/j.pocean.2022.102809>
- Hassett, B. T., Vonnahme, T. R., Peng, X., Jones, E. B. G., & Heuzé, C. (2019). Global diversity and geography of planktonic marine fungi. *Botanica Marina*, 63(2), 121–139. <https://doi.org/10.1515/bot-2018-0113>
- Hatzenpichler, R., & Orphan, V. J. (2015). Detection of Protein-Synthesizing Microorganisms in the Environment via Bioorthogonal Noncanonical Amino Acid Tagging (BONCAT). In *Hydrocarbon and Lipid Microbiology Protocols* (pp. 145–157). [https://doi.org/10.1007/8623\\_2015\\_61](https://doi.org/10.1007/8623_2015_61)
- Hatzenpichler, R., Scheller, S., Tavormina, P. L., Babin, B. M., Tirrell, D. A., & Orphan, V. J. (2014). In situ visualization of newly synthesized proteins in environmental microbes using amino acid tagging and click chemistry. *Environmental Microbiology*, 16(8), 2568–2590. <https://doi.org/10.1111/1462-2920.12436>

- Havird, J. C., & Santos, S. R. (2016). Developmental transcriptomics of the hawaiian anchialine shrimp *halocaridina rubra* holthuis, 1963 (Crustacea: Atyidae). *Integrative and Comparative Biology*, *56*(6), 1170–1182. <https://doi.org/10.1093/icb/icw003>
- He, H., Fu, L., Liu, Q., Fu, L., Bi, N., Yang, Z., & Zhen, Y. (2019). Community Structure, Abundance and Potential Functions of Bacteria and Archaea in the Sansha Yongle Blue Hole, Xisha, South China Sea. *Frontiers in Microbiology*, *10*(October), 1–16. <https://doi.org/10.3389/fmicb.2019.02404>
- He, P., Xie, L., Zhang, X., Li, J., Lin, X., Pu, X., Yuan, C., Tian, Z., & Li, J. (2020). Microbial Diversity and Metabolic Potential in the Stratified Sansha Yongle Blue Hole in the South China Sea. *Scientific Reports*, *10*(1), 1–17. <https://doi.org/10.1038/s41598-020-62411-2>
- Herndl, G. J., & Reinthaler, T. (2013). Microbial control of the dark end of the biological pump. *Nature Geoscience*, *6*(9), 718–724. <https://doi.org/10.1038/ngeo1921>
- Hoehler, T. M., & Jørgensen, B. B. (2013). Microbial life under extreme energy limitation. *Nature Reviews Microbiology*, *11*(2), 83–94. <https://doi.org/10.1038/NRMICRO2939>
- Hoffman, S. K., Seitz, K. W., Havird, J. C., Weese, D. A., & Santos, S. R. (2018). Diversity and the environmental drivers of spatial variation in Bacteria and micro-Eukarya communities from the Hawaiian anchialine ecosystem. *Hydrobiologia*, *806*(1), 265–282. <https://doi.org/10.1007/s10750-017-3365-2>
- Hoffman, S. K., Seitz, K. W., Havird, J. C., Weese, D. A., & Santos, S. R. (2020). Phenotypic comparability from genotypic variability among physically structured microbial consortia. *Integrative and Comparative Biology*, *60*(2), 288–303. <https://doi.org/10.1093/icb/icaa022>
- Hou, J., Sievert, S. M., Wang, Y., Seewald, J. S., Natarajan, V. P., Wang, F., & Xiao, X. (2020). Microbial succession during the transition from active to inactive stages of deep-sea hydrothermal vent sulfide chimneys. *Microbiome*, *8*(1), 1–18. <https://doi.org/10.1186/s40168-020-00851-8>
- Howarth, R. W. (1988). Nutrient limitation of net primary production in marine ecosystems. *Annual Review of Ecology and Systematics*, *19*(1), 89–110. <https://doi.org/10.1146/annurev.es.19.110188.000513>
- Hu, S. K., Connell, P. E., Mesrop, L. Y., & Caron, D. A. (2018). A Hard Day's night: Diel shifts in microbial eukaryotic activity in the North Pacific Subtropical Gyre. *Frontiers in Marine Science*, *5*(OCT), 1–17. <https://doi.org/10.3389/fmars.2018.00351>
- Huang, L., Bae, H. S., Young, C., Pain, A. J., Martin, J. B., & Ogram, A. (2021). Campylobacterota dominate the microbial communities in a tropical karst subterranean estuary, with implications for cycling and export of nitrogen to coastal waters. *Environmental Microbiology*, *23*(11), 6749–6763. <https://doi.org/10.1111/1462-2920.15746>
- Huerta-Cepas, J., Szklarczyk, D., Heller, D., Hernández-Plaza, A., Forslund, S. K., Cook, H., Mende, D. R., Letunic, I., Rattei, T., Jensen, L. J., von Mering, C., & Bork, P. (2019). eggNOG 5.0: a hierarchical, functionally and phylogenetically annotated orthology resource based on 5090 organisms and 2502 viruses. *Nucleic Acids Research*, *47*(D1), D309–D314. <https://doi.org/10.1093/nar/gky1085>

- Humphreys, W. F., Poole, A., Eberhard, S. M., & Warren, D. (1999). Effects of research diving on the physico-chemical profile of Bundera Sinkhole, an anchialine remiped habitat at Cape Range, Western Australia. *Journal of the Royal Society of Western Australia*, 82(3), 99–108.
- Hutchins, D. A., & Fu, F. (2017). Microorganisms and ocean global change. *Nature Microbiology*, 2(May), 1–11. <https://doi.org/10.1038/nmicrobiol.2017.58>
- Hyatt, D., Chen, G.-L., LoCasio, P. F., Land, M. L., Larimer, F. W., & Hauser, L. J. (2010). Prodigal: prokaryotic gene recognition and translation initiation site identification. *BMC Bioinformatics*, 11(1), 119. <https://doi.org/10.1186/1471-2105-11-119>
- Ibarbalz, F. M., Henry, N., Brandão, M. C., Martini, S., Busseni, G., Byrne, H., Coelho, L. P., Endo, H., Gasol, J. M., Gregory, A. C., Mahé, F., Rigonato, J., Royo-Llonch, M., Salazar, G., Sanz-Sáez, I., Scalco, E., Soviadan, D., Zayed, A. A., Zingone, A., ... Wincker, P. (2019). Global Trends in Marine Plankton Diversity across Kingdoms of Life. *Cell*, 179(5), 1084–1097.e21. <https://doi.org/10.1016/j.cell.2019.10.008>
- Iliffe, T. M. (2000). Anchialine cave ecology. In H. Wilkens, D. C. Culver, & W. F. Humphreys (Eds.), *Ecosystems of the World. Subterranean Ecosystems* (pp. 59–76).
- Iliffe, T. M. (2018). Collecting and processing crustaceans from anchialine and marine caves. *Journal of Crustacean Biology*, 38(3), 374–379. <https://doi.org/10.1093/jcbiol/ruy011>
- Iliffe, T. M., & Alvarez, F. (2018). Research in Anchialine Caves. In *Cave Ecology* (pp. 383–397). Springer Nature Switzerland. [https://doi.org/10.1007/978-3-319-98852-8\\_18](https://doi.org/10.1007/978-3-319-98852-8_18)
- Inomura, K., Deutsch, C., Jahn, O., Dutkiewicz, S., & Follows, M. J. (2022). Global patterns in marine organic matter stoichiometry driven by phytoplankton ecophysiology. *Nature Geoscience*, 15(12), 1034–1040. <https://doi.org/10.1038/s41561-022-01066-2>
- Irwin, A. J., & Oliver, M. J. (2009). Are ocean deserts getting larger? *Geophysical Research Letters*, 36(18), L18609. <https://doi.org/10.1029/2009GL039883>
- Iversen, M. H. (2023). Carbon Export in the Ocean: A Biologist's Perspective. *Annual Review of Marine Science*, 15, 357–381. <https://doi.org/10.1146/annurev-marine-032122-035153>
- Jephcott, T. G., Alves-de-Souza, C., Gleason, F. H., van Ogtrop, F. F., Sime-Ngando, T., Karpov, S. A., & Guillou, L. (2016). Ecological impacts of parasitic chytrids, syndiniales and perkinsids on populations of marine photosynthetic dinoflagellates. *Fungal Ecology*, 19(October 2019), 47–58. <https://doi.org/10.1016/j.funeco.2015.03.007>
- Kajan, K., Cukrov, N., Cukrov, N., Bishop-Pierce, R., & Orlić, S. (2022). Microeukaryotic and Prokaryotic Diversity of Anchialine Caves from Eastern Adriatic Sea Islands. *Microbial Ecology*, 83(2), 257–270. <https://doi.org/10.1007/s00248-021-01760-5>
- Kanehisa, M., Furumichi, M., Sato, Y., Kawashima, M., & Ishiguro-Watanabe, M. (2023). KEGG for taxonomy-based analysis of pathways and genomes. *Nucleic Acids Research*, 51(D1), D587–D592. <https://doi.org/10.1093/nar/gkac963>
- Kang, D. D., Li, F., Kirton, E., Thomas, A., Egan, R., An, H., & Wang, Z. (2019). MetaBAT 2: an adaptive binning algorithm for robust and efficient genome reconstruction from metagenome assemblies. *PeerJ*, 7(7), e7359. <https://doi.org/10.7717/peerj.7359>

- Keegstra, J. M., Carrara, F., & Stocker, R. (2022). The ecological roles of bacterial chemotaxis. *Nature Reviews Microbiology*, 20(8), 491–504. <https://doi.org/10.1038/s41579-022-00709-w>
- Kletou, D., & M., J. (2012). Threats to Ultraoligotrophic Marine Ecosystems. *Marine Ecosystems, March*. <https://doi.org/10.5772/34842>
- Ko, Y. H., Lee, K., Takahashi, T., Karl, D. M., Kang, S. H., & Lee, E. (2018). Carbon-Based Estimate of Nitrogen Fixation-Derived Net Community Production in N-Depleted Ocean Gyres. *Global Biogeochemical Cycles*, 32(8), 1241–1252. <https://doi.org/10.1029/2017GB005634>
- Kolde, R. (2012). Package “pheatmap”: Pretty heatmaps. *R Package*, 1–8.
- Korlević, M., Šupraha, L., Ljubešić, Z., Henderiks, J., Ciglenečki, I., Dautović, J., & Orlić, S. (2016). Bacterial diversity across a highly stratified ecosystem: A salt-wedge Mediterranean estuary. *Systematic and Applied Microbiology*, 39(6), 398–408. <https://doi.org/10.1016/j.syapm.2016.06.006>
- Kostešić, E., Mitrović, M., Kajan, K., Marković, T., Hausmann, B., Orlić, S., & Pjevac, P. (2023). Microbial Diversity and Activity of Biofilms from Geothermal Springs in Croatia. *Microbial Ecology*. <https://doi.org/10.1007/s00248-023-02239-1>
- Kršinić, F. (2005). Speleohvarella gamulini gen. et sp. nov., a new copepod (Calanoida, Stephidae) from an anchialine cave in the Adriatic Sea. *Journal of Plankton Research*, 27(6), 607–615. <https://doi.org/10.1093/plankt/fbi028>
- Krstulović, N., Šolić, M., Maršić-Lučić, J., Ordulj, M., & Šestanović, S. (2013). Microbial community structure in two anchialine caves on Mljet Island (Adriatic sea). *Acta Adriatica*, 54(2), 183–197.
- Krukenberg, V., Reichart, N. J., Spietz, R. L., & Hatzenpichler, R. (2021). Microbial Community Response to Polysaccharide Amendment in Anoxic Hydrothermal Sediments of the Guaymas Basin. *Frontiers in Microbiology*, 12(December), 1–11. <https://doi.org/10.3389/fmicb.2021.763971>
- Kubota, K. (2013). CARD-FISH for Environmental Microorganisms: Technical Advancement and Future Applications. *Microbes and Environments*, 28(1), 3. <https://doi.org/10.1264/JSME2.ME12107>
- Kujawinski, E. B. (2011). The impact of microbial metabolism on marine dissolved organic matter. *Annual Review of Marine Science*, 3, 567–599. <https://doi.org/10.1146/annurev-marine-120308-081003>
- Kujawinski, E. B., Longnecker, K., Barott, K. L., Weber, R. J. M., & Soule, M. C. K. (2016). Microbial community structure affects marine dissolved organic matter composition. *Frontiers in Marine Science*, 3(APR), 1–15. <https://doi.org/10.3389/fmars.2016.00045>
- Kumar, V., Sarma, V. V., Thambugala, K. M., Huang, J.-J., Li, X.-Y., & Hao, G.-F. (2021). Ecology and Evolution of Marine Fungi With Their Adaptation to Climate Change. *Frontiers in Microbiology*, 12(August), 1–12. <https://doi.org/10.3389/fmicb.2021.719000>

- Kwokal, Ž., Cukrov, N., & Cuculić, V. (2014). Natural causes of changes in marine environment: Mercury speciation and distribution in anchialine caves. *Estuarine, Coastal and Shelf Science*, *151*, 10–20. <https://doi.org/10.1016/j.ecss.2014.09.016>
- Legendre, L., Rivkin, R. B., Weinbauer, M. G., Guidi, L., & Uitz, J. (2015). The microbial carbon pump concept: Potential biogeochemical significance in the globally changing ocean. In *Progress in Oceanography* (Vol. 134, pp. 432–450). <https://doi.org/10.1016/j.pocean.2015.01.008>
- Letscher, R. T., Knapp, A. N., James, A. K., Carlson, C. A., Santoro, A. E., & Hansell, D. A. (2015). Microbial community composition and nitrogen availability influence DOC remineralization in the South Pacific Gyre. *Marine Chemistry*, *177*, 325–334. <https://doi.org/10.1016/j.marchem.2015.06.024>
- Lever, M. A., Rogers, K. L., Lloyd, K. G., Overmann, J., Schink, B., Thauer, R. K., Hoehler, T. M., & Jørgensen, B. B. (2015). Life under extreme energy limitation: A synthesis of laboratory- and field-based investigations. *FEMS Microbiology Reviews*, *39*(5), 688–728. <https://doi.org/10.1093/femsre/fuv020>
- Li, D., Liu, C.-M., Luo, R., Sadakane, K., & Lam, T.-W. (2015). MEGAHIT: an ultra-fast single-node solution for large and complex metagenomics assembly via succinct de Bruijn graph. *Bioinformatics*, *31*(10), 1674–1676. <https://doi.org/10.1093/bioinformatics/btv033>
- Li, H. (2018). Minimap2: pairwise alignment for nucleotide sequences. *Bioinformatics*, *34*(18), 3094–3100. <https://doi.org/10.1093/bioinformatics/bty191>
- Li, H., Handsaker, B., Wysoker, A., Fennell, T., Ruan, J., Homer, N., Marth, G., Abecasis, G., & Durbin, R. (2009). The Sequence Alignment/Map format and SAMtools. *Bioinformatics*, *25*(16), 2078–2079. <https://doi.org/10.1093/bioinformatics/btp352>
- Liang, Z., Letscher, R. T., & Knapp, A. N. (2023). Global patterns of surface ocean dissolved organic matter stoichiometry. *Authorea Preprints*. <https://doi.org/10.22541/ESSOAR.168056819.90596373/V1>
- Lima-Mendez, G., Faust, K., Henry, N., Decelle, J., Colin, S., Carcillo, F., Chaffron, S., Ignacio-Espinosa, J. C., Roux, S., Vincent, F., Bittner, L., Darzi, Y., Wang, J., Audic, S., Berline, L., Bontempi, G., Cabello, A. M., Coppola, L., Cornejo-Castillo, F. M., ... Velayoudon, D. (2015). Determinants of community structure in the global plankton interactome. *Science*, *348*(6237). <https://doi.org/10.1126/science.1262073>
- Liu, Y., He, H., Fu, L., Liu, Q., Yang, Z., & Zhen, Y. (2019). Environmental DNA sequencing reveals a highly complex eukaryote community in Sansha Yongle Blue Hole, Xisha, south China sea. *Microorganisms*, *7*(12), 1–16. <https://doi.org/10.3390/microorganisms7120624>
- Longhurst, A., Sathyendranath, S., Platt, T., & Caverhill, C. (1995). An estimate of global primary production in the ocean from satellite radiometer data. *J Plankton Res*, *17*(6), 1245–1271. <https://doi.org/10.1093/plankt/17.6.1245>
- Lorrain, A., Savoye, N., Chauvaud, L., Paulet, Y. M., & Naulet, N. (2003). Decarbonation and preservation method for the analysis of organic C and N contents and stable isotope ratios of low-carbonated suspended particulate material. *Analytica Chimica Acta*, *491*(2), 125–133. [https://doi.org/10.1016/S0003-2670\(03\)00815-8](https://doi.org/10.1016/S0003-2670(03)00815-8)

- Louca, S., Parfrey, L. W., & Doebeli, M. (2016). Decoupling function and taxonomy in the global ocean microbiome. *Science*, 353(6305), 1272–1277. <https://doi.org/10.1126/science.aaf4507>
- Louca, S., Polz, M. F., Mazel, F., Albright, M. B. N., Huber, J. A., O'Connor, M. I., Ackermann, M., Hahn, A. S., Srivastava, D. S., Crowe, S. A., Doebeli, M., & Parfrey, L. W. (2018). Function and functional redundancy in microbial systems. *Nature Ecology & Evolution*, 2(6), 936–943. <https://doi.org/10.1038/s41559-018-0519-1>
- Louis, Y., Garnier, C., Lenoble, V., Mounier, S., Cukrov, N., Omanović, D., & Pižeta, I. (2009). Kinetic and equilibrium studies of copper-dissolved organic matter complexation in water column of the stratified Krka River estuary (Croatia). *Marine Chemistry*, 114(3–4), 110–119. <https://doi.org/10.1016/j.marchem.2009.04.006>
- Lozupone, C. A., & Knight, R. (2007). Global patterns in bacterial diversity. *Proceedings of the National Academy of Sciences of the United States of America*, 104(27), 11436–11440. <https://doi.org/10.1073/pnas.0611525104>
- Lu, S., Wang, J., Chitsaz, F., Derbyshire, M. K., Geer, R. C., Gonzales, N. R., Gwadz, M., Hurwitz, D. I., Marchler, G. H., Song, J. S., Thanki, N., Yamashita, R. A., Yang, M., Zhang, D., Zheng, C., Lanczycki, C. J., & Marchler-Bauer, A. (2020). CDD/SPARCLE: the conserved domain database in 2020. *Nucleic Acids Research*, 48(D1), D265–D268. <https://doi.org/10.1093/nar/gkz991>
- Macey, M. C., Fox-Powell, M., Ramkissoon, N. K., Stephens, B. P., Barton, T., Schwenzer, S. P., Pearson, V. K., Cousins, C. R., & Olsson-Francis, K. (2020). The identification of sulfide oxidation as a potential metabolism driving primary production on late Noachian Mars. *Scientific Reports*, 10(1), 10941. <https://doi.org/10.1038/s41598-020-67815-8>
- Magnuson, E., Altshuler, I., Freyria, N. J., Leveille, R. J., & Whyte, L. G. (2023). Sulfur-cycling chemolithoautotrophic microbial community dominates a cold, anoxic, hypersaline Arctic spring. *Microbiome*, 11(1), 1–20. <https://doi.org/10.1186/s40168-023-01628-5>
- Mahé, F., Rognes, T., Quince, C., de Vargas, C., & Dunthorn, M. (2015). Swarm v2: highly-scalable and high-resolution amplicon clustering. *PeerJ*, 3(12), e1420. <https://doi.org/10.7717/peerj.1420>
- Marguš, M., Morales-Reyes, I., Bura-Nakić, E., Batina, N., & Ciglencečki, I. (2015). The anoxic stress conditions explored at the nanoscale by atomic force microscopy in highly eutrophic and sulfidic marine lake. *Continental Shelf Research*, 109, 24–34. <https://doi.org/10.1016/j.csr.2015.09.001>
- Martin, M. (2011). Cutadapt removes adapter sequences from high-throughput sequencing reads. *EMBnet.Journal*, 17(1), 10. <https://doi.org/10.14806/ej.17.1.200>
- Masquelier, S., & Vaultot, D. (2008). Distribution of micro-organisms along a transect in the South-East Pacific Ocean (BIOSCOPE cruise) using epifluorescence microscopy. *Biogeosciences*, 5(2), 311–321. <https://doi.org/10.5194/BG-5-311-2008>
- McClain, C. R., Signorini, S. R., & Christian, J. R. (2004). Subtropical gyre variability observed by ocean-color satellites. *Deep Sea Res Part II Topical Stud Oceanogr*, 51(1–3), 281–301. <https://doi.org/10.1016/j.dsr2.2003.08.002>

- McMurdie, P. J., & Holmes, S. (2013). phyloseq: An R Package for Reproducible Interactive Analysis and Graphics of Microbiome Census Data. *PLoS ONE*, 8(4), e61217. <https://doi.org/10.1371/journal.pone.0061217>
- Meyer, A., Dang, H., & Roland, W. (2019). Myroides spp. cellulitis and bacteremia: A case report. *IDCases*, 18, e00638. <https://doi.org/10.1016/j.idcr.2019.e00638>
- Moore, C. M., Mills, M. M., Arrigo, K. R., Berman-Frank, I., Bopp, L., Boyd, P. W., Galbraith, E. D., Geider, R. J., Guieu, C., Jaccard, S. L., Jickells, T. D., La Roche, J., Lenton, T. M., Mahowald, N. M., Marañón, E., Marinov, I., Moore, J. K., Nakatsuka, T., Oschlies, A., ... Ulloa, O. (2013). Processes and patterns of oceanic nutrient limitation. *Nature Geoscience*, 6(9), 701–710. <https://doi.org/10.1038/ngeo1765>
- Moran, M. A., Kujawinski, E. B., Schroer, W. F., Amin, S. A., Bates, N. R., Bertrand, E. M., Braakman, R., Brown, C. T., Covert, M. W., Doney, S. C., Dyhrman, S. T., Edison, A. S., Eren, A. M., Levine, N. M., Li, L., Ross, A. C., Saito, M. A., Santoro, A. E., Segrè, D., ... Vardi, A. (2022). Microbial metabolites in the marine carbon cycle. *Nature Microbiology*, 7(4), 508–523. <https://doi.org/10.1038/s41564-022-01090-3>
- Moran, M. A., Kujawinski, E. B., Stubbins, A., Fatland, R., Aluwihare, L. I., Buchan, A., Crump, B. C., Dorrestein, P. C., Dyhrman, S. T., Hess, N. J., Howe, B., Longnecker, K., Medeiros, P. M., Niggemann, J., Obernosterer, I., Repeta, D. J., & Waldbauer, J. R. (2016). Deciphering ocean carbon in a changing world. *Proceedings of the National Academy of Sciences of the United States of America*, 113(12), 3143–3151. <https://doi.org/10.1073/pnas.1514645113>
- Morel, A., Gentili, B., Claustre, H., Babin, M., Bricaud, A., Ras, J., & Tièche, F. (2007). Optical properties of the “clearest” natural waters. *Limnology and Oceanography*, 52(1), 217–229. <https://doi.org/10.4319/LO.2007.52.1.0217>
- Moser, M., & Weisse, T. (2011). The outcome of competition between the two chrysoomonads *Ochromonas* sp. and *Poterioochromonas malhamensis* depends on pH. *European Journal of Protistology*, 47(2), 79–85. <https://doi.org/10.1016/j.ejop.2011.01.001>
- Mydroie, J. E., & Mydroie, J. R. (2011). Void development on carbonate coasts: Creation of anchialine habitats. *Hydrobiologia*, 677(1), 15–32. <https://doi.org/10.1007/s10750-010-0542-y>
- Nagahama, T., Hamamoto, M., Nakase, T., Takami, H., & Horikoshi, K. (2001). Distribution and identification of red yeasts in deep-sea environments around the northwest Pacific Ocean. *Antonie van Leeuwenhoek*, 80(2), 101–110. <https://doi.org/10.1023/A:1012270503751>
- Nakagawa, S., Takai, K., Inagaki, F., Hirayama, H., Nunoura, T., Horikoshi, K., & Sako, Y. (2005). Distribution, phylogenetic diversity and physiological characteristics of epsilon-Proteobacteria in a deep-sea hydrothermal field. *Environmental Microbiology*, 7(10), 1619–1632. <https://doi.org/10.1111/J.1462-2920.2005.00856.X>
- Nayfach, S., Roux, S., Seshadri, R., Udwy, D., Varghese, N., Schulz, F., Wu, D., Paez-Espino, D., Chen, I. M., Huntemann, M., Palaniappan, K., Ladau, J., Mukherjee, S., Reddy, T. B. K., Nielsen, T., Kirton, E., Faria, J. P., Edirisinghe, J. N., Henry, C. S., ... Eloe-Fadrosh, E. A. (2021). A genomic catalog of Earth’s microbiomes. *Nature Biotechnology*, 39(4), 499–509. <https://doi.org/10.1038/S41587-020-0718-6>

- Ngugi, D. K., Acinas, S. G., Sánchez, P., Gasol, J. M., Agusti, S., Karl, D. M., & Duarte, C. M. (2023). Abiotic selection of microbial genome size in the global ocean. *Nature Communications*, *14*(1). <https://doi.org/10.1038/s41467-023-36988-x>
- Nguyen, N. H., Song, Z., Bates, S. T., Branco, S., Tedersoo, L., Menke, J., Schilling, J. S., & Kennedy, P. G. (2016). FUNGuild: An open annotation tool for parsing fungal community datasets by ecological guild. *Fungal Ecology*, *20*, 241–248. <https://doi.org/10.1016/j.funeco.2015.06.006>
- Nilsson, R. H., Larsson, K. H., Taylor, A. F. S., Bengtsson-Palme, J., Jeppesen, T. S., Schigel, D., Kennedy, P., Picard, K., Glöckner, F. O., Tedersoo, L., Saar, I., Kõljalg, U., & Abarenkov, K. (2019). The UNITE database for molecular identification of fungi: Handling dark taxa and parallel taxonomic classifications. *Nucleic Acids Research*, *47*(D1), D259–D264. <https://doi.org/10.1093/nar/gky1022>
- Nishitani, G., & Yamaguchi, M. (2018). Seasonal succession of ciliate *Mesodinium* spp. with red, green, or mixed plastids and their association with cryptophyte prey. *Scientific Reports*, *8*(1), 1–9. <https://doi.org/10.1038/s41598-018-35629-4>
- Noell, S. E., Hellweger, F. L., Temperton, B., & Giovannoni, S. J. (2023). A Reduction of Transcriptional Regulation in Aquatic Oligotrophic Microorganisms Enhances Fitness in Nutrient-Poor Environments. *Microbiology and Molecular Biology Reviews*. <https://doi.org/10.1128/mnbr.00124-22>
- Ohtsuka, S., Suzuki, T., Horiguchi, T., Suzuki, N., & Not, F. (2015). Marine protists: Diversity and dynamics. *Marine Protists: Diversity and Dynamics*, 1–637. <https://doi.org/10.1007/978-4-431-55130-0/COVER>
- Oksanen, J., Blanchet, F. G., Friendly, M., Kindt, R., Legendre, P., Mcglinn, D., Minchin, P. R., Hara, R. B. O., Simpson, G. L., Solymos, P., Stevens, M. H. H., & Szoecs, E. (2020). *vegan: Community Ecology Package. R package version 2.5-7*.
- Ollison, G. A., Hu, S. K., Mesrop, L. Y., DeLong, E. F., & Caron, D. A. (2021). Come rain or shine: Depth not season shapes the active protistan community at station ALOHA in the North Pacific Subtropical Gyre. *Deep Sea Research Part I: Oceanographic Research Papers*, *170*, 103494. <https://doi.org/10.1016/j.dsr.2021.103494>
- Oren, A., & Garrity, G. M. (2021). Valid publication of the names of forty-two phyla of prokaryotes. *International Journal of Systematic and Evolutionary Microbiology*, *71*(10), 005056. <https://doi.org/10.1099/ijsem.0.005056>
- Osterholz, H., Kilgour, D. P. A., Storey, D. S., Lavik, G., Ferdelman, T. G., Niggemann, J., & Dittmar, T. (2021). Accumulation of DOC in the South Pacific Subtropical Gyre from a molecular perspective. *Marine Chemistry*, *231*(July 2020), 103955. <https://doi.org/10.1016/j.marchem.2021.103955>
- Pachiadaki, M. G., Yakimov, M. M., Lacono, V., Leadbetter, E., & Edgcomb, V. (2014). Unveiling microbial activities along the halocline of Thetis, a deep-sea hypersaline anoxic basin. *ISME Journal*, *8*(12), 2478–2489. <https://doi.org/10.1038/ismej.2014.100>
- Padilla Crespo, E., Gordils, L., Ramirez, X., & Michael Ceballos, R. (2020). Anoxygenic phototroph pufLM gene sequences derived from tropical aquatic sampling sites: Diversity, distribution, and phylogenetics. *Access Microbiology*, *2*(7A), 971. <https://doi.org/10.1099/acmi.ac2020.po0851>

- Pai, S.-C., Su, Y.-T., Lu, M.-C., Chou, Y., & Ho, T.-Y. (2021). Determination of Nitrate in Natural Waters by Vanadium Reduction and the Griess Assay: Reassessment and Optimization. *ACS ES&T Water*, *1*(6), 1524–1532. <https://doi.org/10.1021/acsestwater.1c00065>
- Pakes, M. J. (2013). *Anchialine Cave Environments: a novel chemosynthetic ecosystem and its ecology*. *15*(4), 250–260. <https://doi.org/10.11436/mssj.15.250>
- Parada, A. E., Needham, D. M., & Fuhrman, J. A. (2016). Every base matters: Assessing small subunit rRNA primers for marine microbiomes with mock communities, time series and global field samples. *Environmental Microbiology*, *18*(5), 1403–1414. <https://doi.org/10.1111/1462-2920.13023>
- Paradis, E., & Schliep, K. (2019). Ape 5.0: An environment for modern phylogenetics and evolutionary analyses in R. *Bioinformatics*, *35*(3), 526–528. <https://doi.org/10.1093/bioinformatics/bty633>
- Parks, D. H., Imelfort, M., Skennerton, C. T., Hugenholtz, P., & Tyson, G. W. (2015). CheckM: assessing the quality of microbial genomes recovered from isolates, single cells, and metagenomes. *Genome Research*, *25*(7), 1043–1055. <https://doi.org/10.1101/gr.186072.114>
- Partensky, F., Hess, W. R., & Vaultot, D. (1999). Prochlorococcus, a Marine Photosynthetic Prokaryote of Global Significance. *Microbiology and Molecular Biology Reviews*, *63*(1), 106–127. <https://doi.org/10.1128/MMBR.63.1.106-127.1999>
- Patin, N. V., Dietrich, Z. A., Stancil, A., Quinan, M., Beckler, J. S., Hall, E. R., Culter, J., Smith, C. G., Taillefert, M., & Stewart, F. J. (2021). Gulf of Mexico blue hole harbors high levels of novel microbial lineages. *The ISME Journal*, *15*(8), 2206–2232. <https://doi.org/10.1038/s41396-021-00917-x>
- Pérez-García, J. A., Díaz-Delgado, Y., García-Machado, E., Martínez-García, A., Gonzalez, B. C., Worsaae, K., & Armenteros, M. (2018). Nematode diversity of freshwater and anchialine caves of Western Cuba. *Proceedings of the Biological Society of Washington*, *131*(1), 144–155. <https://doi.org/10.2988/17-00024>
- Pérez-Moreno, J. L., Iliffe, T. M., & Bracken-Grissom, H. D. (2016). Life in the Underworld: Anchialine cave biology in the era of speleogenomics. *International Journal of Speleology*, *45*(2), 149–170. <https://doi.org/10.5038/1827-806X.45.2.1954>
- Piontek, J., Lunau, M., Händel, N., Borchard, C., Wurst, M., & Engel, A. (2010). Acidification increases microbial polysaccharide degradation in the ocean. *Biogeosciences*, *7*(5), 1615–1624. <https://doi.org/10.5194/bg-7-1615-2010>
- Pjevac, P., Hausmann, B., Schwarz, J., Kohl, G., Herbold, C. W., Loy, A., & Berry, D. (2021). An Economical and Flexible Dual Barcoding, Two-Step PCR Approach for Highly Multiplexed Amplicon Sequencing. *Frontiers in Microbiology*, *12*. <https://doi.org/10.3389/fmicb.2021.669776>
- Pohlman, J. W. (2011). The biogeochemistry of anchialine caves: Progress and possibilities. *Hydrobiologia*, *677*(1), 33–51. <https://doi.org/10.1007/s10750-011-0624-5>

- Pohlman, J. W., Iliffe, T. M., & Cifuentes, L. A. (1997). A stable isotope study of organic cycling and the ecology of an anchialine cave ecosystem. *Marine Ecology Progress Series*, 155, 17–27. <https://doi.org/10.3354/meps155017>
- Poindexter, J. (1981). Oligotrophy: fast and famine existence. In *Advances in Microbial Ecology* (Vol. 5, pp. 63–89).
- Polovina, J. J., Howell, E. A., & Abecassis, M. (2008). Ocean's least productive waters are expanding. *Geophysical Research Letters*, 35(3), 1–6. <https://doi.org/10.1029/2007GL031745>
- R Core Team. (2020). *R: A language and environment for statistical computing*. R Foundation for Statistical Computing, Vienna, Austria. <https://www.R-project.org/>.
- Raimbault, P., & Garcia, N. (2007). Carbon and nitrogen uptake in the South Pacific Ocean: evidence for efficient dinitrogen fixation and regenerated production leading to large accumulation of dissolved organic matter in nitrogen-depleted waters. *Biogeosciences Discuss*, 4(October), 3531–3579. <https://doi.org/10.5194/bgd-4-3531-2007>
- Raimbault, P., & Garcia, N. (2008). Evidence for efficient regenerated production and dinitrogen fixation in nitrogen-deficient waters of the South Pacific Ocean: impact on new and export production estimates. *Biogeosciences*, 5(2), 323–338. <https://doi.org/10.5194/bg-5-323-2008>
- Raimbault, P., Garcia, N., & Cerutti, F. (2008). Distribution of inorganic and organic nutrients in the South Pacific Ocean – evidence for long-term accumulation of organic matter in nitrogen-depleted waters. *Biogeosciences*, 5(2), 281–298. <https://doi.org/10.5194/bg-5-281-2008>
- Raina, J. B., Giardina, M., Brumley, D. R., Clode, P. L., Pernice, M., Guagliardo, P., Bougoure, J., Mendis, H., Smriga, S., Sonnenschein, E. C., Ullrich, M. S., Stocker, R., & Seymour, J. R. (2023). Chemotaxis increases metabolic exchanges between marine picophytoplankton and heterotrophic bacteria. *Nature Microbiology*, 8(3), 510–521. <https://doi.org/10.1038/s41564-023-01327-9>
- Reczuga, M. K., Seppey, C. V. W., Mulo, M., Jassey, V. E. J., Buttler, A., Słowińska, S., Słowiński, M., Lara, E., Lamentowicz, M., & Mitchell, E. A. D. (2020). Assessing the responses of Sphagnum micro-eukaryotes to climate changes using high throughput sequencing. *PeerJ*, 8, e9821. <https://doi.org/10.7717/peerj.9821>
- Reintjes, G., Fuchs, B. M., Amann, R., & Arnosti, C. (2020). Extensive Microbial Processing of Polysaccharides in the South Pacific Gyre via Selfish Uptake and Extracellular Hydrolysis. *Frontiers in Microbiology*, 11(December), 1–14. <https://doi.org/10.3389/fmicb.2020.583158>
- Reintjes, G., Tegetmeyer, H. E., Bürgisser, M., Orlić, S., Tews, I., Zubkov, M., Voß, D., Zielinski, O., Quast, C., Glöckner, F. O., Amann, R., Ferdelman, T. G., & Fuchs, B. M. (2016). *On-board sequencing of the microbial community of the South Pacific Gyre*. <https://doi.org/https://doi.org/10.1594/PANGAEA.882015>
- Reintjes, G., Tegetmeyer, H. E., Bürgisser, M., Orlić, S., Tews, I., Zubkov, M., Voß, D., Zielinski, O., Quast, C., Glöckner, F. O., Amann, R., Ferdelman, T. G., & Fuchs, B. M. (2019). On-Site Analysis of Bacterial Communities of the Ultraoligotrophic South Pacific

- Gyre. *Applied and Environmental Microbiology*, 85(14), 1–14. <https://doi.org/10.1128/AEM.00184-19>
- Richards, T. A., Jones, M. D. M., Leonard, G., & Bass, D. (2012). Marine fungi: Their ecology and molecular diversity. *Annual Review of Marine Science*, 4(January), 495–522. <https://doi.org/10.1146/annurev-marine-120710-100802>
- Richardson, K., & Bendtsen, J. (2019). Vertical distribution of phytoplankton and primary production in relation to nutricline depth in the open ocean. *Mar Ecol Prog Ser*, 620, 33–46. <https://doi.org/10.3354/meps12960>
- Riser, S. C., & Johnson, K. S. (2008). Net production of oxygen in the subtropical ocean. *Nature*, 451(7176), 323–325. <https://doi.org/10.1038/nature06441>
- Rizos, I., Debeljak, P., Finet, T., Klein, D., Ayata, S.-D., Not, F., & Bittner, L. (2023). Beyond the limits of the unassigned protist microbiome: inferring large-scale spatio-temporal patterns of Syndiniales marine parasites. *ISME Communications*, 3(1), 16. <https://doi.org/10.1038/s43705-022-00203-7>
- Roshan, S., & DeVries, T. (2017). Efficient dissolved organic carbon production and export in the oligotrophic ocean. *Nature Communications*, 8(1). <https://doi.org/10.1038/s41467-017-02227-3>
- Rossi, I. R., & Cukrov, N. (2017). Archaeological Potential of the Anchialine Caves in Croatia. In *Under the Sea: Archaeology and Palaeolandscapes* (pp. 255–266). [https://doi.org/10.1007/978-3-319-53160-1\\_17](https://doi.org/10.1007/978-3-319-53160-1_17)
- Ruiz-González, C., Rodellas, V., & Garcia-Orellana, J. (2021). The microbial dimension of submarine groundwater discharge: Current challenges and future directions. In *FEMS Microbiology Reviews* (Vol. 45, Issue 5). Oxford University Press. <https://doi.org/10.1093/femsre/fuab010>
- Sanz-Sáez, I., Salazar, G., Sánchez, P., Lara, E., Royo-Llonch, M., Sà, E. L., Lucena, T., Pujalte, M. J., Vaqué, D., Duarte, C. M., Gasol, J. M., Pedrós-Alió, C., Sánchez, O., & Acinas, S. G. (2020). Diversity and distribution of marine heterotrophic bacteria from a large culture collection. *BMC Microbiology*, 20(1), 1–16. <https://doi.org/10.1186/s12866-020-01884-7>
- Schmidt, H., Eickhorst, T., & Tippkötter, R. (2012). Evaluation of tyramide solutions for an improved detection and enumeration of single microbial cells in soil by CARD-FISH. *Journal of Microbiological Methods*, 91(3), 399–405. <https://doi.org/10.1016/j.mimet.2012.09.021>
- Schnetzer, A., Moorthi, S. D., Countway, P. D., Gast, R. J., Gilg, I. C., & Caron, D. A. (2011). Depth matters: Microbial eukaryote diversity and community structure in the eastern North Pacific revealed through environmental gene libraries. *Deep Sea Research Part I: Oceanographic Research Papers*, 58(1), 16–26. <https://doi.org/10.1016/J.DSR.2010.10.003>
- Scoble, J. M., & Cavalier-Smith, T. (2014). Scale evolution in paraphysomonadida (Chrysophyceae): Sequence phylogeny and revised taxonomy of paraphysomonas, new genus clathromonas, and 25 new species. *European Journal of Protistology*, 50(5), 551–592. <https://doi.org/10.1016/j.ejop.2014.08.001>

- Sebastián, M., Estrany, M., Ruiz-González, C., Forn, I., Montserrat Sala, M., Gasol, J. M., & Marrasé, C. (2019). High growth potential of long-term starved deep ocean opportunistic heterotrophic bacteria. *Frontiers in Microbiology*, *10*(APR), 760. <https://doi.org/10.3389/fmicb.2019.00760>
- Seemann, T. (2014). Prokka: rapid prokaryotic genome annotation. *Bioinformatics*, *30*(14), 2068–2069. <https://doi.org/10.1093/bioinformatics/btu153>
- Sehein, T. R., Gast, R. J., Pachiadaki, M., Guillou, L., & Edgcomb, V. P. (2022). Parasitic infections by Group II Syndiniales target selected dinoflagellate host populations within diverse protist assemblages in a model coastal pond. *Environmental Microbiology*, *24*(4), 1818–1834. <https://doi.org/10.1111/1462-2920.15977>
- Sen, K., Sen, B., & Wang, G. (2022). Diversity, Abundance, and Ecological Roles of Planktonic Fungi in Marine Environments. *Journal of Fungi*, *8*(5), 491. <https://doi.org/10.3390/jof8050491>
- Seymour, J. R., Amin, S. A., Raina, J. B., & Stocker, R. (2017). Zooming in on the phycosphere: The ecological interface for phytoplankton-bacteria relationships. *Nature Microbiology*, *2*(May). <https://doi.org/10.1038/nmicrobiol.2017.65>
- Seymour, J. R., Humphreys, W. F., & Mitchell, J. G. (2007). Stratification of the microbial community inhabiting an anchialine sinkhole. *Aquatic Microbial Ecology*, *50*(1), 11–24. <https://doi.org/10.3354/ame01153>
- Shea, C. H., Wojtal, P. K., Close, H. G., Maas, A. E., Stamieszkin, K., Cope, J. S., Steinberg, D. K., Wallsgrove, N., & Popp, B. N. (2023). Small particles and heterotrophic protists support the mesopelagic zooplankton food web in the subarctic northeast Pacific Ocean. *Limnology and Oceanography*, *68*(8), 1949–1963. <https://doi.org/10.1002/lno.12397>
- Shi, X. L., Lepère, C., Scanlan, D. J., & Vaultot, D. (2011). Plastid 16S rRNA Gene Diversity among Eukaryotic Picophytoplankton Sorted by Flow Cytometry from the South Pacific Ocean. *PLoS ONE*, *6*(4), e18979. <https://doi.org/10.1371/journal.pone.0018979>
- Shiozaki, T., Bombar, D., Riemann, L., Sato, M., Hashihama, F., Kodama, T., Tanita, I., Takeda, S., Saito, H., Hamasaki, K., & Furuya, K. (2018). Linkage Between Dinitrogen Fixation and Primary Production in the Oligotrophic South Pacific Ocean. *Global Biogeochemical Cycles*, *32*(7), 1028–1044. <https://doi.org/10.1029/2017GB005869>
- Siegel, D. A., Buesseler, K. O., Doney, S. C., Sailley, S. F., Behrenfeld, M. J., & Boyd, P. W. (2014). Global assessment of ocean carbon export by combining satellite observations and food-web models. *Global Biogeochemical Cycles*, *28*(3), 181–196. <https://doi.org/10.1002/2013GB004743>
- Siegel, D. A., Devries, T., Cetinić, I., & Bisson, K. M. (2023). Quantifying the Ocean's Biological Pump and Its Carbon Cycle Impacts on Global Scales. *Annual Review of Marine Science*, *15*, 329–356. <https://doi.org/10.1146/annurev-marine-040722-115226>
- Signorini, S. R., Franz, B. A., & McClain, C. R. (2015). Chlorophyll variability in the oligotrophic gyres: Mechanisms, seasonality and trends. *Frontiers in Marine Science*, *2*(FEB). <https://doi.org/10.3389/fmars.2015.00001>
- Šimek, K., Kasalický, V., Jezbera, J., Horňák, K., Nedoma, J., Hahn, M. W., Bass, D., Jost, S., & Boenigk, J. (2013). Differential freshwater flagellate community response to bacterial

- food quality with a focus on Limnohabitans bacteria. *The ISME Journal*, 7(8), 1519–1530. <https://doi.org/10.1038/ismej.2013.57>
- Simon, M., Grossart, H. P., Schweitzer, B., & Ploug, H. (2002). Microbial ecology of organic aggregates in aquatic ecosystems. *Aquatic Microbial Ecology*, 28(2), 175–211. <https://doi.org/10.3354/ame028175>
- Sket, B. (1996). The ecology of anchialine caves. *Trends in Ecology and Evolution*, 11(5), 221–225. [https://doi.org/10.1016/0169-5347\(96\)20031-X](https://doi.org/10.1016/0169-5347(96)20031-X)
- Smith, S. V. (1984). Phosphorus versus nitrogen limitation in the marine environment. *Limnology and Oceanography*, 29(6), 1149–1160. <https://doi.org/10.4319/lo.1984.29.6.1149>
- Sobol, M. S., Hoshino, T., Delgado, V., Futagami, T., Kadooka, C., Inagaki, F., & Kiel Reese, B. (2023). Genome characterization of two novel deep-sea sediment fungi, *Penicillium pacificagyrum* sp. nov. and *Penicillium pacificasedimenti* sp. nov., from South Pacific Gyre subseafloor sediments, highlights survivability. *BMC Genomics*, 24(1), 249. <https://doi.org/10.1186/s12864-023-09320-6>
- Sogawa, S., Nakamura, Y., Nagai, S., Nishi, N., Hidaka, K., Shimizu, Y., & Setou, T. (2022). DNA metabarcoding reveals vertical variation and hidden diversity of Alveolata and Rhizaria communities in the western North Pacific. *Deep-Sea Research Part I: Oceanographic Research Papers*, 183, 103765. <https://doi.org/10.1016/j.dsr.2022.103765>
- Steele, J. A., Countway, P. D., Xia, L., Vigil, P. D., Beman, J. M., Kim, D. Y., Chow, C.-E. T., Sachdeva, R., Jones, A. C., Schwalbach, M. S., Rose, J. M., Hewson, I., Patel, A., Sun, F., Caron, D. A., & Fuhrman, J. A. (2011). Marine bacterial, archaeal and protistan association networks reveal ecological linkages. *The ISME Journal*, 5(9), 1414–1425. <https://doi.org/10.1038/ismej.2011.24>
- Stegen, J. C., Lin, X., Fredrickson, J. K., Chen, X., Kennedy, D. W., Murray, C. J., Rockhold, M. L., & Konopka, A. (2013). Quantifying community assembly processes and identifying features that impose them. *ISME Journal*, 7(11), 2069–2079. <https://doi.org/10.1038/ismej.2013.93>
- Stegen, J. C., Lin, X., Fredrickson, J. K., & Konopka, A. E. (2015). Estimating and mapping ecological processes influencing microbial community assembly. *Frontiers in Microbiology*, 6(MAY), 1–15. <https://doi.org/10.3389/fmicb.2015.00370>
- Steinberg, D. K., & Landry, M. R. (2017). Zooplankton and the Ocean Carbon Cycle. *Annual Review of Marine Science*, 9(1), 413–444. <https://doi.org/10.1146/annurev-marine-010814-015924>
- Steward, K. F., Eilers, B., Tripet, B., Fuchs, A., Dorle, M., Rawle, R., Soriano, B., Balasubramanian, N., Copié, V., Bothner, B., & Hatzenpichler, R. (2020). Metabolic Implications of Using BioOrthogonal Non-Canonical Amino Acid Tagging (BONCAT) for Tracking Protein Synthesis. *Frontiers in Microbiology*, 11(February), 1–12. <https://doi.org/10.3389/fmicb.2020.00197>
- Stock, A., Edgcomb, V., Orsi, W., Filker, S., Breiner, H. W., Yakimov, M. M., & Stoeck, T. (2013). Evidence for isolated evolution of deep-sea ciliate communities through geological separation and environmental selection. *BMC Microbiology*, 13, 1–15. <https://doi.org/10.1186/1471-2180-13-150>

- Stocker, R. (2012). Marine microbes see a sea of gradients. *Science*, *338*(6107), 628–633. <https://doi.org/10.1126/science.1208929>
- Stoeck, T., Bass, D., Nebel, M., Christen, R., Jones, M. D. M., Breiner, H.-W., & Richards, T. A. (2010). Multiple marker parallel tag environmental DNA sequencing reveals a highly complex eukaryotic community in marine anoxic water. *Molecular Ecology*, *19*, 21–31. <https://doi.org/10.1111/j.1365-294X.2009.04480.x>
- Strickland, J. D., & Parsons, T. R. (1972). *A Practical Hand Book of Seawater Analysis* (Issue 167). Fisheries Research Board of Canada Bulletin.
- Sunagawa, S., Coelho, L. P., Chaffron, S., Kultima, J. R., Labadie, K., Salazar, G., Djahanschiri, B., Zeller, G., Mende, D. R., Alberti, A., Cornejo-Castillo, F. M., Costea, P. I., Cruaud, C., D’Ovidio, F., Engelen, S., Ferrera, I., Gasol, J. M., Guidi, L., Hildebrand, F., ... Bork, P. (2015). Structure and function of the global ocean microbiome. *Science*, *348*(6237), 1–10. <https://doi.org/10.1126/science.1261359>
- Surić, M., Lončarić, R., & Lončar, N. (2010). Submerged caves of Croatia: Distribution, classification and origin. *Environmental Earth Sciences*, *61*(7), 1473–1480. <https://doi.org/10.1007/s12665-010-0463-0>
- Suter, E. A., Pachiadaki, M., Taylor, G. T., & Edgcomb, V. P. (2022). Eukaryotic Parasites Are Integral to a Productive Microbial Food Web in Oxygen-Depleted Waters. *Frontiers in Microbiology*, *12*(January), 1–16. <https://doi.org/10.3389/fmicb.2021.764605>
- Tedersoo, L., Anslan, S., Bahram, M., Põlme, S., Riit, T., Liiv, I., Kõljalg, U., Kisand, V., Nilsson, H., Hildebrand, F., Bork, P., & Abarenkov, K. (2015). Shotgun metagenomes and multiple primer pair-barcode combinations of amplicons reveal biases in metabarcoding analyses of fungi. *MycKeys*, *10*, 1–43. <https://doi.org/10.3897/mycokeys.10.4852>
- Tedersoo, L., Bahram, M., Zinger, L., Nilsson, R. H., Kennedy, P. G., Yang, T., Anslan, S., & Mikryukov, V. (2022). Best practices in metabarcoding of fungi: from experimental design to results. *Molecular Ecology*, *February*, 2769–2795. <https://doi.org/10.1111/mec.16460>
- Thompson, L. R., Sanders, J. G., McDonald, D., Amir, A., Ladau, J., Locey, K. J., Prill, R. J., Tripathi, A., Gibbons, S. M., Ackermann, G., Navas-Molina, J. A., Janssen, S., Kopylova, E., Vázquez-Baeza, Y., González, A., Morton, J. T., Mirarab, S., Zech Xu, Z., Jiang, L., ... Zhao, H. (2017). A communal catalogue reveals Earth’s multiscale microbial diversity. *Nature*, *551*(7681), 457–463. <https://doi.org/10.1038/nature24621>
- Thornton, D. C. O. (2014). Dissolved organic matter (DOM) release by phytoplankton in the contemporary and future ocean. *European Journal of Phycology*, *49*(1), 20–46. <https://doi.org/10.1080/09670262.2013.875596>
- van Hengstum, P. J., Cresswell, J. N., Milne, G. A., & Iliffe, T. M. (2019). Development of anchialine cave habitats and karst subterranean estuaries since the last ice age. *Scientific Reports*, *9*(1), 1–10. <https://doi.org/10.1038/s41598-019-48058-8>
- Vigneron, A., Cruaud, P., Culley, A. I., Couture, R. M., Lovejoy, C., & Vincent, W. F. (2021). Genomic evidence for sulfur intermediates as new biogeochemical hubs in a model aquatic microbial ecosystem. *Microbiome*, *9*(1), 1–14. <https://doi.org/10.1186/s40168-021-00999-x>

- Vigneron, A., Cruaud, P., Lovejoy, C., & Vincent, W. F. (2022). Genomic evidence of functional diversity in DPANN archaea, from oxic species to anoxic vampiristic consortia. *ISME Communications*, 2(1), 1–10. <https://doi.org/10.1038/s43705-022-00088-6>
- Wagener, T., Guieu, C., Losno, R., Bonnet, S., & Mahowald, N. (2008). Revisiting atmospheric dust export to the Southern Hemisphere ocean: Biogeochemical implications. *Global Biogeochemical Cycles*, 22(2), 2006. <https://doi.org/10.1029/2007GB002984>
- Wallace, R. B., Baumann, H., Grear, J. S., Aller, R. C., & Gobler, C. J. (2014). Coastal ocean acidification: The other eutrophication problem. *Estuarine, Coastal and Shelf Science*, 148, 1–13. <https://doi.org/10.1016/j.ecss.2014.05.027>
- Walsh, E., Smith, D., Sogin, M., & D'Hondt, S. (2015). Bacterial and archaeal biogeography of the deep chlorophyll maximum in the South Pacific Gyre. *Aquatic Microbial Ecology*, 75(1), 1–13. <https://doi.org/10.3354/ame01746>
- Wang, B., Qin, W., Ren, Y., Zhou, X., Jung, M.-Y., Han, P., Eloë-Fadrosh, E. A., Li, M., Zheng, Y., Lu, L., Yan, X., Ji, J., Liu, Y., Liu, L., Heiner, C., Hall, R., Martens-Habben, W., Herbold, C. W., Rhee, S., ... Jia, Z. (2019). Expansion of Thaumarchaeota habitat range is correlated with horizontal transfer of ATPase operons. *The ISME Journal*, 13(12), 3067–3079. <https://doi.org/10.1038/s41396-019-0493-x>
- West, N. J., Lepère, C., Manes, C.-L. de O., Catala, P., Scanlan, D. J., & Lebaron, P. (2016). Distinct Spatial Patterns of SAR11, SAR86, and Actinobacteria Diversity along a Transect in the Ultra-oligotrophic South Pacific Ocean. *Frontiers in Microbiology*, 7(MAR), 234. <https://doi.org/10.3389/fmicb.2016.00234>
- Wickham, H. (2016). ggplot2: Elegant Graphics for Data Analysis. In *Media* (Vol. 35, Issue July). <http://had.co.nz/ggplot2/book>
- Wickham, H., Averick, M., Bryan, J., Chang, W., McGowan, L., François, R., Grolemund, G., Hayes, A., Henry, L., Hester, J., Kuhn, M., Pedersen, T., Miller, E., Bache, S., Müller, K., Ooms, J., Robinson, D., Seidel, D., Spinu, V., ... Yutani, H. (2019). Welcome to the Tidyverse. *Journal of Open Source Software*, 4(43), 1686. <https://doi.org/10.21105/joss.01686>
- Wickham, H., François, R., Henry, L., Müller, K., & Vaughan, D. (2023). *dplyr: A Grammar of Data Manipulation*. <https://dplyr.tidyverse.org/authors.html#citation>
- Worden, A. Z., Follows, M. J., Giovannoni, S. J., Wilken, S., Zimmerman, A. E., & Keeling, P. J. (2015). Rethinking the marine carbon cycle: Factoring in the multifarious lifestyles of microbes. *Science*, 347(6223). <https://doi.org/10.1126/science.1257594>
- Wurzbacher, C., Nilsson, R. H., Rautio, M., & Peura, S. (2017). Poorly known microbial taxa dominate the microbiome of permafrost thaw ponds. *The ISME Journal*, 11(8), 1938–1941. <https://doi.org/10.1038/ismej.2017.54>
- Xiang, Y., Quay, P. D., Sonnerup, R. E., & Fassbender, A. J. (2023). Subtropical Gyre Nutrient Cycling in the Upper Ocean: Insights From a Nutrient-Ratio Budget Method. *Geophysical Research Letters*, 50(13), 1–10. <https://doi.org/10.1029/2023GL103213>
- Yan, Y., Lin, T., Xie, W., Zhang, D., Jiang, Z., Han, Q., Zhu, X., & Zhang, H. (2023). Contrasting Mechanisms Determine the Microeukaryotic and Syndiniales Community

- Assembly in a Eutrophic bay. *Microbial Ecology*, 86(3), 1575–1588. <https://doi.org/10.1007/s00248-023-02175-0>
- Yeh, Y.-C., & Fuhrman, J. A. (2022). Contrasting diversity patterns of prokaryotes and protists over time and depth at the San-Pedro Ocean Time series. *ISME Communications 2022 2:1*, 2(1), 1–12. <https://doi.org/10.1038/s43705-022-00121-8>
- York, A. (2022). Chemotaxis in the ocean. *Nature Reviews Microbiology*, 20(7), 381. <https://doi.org/10.1038/S41579-022-00743-8>
- Yoshida-Takashima, Y., Takaki, Y., Yoshida, M., Zhang, Y., Nunoura, T., & Takai, K. (2022). Genomic insights into phage-host interaction in the deep-sea chemolithoautotrophic Campylobacterota, Nitratiruptor. *ISME Communications*, 2(1), 1–10. <https://doi.org/10.1038/s43705-022-00194-5>
- Zamora-Terol, S., Novotny, A., & Winder, M. (2021). Molecular evidence of host-parasite interactions between zooplankton and Syndiniales. *Aquatic Ecology*, 55(1), 125–134. <https://doi.org/10.1007/s10452-020-09816-3>
- Zhang, C. L., Xie, W., Martin-Cuadrado, A. B., & Rodriguez-Valera, F. (2015). Marine Group II Archaea, potentially important players in the global ocean carbon cycle. *Frontiers in Microbiology*, 6(OCT). <https://doi.org/10.3389/fmicb.2015.01108>
- Zhang, J. Z., & Fischer, C. J. (2006). A simplified resorcinol method for direct spectrophotometric determination of nitrate in seawater. *Marine Chemistry*, 99(1–4), 220–226. <https://doi.org/10.1016/j.marchem.2005.09.008>
- Zhang, T., Fan, X., Gao, F., Al-Farraj, S. A., El-Serehy, H. A., & Song, W. (2019). Further analyses on the phylogeny of the subclass Scuticociliatia (Protozoa, Ciliophora) based on both nuclear and mitochondrial data. *Molecular Phylogenetics and Evolution*, 139(March), 106565. <https://doi.org/10.1016/j.ympev.2019.106565>
- Zhang, Y., Huang, N., & Jing, H. (2022). Biogeography and Population Divergence of Microeukaryotes Associated with Fluids and Chimneys in the Hydrothermal Vents of the Southwest Indian Ocean. *Microbiology Spectrum*. <https://doi.org/10.1128/spectrum.02632-21>
- Zhou, Z., Tran, P. Q., Breister, A. M., Liu, Y., Kieft, K., Cowley, E. S., Karaoz, U., & Anantharaman, K. (2022). METABOLIC: high-throughput profiling of microbial genomes for functional traits, metabolism, biogeochemistry, and community-scale functional networks. *Microbiome*, 10(1), 1–22. <https://doi.org/10.1186/s40168-021-01213-8>
- Zhu, H. Z., Zhang, Z. F., Zhou, N., Jiang, C. Y., Wang, B. J., Cai, L., & Liu, S. J. (2019). Diversity, distribution and co-occurrence patterns of bacterial communities in a karst cave system. *Frontiers in Microbiology*, 10(JULY), 1–12. <https://doi.org/10.3389/fmicb.2019.01726>
- Žic, V., Truesdale, V. W., Cuculić, V., & Cukrov, N. (2011). Nutrient speciation and hydrography in two anchialine caves in Croatia: Tools to understand iodine speciation. *Hydrobiologia*, 677(1), 129–148. <https://doi.org/10.1007/s10750-011-0686-4>
- Žic, V., Truesdale, V. W., & Cukrov, N. (2008). The distribution of iodide and iodate in anchialine cave waters — Evidence for sustained localised oxidation of iodide to iodate in

marine water. *Marine Chemistry*, 112, 168–178.  
<https://doi.org/10.1016/j.marchem.2008.09.001>

Zielinski, O., Henkel, R., Voß, D., & Ferdelman, T. G. (2018). *Physical oceanography during SONNE cruise SO245 (UltraPac)*. <https://doi.pangaea.de/10.1594/PANGAEA.890394>

Zwirgmaier, K., Keiz, K., Engel, M., Geist, J., & Raeder, U. (2015). Seasonal and spatial patterns of microbial diversity along a trophic gradient in the interconnected lakes of the Osterseen Lake District, Bavaria. *Frontiers in Microbiology*, 6(OCT), 165646. <https://doi.org/10.3389/fmicb.2015.01168>

## SUPPLEMENTARY MATERIALS

The supplementary materials are categorized into four sections corresponding to distinct chapters within the doctoral dissertation. Each section is accompanied by a notation indicating the relevant chapter, followed by the tables and figures that relate to it. The content descriptions for tables and figures are provided within their respective chapters. In total, there are 11 tables and 11 figures included in the supplementary materials.

### Supplementary material 1

**Chapter Material and methods:** 2.3. Study area: anchialine speleological object in the Martinska area

**Table S1.** 16S rRNA-targeted oligonucleotide probes and hybridization conditions used for CARD-FISH experiments.

Probe	Target group	Sequence (5'→ 3')	HB (%) <sup>a</sup>	Reference
EUB I*	Most Bacteria	5'-GCT GCC TCC CGT AGG AGT-3'	35	Amann et al. (1995)
EUB II*	Planctomycetota	5'-GCA GCC ACC CGT AGG TGT-3'	35	Daims et al. (1999)
EUB III*	Verrucomicrobiota	5'-GCT GCC ACC CGT AGG TGT-3'	35	Daims et al. (1999)

<sup>a</sup> HB, formamide concentration in the hybridization buffer

\*Used in equimolar mixture EUBI-III

## Supplementary material 2

**Chapter Results:** 3.1. Diversity patterns of protists and fungi in the water column of the ultra-oligotrophic South Pacific Gyre area

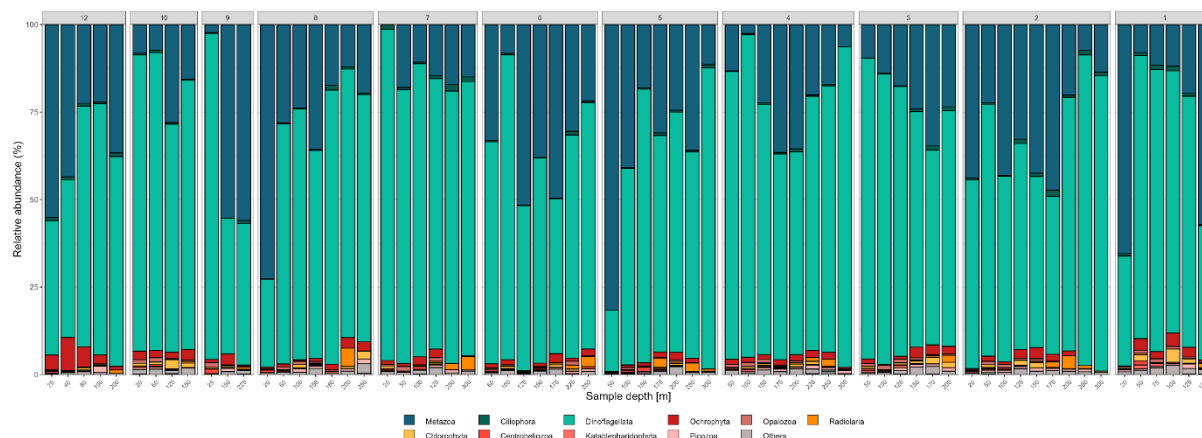


**Figure S1.** Diversity of the community based on the 18S dataset across vertical profile from 20 to 300 m per sampling station at the phyla level.

**Table S2.** PERMANOVA results based on the Bray-Curtis distance of the protistan and parasitic protistan community.

		Group	R <sup>2</sup>	P value
Protists	Sampling station		0.193	0.016 *
	Sampling depth		0.422	0.001 ***
	Radiance zone		0.196	0.001 ***
Parasitic protists	Sampling station		0.188	0.018 *
	Sampling depth		0.438	0.001 ***
	Radiance zone		0.197	0.001 ***

**Table S3.** Mantel tests between the Bray-Curtis distance of the protistan community and Euclidean distances of environmental variables using Spearman's rank correlation.

		Parameter	Mantel correlation r	P value
Protists		Temperature	0.603	0.001 ***
		Salinity	0.396	0.001 ***
		Chl <i>a</i>	0.110	0.07
		Oxygen (μmol L <sup>-1</sup> )	0.429	0.001 ***
		PO <sub>4</sub> (μmol L <sup>-1</sup> )	0.517	0.001 ***
		NO <sub>2</sub> (μmol L <sup>-1</sup> )	0.069	0.18
		NO <sub>x</sub> (μmol L <sup>-1</sup> )	0.594	0.001 ***
		SiOH <sub>4</sub> (μmol L <sup>-1</sup> )	0.317	0.001 ***
		NO <sub>3</sub> (μmol L <sup>-1</sup> )	0.593	0.001 ***
		Temperature	0.532	0.001 ***
	Salinity	0.323	0.001 ***	

	Chl <i>a</i>	0.162	0.004 **
	Oxygen ( $\mu\text{mol L}^{-1}$ )	0.354	0.001 ***
Parasitic protists	PO <sub>4</sub> ( $\mu\text{mol L}^{-1}$ )	0.381	0.001 ***
	NO <sub>2</sub> ( $\mu\text{mol L}^{-1}$ )	0.025	0.346
	NO <sub>x</sub> ( $\mu\text{mol L}^{-1}$ )	0.437	0.001 ***
	SiOH <sub>4</sub> ( $\mu\text{mol L}^{-1}$ )	0.212	0.001 ***
	NO <sub>3</sub> ( $\mu\text{mol L}^{-1}$ )	0.436	0.001 ***

**Table S4.** PERMANOVA results based on the Bray-Curtis distance of protistan community diel variation at station 8.

	Group	R <sup>2</sup>	P value
	Sampling depth	0.580	0.001 ***
Protists	Radiance zone	0.259	0.001 ***
	Sampling hour	0.116	0.516

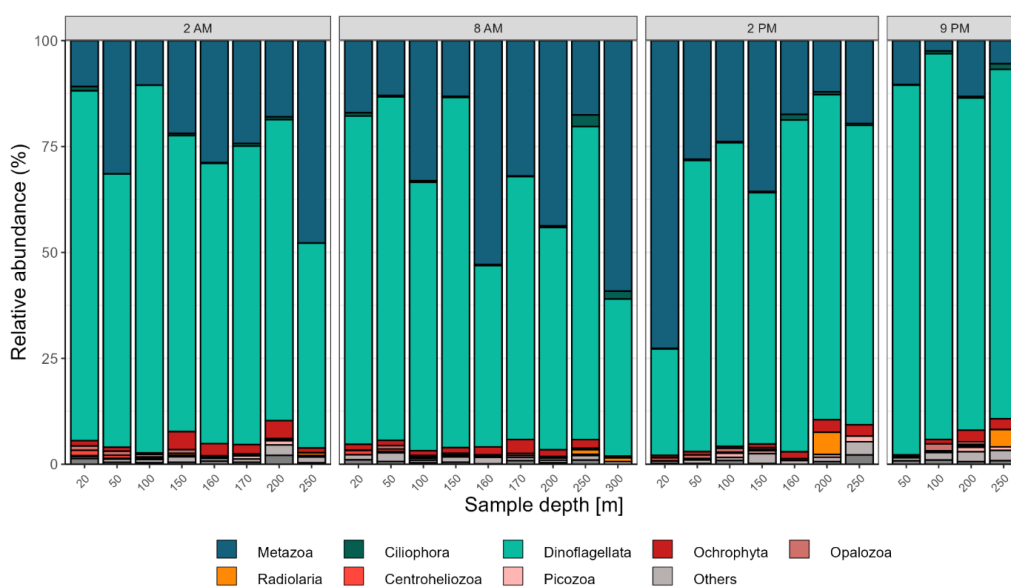


**Figure S2.** Diurnal community diversity based on the 18S dataset across vertical profile from 20 to 300m at station 8 on the phyla level.

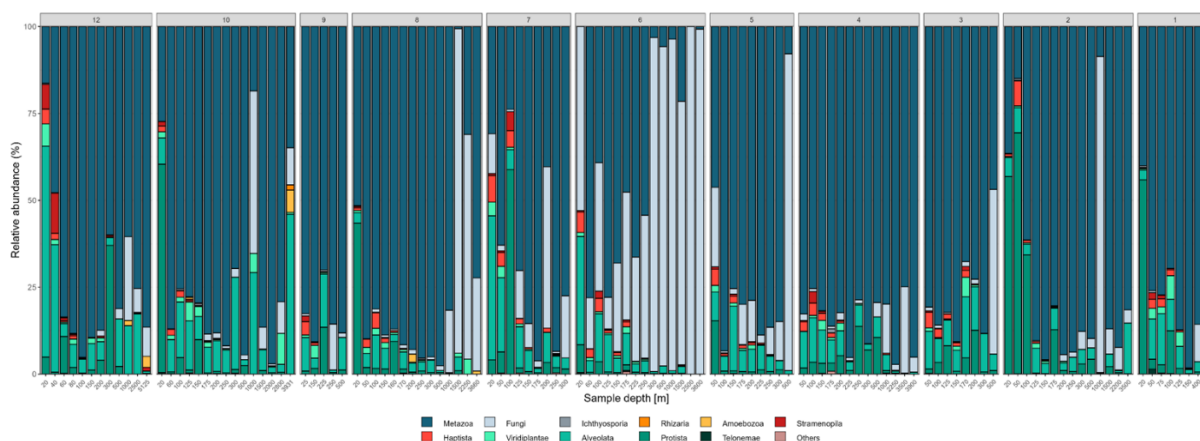


**Figure S3.** Diversity of the community based on the ITS dataset across vertical profile from 20 to 5125m per sampling station on the phyla level.

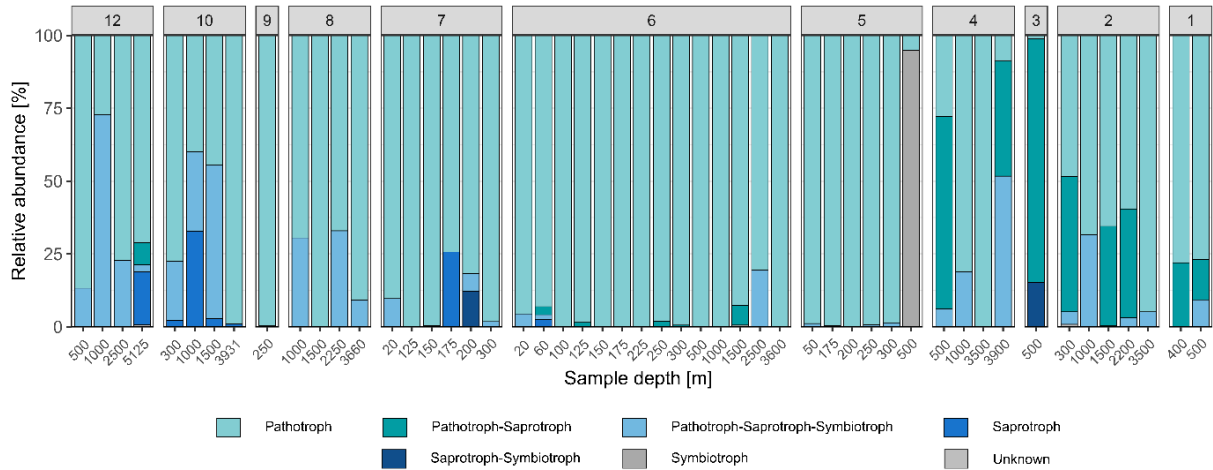


**Figure S4.** Relative abundance of fungal trophic functional groups per sampling station and depth.

**Table S5.** PERMANOVA results based on the Bray-Curtis distance of the fungal community.

	Group	R <sup>2</sup>	P value
	Sampling station	0.545	0.001 ***
Fungi	Sampling depth	0.537	0.051 .
	Radiance zone	0.105	0.008**
	Pelagic zone	0.223	0.001 ***

**Table S6.** Mantel tests between the Bray-Curtis distance of the fungal community and Euclidean distances of environmental variables using Spearman's rank correlation.

	Parameter	Mantel correlation r	P value
	Temperature	0.167	0.007 **
	Salinity	0.057	0.137
	Chl <i>a</i>	-0.087	0.916
Fungi	Oxygen (μmol L <sup>-1</sup> )	0.294	0.001 ***
	PO <sub>4</sub> (μmol L <sup>-1</sup> )	0.231	0.001 ***
	NO <sub>2</sub> (μmol L <sup>-1</sup> )	-0.088	0.921
	NO <sub>x</sub> (μmol L <sup>-1</sup> )	0.244	0.002 **
	SiOH <sub>4</sub> (μmol L <sup>-1</sup> )	0.176	0.005
	NO <sub>3</sub> (μmol L <sup>-1</sup> )	0.245	0.001 ***

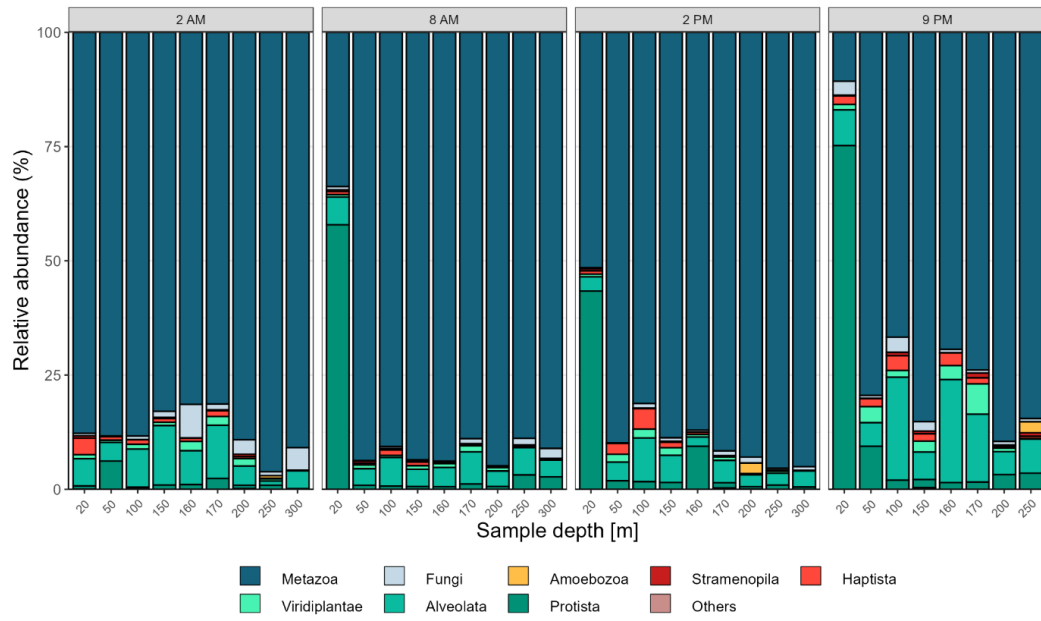


**Figure S5.** Diurnal community diversity based on the ITS dataset across vertical profile from 20 to 300m at station 8 on the phyla level.

**Supplementary material 3**

**Chapter Results:** 3.2. Diversity patterns of prokaryotes and protists in the water column of anchialine pits and caves in the area of National Park Kornati

**Table S7.** Values of measured chemical parameters in anchialine speleological objects.

Anchialine speleological object	Sample	TN (mg L <sup>-1</sup> )	Nitrate (mg L <sup>-1</sup> )	Nitrite (mg L <sup>-1</sup> )	Ammonium + Norg (mg L <sup>-1</sup> )	orto-P (mg L <sup>-1</sup> )	TOC (mg L <sup>-1</sup> )
Vjetruša	VG-AH	7	2.7	0.003	4.297	0.044	0.71
	VG-H	1.3	0.41	0.001	0.89	0.033	0.49
	VG-BH	0.15	0.12	0.001	0.03	0.011	0.4
Blitvica	BP-AH	0.39	0.17	0.002	0.218	0.017	1
	BP-H	0.15	0.015	0.001	0.15	0.019	0.67
	BP-BH	0.2	0.11	0.001	0.089	0.019	0.47
Gravrnjača	GKV-AH	1.4	0.04	0.001	1.36	0.009	1.2
	GKV-H	0.15	0.09	0.001	0.06	0.006	1.1
	GKV-BH	0.08	0.03	0.001	0.05	0.011	0.49
Živa Voda	ZVP-AH	3	0.78	0.007	2.213	0.006	1.3
	ZVP-H	0.54	0.02	0.002	0.518	0.033	1.2
	ZVP-BH	0.36	0.015	0.001	0.36	0.032	0.87

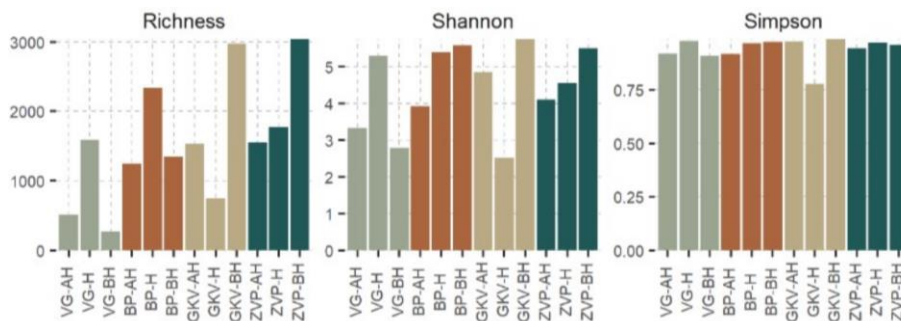


**Figure S6.** Alpha diversity of prokaryotic community in anchialine speleological objects. Sample name abbreviations refer to the area of a sampling point: above the halocline (AH), in the halocline (H), and below the halocline (BH).

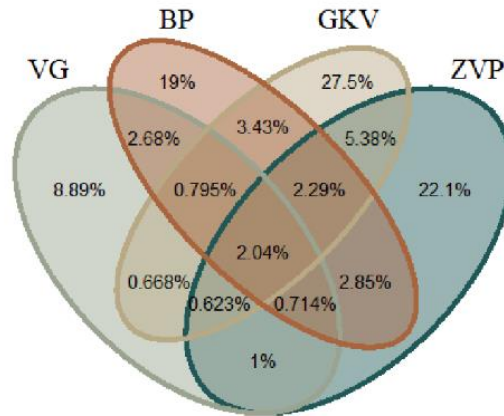


**Figure S7.** Venn diagram showing the percentage of prokaryotic OTUs overlapping between the anchialine speleological objects.

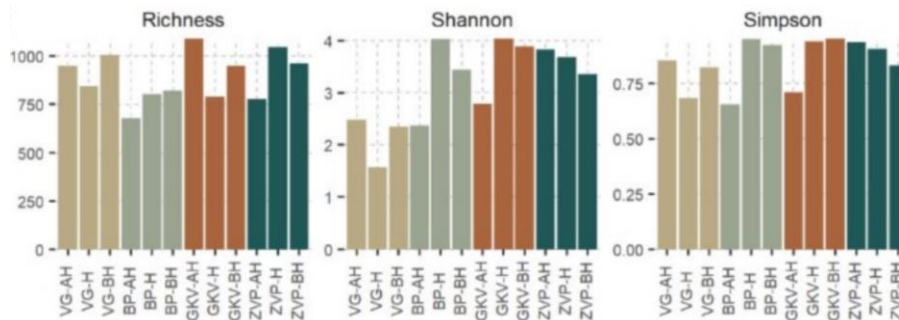


**Figure S8.** Alpha diversity of protistan and fungal community. Sample name abbreviations refer to the area of a sampling point: above the halocline (AH), in the halocline (H), and below the halocline (BH).

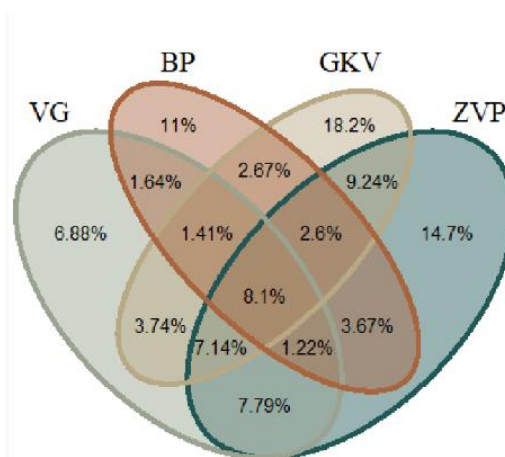


**Figure S9.** Venn diagram showing the percentage of protistan and fungal OTUs overlapping between the anchialine speleological objects.

## Supplementary material 4

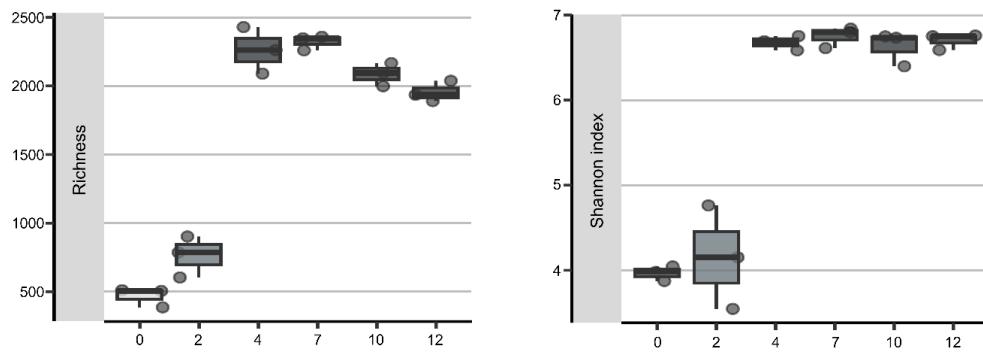
**Chapter Results:** 3.3. Diversity patterns of prokaryotes in the water column of the anchialine speleological object in the Martinska area

**Table S8.** Values of measured physical and chemical parameters in anchialine speleological object.

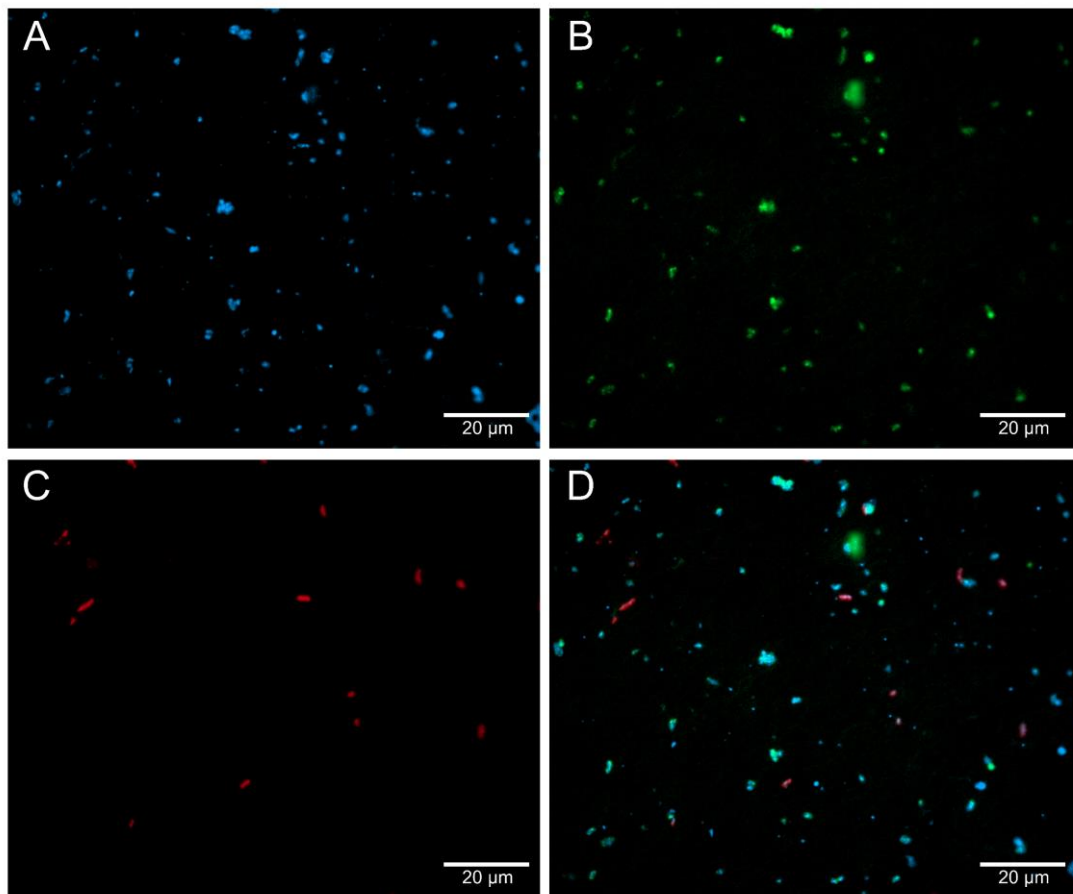
Sample	Sampling date	Depth (m)	Temperature (°C)	Salinity (‰)	Cond ( $\mu\text{S cm}^{-1}$ )	ODO (%)	ODO ( $\text{mg L}^{-1}$ )	pH	TDS ( $\text{mg L}^{-1}$ )	Chlorophyll ( $\mu\text{g L}^{-1}$ )
SC1	17/3/2021	0	13.3	0.9	1415.3	72.7	7.6	7.9	1183.2	0.4
SC2	17/3/2021	2	13.4	1.1	1670.6	17.3	1.8	7.2	1395.7	6.2
SC3	17/3/2021	4	15.4	10.5	14415.9	4.1	0.4	7.0	11466.7	1.0
SC4	17/3/2021	7	15.5	23.1	29857.3	3.9	0.3	7.0	23726.2	0.7
SC5	17/3/2021	10	15.3	31.1	38941.9	3.7	0.3	7.2	31041.7	0.4
SC6	17/3/2021	12	15.3	33.2	41204.4	3.7	0.3	7.3	32842.1	1.3
SC1	14/4/2021	0	13.1	1.1	1688.5	85.8	9.0	8.1	1420.1	0.1
SC2	14/4/2021	2	13.5	1.8	2614.8	15.5	1.6	7.3	2176.0	3.5
SC3	14/4/2021	4	15.3	15.4	20537.4	3.9	0.4	7.0	16401.1	0.9
SC4	14/4/2021	7	15.4	25.1	32122.4	3.6	0.3	7.1	25557.4	0.8
SC5	14/4/2021	10	15.3	31.8	39681.9	3.5	0.3	7.2	31637.4	0.5
SC6	14/4/2021	12	15.3	33.9	42003.5	3.5	0.3	7.3	33489.5	1.7
SC1	30/8/2021	0	15.8	1.5	2373.9	74.2	7.2	8.6	1870.6	0.6
SC2	30/8/2021	2	14.7	9.1	12422.4	7.2	0.7	7.0	10054.6	1.9
SC3	30/8/2021	4	14.4	20.2	25791.0	3.6	0.3	7.0	21016.6	0.9
SC4	30/8/2021	7	14.7	26.2	32836.9	3.4	0.3	7.2	26576.6	0.8
SC5	30/8/2021	10	14.8	31.7	39159.4	3.2	0.3	7.3	31593.6	0.6
SC6	30/8/2021	12	14.8	34.1	41808.6	3.2	0.3	7.3	33713.8	0.4

Table S8. *Continued*

Sample	Depth (m)	DOC (mg L <sup>-1</sup> )	HS <sup>-</sup> (μg L <sup>-1</sup> )	SO <sub>4</sub> <sup>2-</sup> (mg L <sup>-1</sup> )	NH <sub>4</sub> <sup>+</sup> (μg L <sup>-1</sup> )	NO <sub>2</sub> <sup>-</sup> (μg L <sup>-1</sup> )	NO <sub>3</sub> <sup>-</sup> (μg L <sup>-1</sup> )	SiO <sub>4</sub> <sup>2-</sup> (mg L <sup>-1</sup> )	PO <sub>4</sub> <sup>-</sup> (μg L <sup>-1</sup> )	Ca <sup>2+</sup> (mg L <sup>-1</sup> )	Mg <sup>2+</sup> (mg L <sup>-1</sup> )	Na <sup>+</sup> (mg L <sup>-1</sup> )	Cl <sup>-</sup> (mg L <sup>-1</sup> )
SC1	0	1.3	0.0	NA	2.9	1.5	967.0	48.4	135.6	NA	NA	NA	NA
SC2	2	0.7	0.0	NA	4.5	3.7	636.6	50.2	146.0	NA	NA	NA	NA
SC3	4	0.4	1535.1	NA	217.4	3.6	88.7	59.7	455.0	NA	NA	NA	NA
SC4	7	0.3	6680.1	NA	301.4	1.3	342.1	22.4	351.2	NA	NA	NA	NA
SC5	10	0.3	23.5	NA	199.8	1.2	907.0	24.8	246.8	NA	NA	NA	NA
SC6	12	0.4	44.7	NA	157.2	0.8	815.3	11.3	218.6	NA	NA	NA	NA
SC1	0	1.3	0.0	55.1	4.7	1.2	1147.5	28.5	153.1	146.3	30.6	447.9	688.9
SC2	2	1.1	0.0	55.4	15.0	2.3	992.6	34.1	139.3	147.6	33.8	573.8	780.3
SC3	4	0.4	12368.2	387.9	374.5	3.2	1275.4	18.1	581.1	254.7	303.2	6190.9	9541.2
SC4	7	0.4	13393.4	386.7	401.3	3.9	526.8	12.6	530.8	228.1	369.2	8242.2	12330.0
SC5	10	0.3	23.4	705.8	362.5	2.0	822.0	9.5	498.2	117.7	219.6	11890.8	17400.0
SC6	12	0.2	26.9	802.4	229.7	0.8	2171.4	6.5	364.3	102.7	238.6	12005.1	17825.0
SC1	0	3.0	0.0	90.8	211.3	29.6	4208.9	26.0	603.9	177.1	43.2	380.7	1024.9
SC2	2	1.5	4828.2	318.0	502.4	3.0	1058.6	23.0	736.9	256.3	162.1	1432.8	4633.4
SC3	4	0.8	10417.1	1493.3	521.8	0.6	631.7	12.8	653.2	460.4	762.0	7003.8	18864.8
SC4	7	0.7	8036.0	2532.6	586.0	0.3	2599.3	9.8	842.0	468.7	967.8	8973.6	25025.7
SC5	10	2.4	5621.9	3006.6	469.0	1.7	1165.8	7.4	245.3	483.2	1151.0	10696.4	30526.4
SC6	12	0.1	780.5	3205.8	238.1	0.8	803.9	6.2	443.3	479.1	1193.2	11111.0	31880.7



**Figure S10.** Average alpha diversity of the microbial community in anchialine speleological object per depth assessed by 16S rRNA data analysis: richness and Shannon index. Boxplots represent the 1st and 3rd quartiles, the line represents the median, and the points are the established data in three sampling timepoints (March, April and August).



**Figure S11.** Images of prokaryotic cells in HPG-incubated water sample collected in August at 4 m depth (SC3) in anchialine speleological object. (A) DAPI-stained cells (BLUE), (B) cells labeled with Alexa Fluor 488 (GREEN) for CARD-FISH signal: EUBI-III, (C) labeled with Cy5,5 (RED) for BONCAT signal, and (D) all three overlapping signals.

**Table S9.** Percentage of DAPI-BONCAT positive cells (active cells) and DAPI-CARD-FISH (EUBI-III) cells in HPG-incubated water sample, and total, active and EUB cell count in anchialine speleological object.

Sample	Month	Depth (m)	Active cells (%)	EUB cells (%)	Total cell count (cell mL <sup>-1</sup> )	Active cell count (cell mL <sup>-1</sup> )	EUB cell count (cell mL <sup>-1</sup> )
SC1	April	0	38.20	45.06	3.40x10 <sup>6</sup>	1.30x10 <sup>6</sup>	1.53x10 <sup>6</sup>
SC2	April	2	40.46	37.50	4.43x10 <sup>6</sup>	1.79x10 <sup>6</sup>	1.66x10 <sup>6</sup>
SC3	April	4	6.45	26.88	7.75x10 <sup>5</sup>	5.00x10 <sup>4</sup>	2.08x10 <sup>5</sup>
SC4	April	7	2.92	14.62	1.42x10 <sup>6</sup>	4.17x10 <sup>4</sup>	2.08x10 <sup>5</sup>
SC5	April	10	3.33	24.17	1.00x10 <sup>6</sup>	3.33x10 <sup>4</sup>	2.42x10 <sup>5</sup>
SC6	April	12	2.42	15.32	1.03x10 <sup>6</sup>	2.50x10 <sup>4</sup>	1.58x10 <sup>5</sup>
SC1	August	0	66.41	52.20	5.64x10 <sup>6</sup>	3.75x10 <sup>6</sup>	2.95x10 <sup>6</sup>
SC2	August	2	52.45	46.57	2.97x10 <sup>6</sup>	1.56x10 <sup>6</sup>	1.39x10 <sup>6</sup>
SC3	August	4	11.95	45.28	1.32x10 <sup>6</sup>	1.58x10 <sup>5</sup>	6.00x10 <sup>5</sup>
SC4	August	7	7.09	28.35	1.06x10 <sup>6</sup>	7.50x10 <sup>4</sup>	3.00x10 <sup>5</sup>
SC5	August	10	10.40	28.00	1.04x10 <sup>6</sup>	1.08x10 <sup>5</sup>	2.92x10 <sup>5</sup>
SC6	August	12	1.56	10.94	5.33x10 <sup>5</sup>	8.33x10 <sup>3</sup>	5.83x10 <sup>4</sup>

**Table S10.** Relative abundance (%) of major protein functional categories identified in Metagenome Assembled Genomes (MAGs) per depth of anchialine speleological object. Data was obtained by KEGG annotations.

<b>KEGG category</b>	<b>SC1</b>	<b>SC2</b>	<b>SC3</b>	<b>SC4</b>	<b>SC5</b>	<b>SC6</b>
Protein families: genetic information processing	11.98%	10.54%	11.61%	11.68%	11.59%	11.62%
Metabolism - Carbohydrate metabolism	10.48%	8.72%	9.48%	9.56%	9.41%	9.54%
Genetic Information Processing - Translation	5.50%	6.88%	8.60%	8.66%	9.09%	10.24%
Protein families: signaling and cellular processes	7.71%	9.02%	7.79%	7.76%	7.35%	7.32%
Metabolism - Amino acid metabolism	7.51%	6.72%	6.21%	6.21%	6.14%	6.10%
Metabolism - Metabolism of cofactors and vitamins	5.81%	6.65%	5.85%	5.71%	5.99%	5.51%
Unclassified: metabolism	5.80%	5.58%	5.89%	5.87%	5.63%	5.65%
Poorly characterized	4.80%	4.79%	5.25%	5.13%	5.34%	5.23%
Metabolism - Energy metabolism	5.33%	5.78%	4.91%	4.78%	5.06%	4.54%
Metabolism - Nucleotide metabolism	3.99%	3.94%	4.27%	4.33%	4.47%	4.55%
Genetic Information Processing - Replication and repair	2.86%	3.45%	3.62%	3.52%	3.78%	3.84%
Environmental Information Processing - Membrane transport	4.53%	2.98%	2.93%	2.96%	2.77%	2.69%
Protein families: metabolism	2.62%	2.51%	2.91%	2.93%	2.87%	2.89%
Genetic Information Processing - Folding, sorting and degradation	2.27%	2.82%	2.82%	2.79%	2.98%	2.94%
Metabolism - Glycan biosynthesis and metabolism	2.21%	3.04%	2.66%	2.77%	2.85%	2.87%
Environmental Information Processing - Signal transduction	2.32%	3.15%	2.32%	2.28%	1.99%	1.89%
Metabolism - Lipid metabolism	2.19%	2.00%	1.96%	2.00%	2.02%	1.88%
Unclassified: signaling and cellular processes	1.94%	1.84%	1.94%	1.92%	2.03%	1.81%
Unclassified: genetic information processing	1.58%	1.81%	1.94%	1.96%	2.09%	2.09%
Metabolism - Metabolism of other amino acids	1.16%	1.05%	1.13%	1.14%	1.21%	1.14%
Metabolism - Metabolism of terpenoids and polyketides	1.08%	0.86%	0.94%	0.95%	0.98%	0.99%
Cellular Processes - Cell motility	1.06%	2.02%	0.76%	0.85%	0.46%	0.46%
Cellular Processes - Cellular community - prokaryotes	1.02%	0.98%	0.91%	0.90%	0.88%	0.91%
Metabolism - Xenobiotics biodegradation and metabolism	1.72%	0.24%	0.36%	0.44%	0.25%	0.30%

**Table S11.** Relative abundance (%) of major protein functional pathways identified in Metagenome Assembled Genomes (MAGs) per depth of anchialine speleological object. Data was obtained by KEGG annotations.

<b>KEGG pathway</b>	<b>SC1</b>	<b>SC2</b>	<b>SC3</b>	<b>SC4</b>	<b>SC5</b>	<b>SC6</b>
ko03010 Ribosome	3.72%	4.69%	5.55%	5.57%	5.87%	6.61%
ko02000 Transporters	5.24%	5.18%	5.09%	5.07%	5.03%	4.80%
ko99980 Enzymes with EC numbers	4.58%	3.81%	4.49%	4.49%	4.34%	4.39%
ko99997 Function unknown	3.52%	3.74%	4.07%	4.02%	4.14%	4.10%
ko02010 ABC transporters	3.93%	2.41%	2.45%	2.44%	2.11%	2.05%
ko02020 Two-component system	2.17%	3.03%	2.11%	2.10%	1.79%	1.71%
ko00190 Oxidative phosphorylation	2.55%	2.90%	2.30%	2.16%	2.34%	2.05%
ko00230 Purine metabolism	2.56%	2.71%	2.65%	2.67%	2.78%	2.77%
ko03009 Ribosome biogenesis	2.59%	2.71%	2.46%	2.43%	2.44%	2.28%
ko00970 Aminoacyl-tRNA biosynthesis	1.50%	1.89%	2.34%	2.35%	2.48%	2.69%
ko00010 Glycolysis/Gluconeogenesis	1.82%	1.79%	2.17%	2.15%	2.23%	2.32%
ko03016 Transfer RNA biogenesis	2.00%	1.97%	2.26%	2.25%	2.32%	2.32%
ko01002 Peptidases and inhibitors	1.57%	1.39%	1.85%	1.89%	1.90%	1.93%
ko03000 Transcription factors	1.82%	0.99%	1.23%	1.26%	1.04%	1.09%
ko00240 Pyrimidine metabolism	1.43%	1.23%	1.62%	1.66%	1.69%	1.78%
ko00540 Lipopolysaccharide biosynthesis	0.97%	1.70%	1.27%	1.35%	1.40%	1.30%
ko03030 DNA replication	0.98%	1.24%	1.47%	1.45%	1.55%	1.68%
ko02040 Flagellar assembly	0.91%	1.59%	0.59%	0.66%	0.33%	0.35%
ko00020 Citrate cycle (TCA cycle)	0.99%	1.59%	1.05%	1.02%	0.97%	0.90%
ko00790 Folate biosynthesis	1.17%	1.54%	1.22%	1.22%	1.35%	1.22%
ko02048 Prokaryotic defense system	0.96%	1.52%	0.93%	0.91%	0.65%	0.78%
ko00630 Glyoxylate and dicarboxylate metabolism	1.47%	0.80%	0.95%	0.95%	0.91%	0.88%
ko99982 Energy metabolism	0.57%	1.47%	0.90%	0.92%	0.87%	0.86%
ko03060 Protein export	1.03%	1.32%	1.33%	1.35%	1.47%	1.45%
ko00520 Amino sugar and nucleotide sugar metabolism	1.00%	1.21%	1.24%	1.29%	1.39%	1.40%
ko03110 Chaperones and folding catalysts	1.33%	1.21%	1.32%	1.32%	1.34%	1.30%
ko03012 Translation factors	0.92%	1.08%	1.21%	1.18%	1.23%	1.31%
ko00400 Phenylalanine, tyrosine and tryptophan biosynthesis	1.01%	1.29%	1.05%	1.10%	1.25%	1.23%
ko00920 Sulfur metabolism	1.29%	1.15%	1.02%	1.01%	1.11%	0.98%
ko00860 Porphyrin and chlorophyll metabolism	1.28%	0.94%	1.14%	1.02%	0.96%	0.83%
ko99996 General function prediction only	1.28%	1.06%	1.18%	1.12%	1.20%	1.13%
ko02044 Secretion system	0.44%	1.27%	0.67%	0.69%	0.62%	0.64%
ko00910 Nitrogen metabolism	0.85%	1.27%	0.85%	0.84%	0.85%	0.72%
ko03018 RNA degradation	0.75%	0.91%	0.95%	0.92%	1.01%	0.99%
ko03036 Chromosome and associated proteins	1.00%	0.72%	0.91%	0.95%	0.98%	0.98%

## CURRICULUM VITAE

Katarina Kajan was born on 19<sup>th</sup> April 1992 in Augsburg (Germany). She finished elementary school in Erdut and Dalj, and continued her high school education in Second Gymnasium Osijek in Osijek. She completed her undergraduate studies at the Department of Biology, University of J.J. Strossmayer in Osijek in 2013 and the Graduate University Study Programme in Biology at the Department of Biology, University of J.J. Strossmayer in Osijek in 2017 with the title of Master of Biology (mag. biol.). In April 2018, she started working as a research assistant in the Laboratory for Precipitation Processes, Division of Materials Chemistry, Ruđer Bošković Institute, Zagreb, under the project “STIM-REI” of Center of Excellence for Science and Technology-Integration of Mediterranean Region (STIM), University of Split, Split, Croatia. In October 2018, she enrolled in a PhD program at Interdisciplinary doctoral study in Oceanology, Department of Geology, Faculty of Science, University of Zagreb.

She is the first author of three and co-author of eight published scientific papers. She participated in international scientific conferences with one oral and five poster presentations and co-authored on 21 conference abstracts. During her doctoral studies, she has undergone several trainings abroad and participated in several workshops. She has also contributed to scientific popularization in the event of the 5<sup>th</sup> Faculty of Science PhD Student Symposium. She is the recipient of a Rector’s award (2016), the annual award to young scientists "Jasenka Pigac" for 2021 (Croatian Microbiological Society), and the annual award for the best scientific work of an RBI employee for 2021.

**CROSBİ PROFILE: Katarina Kajan**

(Crosbi Profile: 35318, MBZ: 372775)

**Scientific publications**

**Kajan K**, Osterholz H, Stegen J, Gligora Udovič M, Orlić S. Mechanisms shaping dissolved organic matter and microbial community in lake ecosystems. *Water research* (2023) doi: 10.1016/j.watres.2023.120653 (IF: 12.8, Q1)

Hanžek N, Gligora Udovič M, **Kajan K**, Borics G, Várбірó G, Stoeck T, Orlić S, Stanković I. Comparative identification of phytoplankton taxonomic and functional group approach in karst lakes using classical microscopy and eDNA metabarcoding for ecological status assessment. *Hydrobiologia* (2023) doi: <https://doi.org/10.1007/s10750-023-05344-x> (IF: 2.8, Q1)

Kostešić E, Mitrović M, **Kajan K**, Marković T, Hausmann B, Orlić S, Pjevac P. Microbial diversity and activity of biofilms from geothermal springs in Croatia. *Microbial ecology* (2023) doi: <https://doi.org/10.1007/s00248-023-02239-1> (IF: 3.6, Q1)

Čačković A, **Kajan K**, Selak L, Marković T, Brozinčević A, Pjevac P, Orlić S. Hydrochemical and Seasonally Conditioned Changes of Microbial Communities in the Tufa-Forming Freshwater Network Ecosystem. *mSphere*, (2023), e00602-22, doi:10.1128/msphere.00602-22 (IF: 4.8, Q2)

Marković T, Karlović I, Orlić S, **Kajan K**, Smith AC. Tracking the nitrogen cycle in a vulnerable alluvial system using a multi proxy approach: Case study Varaždin alluvial aquifer, Croatia. *Science of The Total Environment* 853 (2022), 158632, doi:10.1016/j.scitotenv.2022.158632 (IF: 9.8, Q1)

**Kajan K**, Cukrov N, Cukrov N, Bishop-Pierce R, Orlić S. Microeukaryotic and Prokaryotic Diversity of Anchialine Caves from Eastern Adriatic Sea Islands. *Microbial ecology* (2021) doi:10.1007/s00248-021-01760-5 (IF: 3.6, Q1)

Hanžek N, Gligora Udovič M, **Kajan K**, Borics G, Várбірó G, Stoeck T, Žutinić P, Orlić S, Stanković I. Assessing ecological status in karstic lakes through the integration of phytoplankton functional groups, morphological approach and environmental DNA metabarcoding. *Ecological Indicators*, 131 (2021), 108166, 13 doi:10.1016/j.ecolind.2021.108166 (IF: 6.9, Q1)

Kulaš A, Gulin V, Matoničkin Kepčija R, Žutinić P, Sertić Perić M, Orlić S, **Kajan K**, Stoeck T, Lentendu G, Čanjevac I, et al. Ciliates (Alveolata, Ciliophora) as bioindicators of environmental pressure: A karstic river case. *Ecological indicators*, 124 (2021), 107430, 12 doi:10.1016/j.ecolind.2021.107430 (IF: 6.9, Q1)

Jokanović S\*, **Kajan K\***, Perović S, Ivanić M, Mačić V, Orlić S. Anthropogenic influence on the environmental health along Montenegro coast based on the bacterial and chemical characterization. *Environmental pollution*, 271 (2021), 116383, 13 doi:10.1016/j.envpol.2020.116383 (IF: 8.9, Q1)

Kulaš A, Marković T, Žutinić P, **Kajan K**, Karlović I, Orlić S, Keskin E, Filipović V, Gligora Udovič M. Succession of Microbial Community in a Small Water Body within the Alluvial Aquifer of a Large River. *Water*, 13 (2021), 2; 115, 23 doi:10.3390/w13020115 (IF: 3.4, Q2)

Žuna Pfeiffer T, Špoljarić Maronić D, Zahirović V, Stević F, Zjalić M, **Kajan K**, Ozimec S, Mihaljević M. 2016. Early spring flora of the Sub-Pannonic steppic grassland (NATURA 2000

site) in Bilje, northeast Croatia. *Acta Botanica Croatica* 75 (2):157-163. doi: 10.1515/botcro-2016-0029 (IF: 1.3, Q3)

### Conference proceedings

Čačković A, Selak L, **Kajan K**, Marković T, Brozinčević A, Pjevac P, Orlić S. 2023. Stability of the freshwater network ecosystem despite seasonal and downstream changes in environmental conditions and diversity of microbial communities. *7th Faculty of science PhD student symposium*. Zagreb, Croatia

**Kajan K**, Jalžić B, Cukrov N, Marguš M, Marković T, Pjevac P, Orlić S. 2022. Effects of salinity gradient on microbial diversity: case study of Sarcophagus cave. *5th International Symposium on Anchialine Ecosystems*. Kona, Hawaii

**Kajan K**, Osterholz H, Orlić S. 2022. Influence of assembly processes on the diversity of microbial communities and dissolved organic compounds in lake ecosystems. *18th International Symposium on Microbial Ecology*. Lausanne, Switzerland

Čačković A, Selak L, **Kajan K**, Mitrović M, Marković T, Brozinčević A, Pjevac P, Orlić S. 2022. The spatial-seasonal differences of microbial communities in the freshwater network ecosystem. *18th International Symposium on Microbial Ecology*. Lausanne, Switzerland

Stanić I, Selak L, **Kajan K**, Čačković A, Pjevac P, Orlić S. 2022. Distribution of methanotrophs along the oxycline in two lake systems. *18th International Symposium on Microbial Ecology*. Lausanne, Switzerland

Marković T, Karlović I, Kolarić J, Šparica Miko M, Heski AM, Stanić N, Pomper N, Smith A, Kulaš A, Gligora Udovič, M, **Kajan, K**, et al. 2022. Gramoznice v aluvijalnih vodonosnikih: ali so vir ali ponor onesnaženja - primer Varaždinskega vodonosnika. *Hidrogeološki kolokvij i 25. Skupština društva SKIAH*. Ljubljana, Slovenia

Hanžek, N, Gligora Udovič M, **Kajan K**, Borics G, Várbíró G, Stoeck T, Žutinić P, Orlić S, Stanković I. 2022. Phytoplankton functional classification and eDNA metabarcoding for biomonitoring assessment of karstic lakes. *19th Workshop of the International Association of Phytoplankton Taxonomy and Ecology*. Tiszafüred: Department of Tisza Research, Danube Research Institute, Centre for Ecological Research, Hungary

Čačković A, **Kajan K**, Mitrović M, Selak L, Brozinčević A, Orlić S. 2022. Bacterial diversity of Plitvice Lakes catchment area during the summer season. *FEMS Conference on Microbiology*. Beograd, Srbija

Hanžek N, Gligora Udovič M, **Kajan K**, Borics G, Várbíró G, Stoeck T, Orlić S, Stanković I. 2022. eDNA metabarkoding fitoplanktona u usporedbi s klasičnom mikroskopskom analizom. *14th Croatian Biological Congress*. Zagreb, Croatia

Grgić M, Kuharić N, **Kajan K**, Dražina T, Orlić S, Bilandžija H. 2022. Testing the utility of eDNA metabarcoding for studying groundwater biodiversity. *3rd Dinaric Symposium on Subterranean Biology*. Trebinje, Bosna i Hercegovina

- Stanić I, Selak L, **Kajan K**, Čačković A, Brozinčević A, Orlić S. 2022. Microbial community comparison of two lake systems in Croatia. *6th Faculty of Science PhD student symposium*. Zagreb, Croatia
- Čačković A, **Kajan K**, Mitrović M, Selak L, Brozinčević A, Orlić S. 2022. Seasonal changes of microbial community in Plitvice Lakes. *6th Faculty of Science PhD student symposium*. Zagreb, Croatia
- Selak L, Osterholz H, **Kajan K**, Dittmar T, Orlić S. 2021. Strong ties of microbes and dissolved organics over a productive season in a shallow coastal Mediterranean lake. *ASLO 2021*, virtual meeting
- Kulaš A, Gulin V, Matoničkin Kepčija R, Žutinić P, Sertić Perić M, Orlić S, **Kajan K**, Stoeck T, Lentendu G, Čanjevac I, et al. 2021. Ciliates as bioindicators of environmental pressure in a karstic river. *DNAQUA Conference*, virtual meeting
- Kamberović J, Gligora Udovič M, Kahlert M, Tapolczai K, Lukić Z, Ahmić A, Dedić A, Kulaš A, **Kajan K**, Hanjalić J et al. 2021. Composition of diatom communities on travertine barriers of the Una River (Bosnia and Herzegovina) obtained by DNA metabarcoding and morphological analysis. *DNAQUA Conference*, virtual meeting
- Kajan K**, Cukrov N, Orlić S. 2020. Mikrobiološka raznolikost anhijalinih ekosustava na području NP Kornati. *Simpozij studenata doktorskih studija PMF-a*. Zagreb, Croatia
- Kajan K**, Cukrov N, Orlić S. 2019. Microbial community composition of anchialine caves on the Kornati islands (Adriatic Sea). *Interdisciplinary Endeavour in Technology at Nanoscale, Water and Environment*. Split, Croatia
- Kajan K**, Filker S, Stoeck T, Hanžek N, Stanković I, Orlić S. 2019. Dynamics of eukaryotic and prokaryotic communities in Croatian karst lakes. *16th Symposium of Aquatic Microbial Ecology*. Potsdam, Germany
- Kajan K**, Osterholz H, Dittmar T, Hanžek N, Stanković I, Orlić S. 2019. Microbial community response to salinity variation in a coastal Mediterranean lake. *16th Symposium of Aquatic Microbial Ecology*. Potsdam, Germany
- Kajan K**, Cukrov N, Orlić S. 2019. Microbial diversity in Adriatic anchialine caves. *8th Congress of European Microbiologist*. Glasgow, UK
- Herrero S, Stratmann C, ... , **Kajan K**, et al. 2019. Urban Algae - Ecological Status and the Perception of Ecosystem Services of Urban Ponds. *ESP World conferences*. Hannover, Germany
- Orlić S, **Kajan K**, Selak L. 2019. The potential of Adriatic microbiome in the blue biotechnology. *Interdisciplinary Endeavour in Technology at Nanoscale, Water and Environment*. Split, Croatia
- Jokanović S, **Kajan K**, Huter A, Perović S, Mačić V, Orlić S. 2019. Potential impact of contamination on microbial communities in sediments of Montenegrin coast (southern Adriatic Sea). *16th Symposium of Aquatic Microbial Ecology*. Potsdam, Germany

Osterholz H, **Kajan K**, Bourceau P, Stanković I, Dittmar T, Orlić S. 2019. Dissolved organic matter in Croatian lakes – the influence of catchment, season and microbes. *16th Symposium of Aquatic Microbial Ecology*. Potsdam, Germany

Šimunović M, Šušnjara M, Žutinić P, Kulaš A, Plenković-Moraj A, Orlić S, **Kajan K**, Valić D, Žunić J, Goreta G, Gligora Udovič M. 2019. Application of new tools in biomonitoring of a freshwater karstic Lake Visovac (Croatia). *Seventh European Phycological Congress*. Zagreb, Croatia

Kulaš A, Gulin V, Matoničkin Kepčija R, Sertić Perić M, Žutinić P, Šušnjara M, Orlić S, **Kajan K**, Stoeck T, Lentendu G, Martinić I, et al. 2019. Diversity and ecological preference of ciliates assemblage in a freshwater karstic river. *SEFS11 Symposium for European Freshwater Sciences*. Zagreb, Croatia

Stratmann C, Herrero S, ..., **Kajan K**, et al. 2019. Urban Algae - ecological status of urban ponds and the public perception of their ecosystem services. *SEFS11 Symposium for European Freshwater Sciences*. Zagreb, Croatia

### Workshops and Trainings

10/2022 AQUACOSM-plus Fall School, Cluj-Napoca, Romania

03/2022 Workshop Srce: Korištenje računalnog klastera Isabella (online)

07/2021 Workshop user! 2021 - The R Conference (online)

07/2020 Advanced Programming in R workshop, Physalia-courses (online)

11/2018 EukRef Workshop: A phylogenetically informed curation of Eukaryotic 18S rDNA Station Biologique Roscoff, Roscoff, France

09/2018 Training School 4: Deep Life in Buried Salt Deposits School of Biological Sciences University of Essex, University of Essex, Colchester, UK

07/2022 Research visit at the Department of Aquatic Sciences and Assessment, Swedish University of Agricultural Sciences, Uppsala, Sweden. Supervision: dr. sc. Maliheh Mehrshad

02-03/2019 + 10/2021 + 04/2022 Research visit at the Division of Microbial Ecology, Department of Microbiology and Ecosystem Science, University of Vienna in Vienna, Austria. Supervision: dr.rer.nat. Petra Pjevac (STSM financed by Cost Action (grant) and RBI grant)

06-08/2018 Research visit at the University of Kaiserslautern, Faculty of Biology, Ecology Department in Kaiserslautern, Germany. Supervision: Prof Thorsten Stoeck (STSM financed by Cost Action (grant))

11/2017-03/2018 Student trainee at the Biology Centre CAS, Institute of Hydrobiology, Department of Aquatic Microbial Ecology in České Budějovice, Czech Republic. Supervision: Dr.sc. Tatiana Shabarova (Erasmus+ grant)

01/2016-04/2016 Student trainee at the University of Pannonia, Department of Limnology in Veszprém, Hungary. Supervision: Prof. Judit Padisák (Erasmus+ grant)

### **Activities**

2021 Member of the Organizing Committee of the 5<sup>th</sup> PhD Student Symposium 2021 at the Faculty of Science, University of Zagreb, Zagreb, Croatia and Online

2018 member of the „Urban Algae“ project, <https://freshproject-urbanalgae.jimdofree.com/citizen-science/>

### **Awards**

2023 Annual award for the best scientific work of an RBI employee for 2021

2022 Annual award to young scientists "Jasenka Pigac" for 2021 (Croatian Microbiological Society)

2019 Poster award at Interdisciplinary Endeavor in Technology at Nanoscale, Water and Environment, Split, Croatia

2016 Rector's award for the academic year 2015/2016